DETERMINATION OF THE PHYSICAL CHARACTERISTICS OF SMOKE PARTICULATES GENERATED BY BURNING POLYMERS

A THESIS

Presented to

The Faculty of the Division of Graduate Studies

By

Clyde Perry Bankston

In Partial Fulfillment

of the Requirements for the Degree

Doctor of Philosophy

in the School of Aerospace Engineering

Georgia Institute of Technology

March, 1976

In presenting the dissertation as a partial fulfillment of the requirements for an advanced degree from the Georgia Institute of Technology, I agree that the Library of the Institute shall make it available for inspection and circulation in accordance with its regulations governing materials of this type. I agree that permission to copy from, or to publish from, this dissertation may be granted by the professor under whose direction it was written, or, in his absence, by the Dean of the Graduate Division when such copying or publication is solely for scholarly purposes and does not involve potential financial gain. It is understood that any copying from, or publication of, this dissertation which involves potential financial gain will not be allowed without written permission.

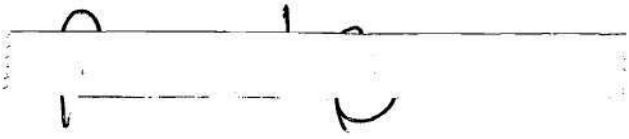

7/25/68

DETERMINATION OF THE PHYSICAL CHARACTERISTICS OF SMOKE PARTICULATES GENERATED BY BURNING POLYMERS

Approved:

Ben T. Zinn, Chairman

Edward W. Price

Eugene A. Powell

Date approved by Chairman: 3/19/76

ACKNOWLEDGMENTS

I would like to express my sincere appreciation to those people who have helped make this thesis possible. First, I would like to thank Dr. Ben T. Zinn for his suggestion of the thesis topic and for his guidance during the course of this research. I would also like to thank Professor Edward W. Price and Dr. Eugene A. Powell for their careful examination of the manuscript. Dr. Powell's frequent counsel and advice concerning various aspects of the research is also appreciated.

I am grateful to Dr. Robert A. Cassanova for his assistance in the development of the experimental techniques utilized in this research, and for his valuable insight into various aspects of the test program.

The financial support of the National Science Foundation RANN Program and the Georgia Institute of Technology are gratefully acknowledged.

My wife Mary has provided continued enthusiastic support and assistance during my graduate work and I am sincerely thankful for her patience and understanding. Finally, I thank my parents, Mr. and Mrs. Clyde Bankston, for their guidance and support during the years of my education.

TABLE OF CONTENTS

Page

SUMMARY

Available evidence indicates that additional information is needed on the characteristics and hazards of smoke particulates produced by burning materials. The purpose of this research is to provide such information on smoke particulates generated by burning three commonly used building materials. In order to accomplish this goal, small-scale test methods have been developed to simulate "real-fire" conditions. An aerosol sampling and analysis system has been utilized to measure smoke particulate size distributions and particulate mass concentrations produced by burning wood, rigid urethane foam, and rigid polyvinyl chloride plastic under different environmental conditions.

Effects of changes in the following environmental parameters on smoke particulate characteristics have been determined: (1) atmospheric composition, (2) type of combustion; i.e., flaming or smoldering, and (3) in the case of smoldering combustion, the level of radiant heating received by the material. Results show that particulate characteristics are relatively insensitive to changes in atmospheric composition for both flaming and non-flaming combustion. However, particulate characteristics observed during non-flaming combustion were found to be quite different from particulate characteristics observed during flaming combustion. Specifically, smoke particle sizes were generally smaller and particulate mass concentrations

were less during flaming combustion. Particle size distribution peaks are in the range 0.1-0.3 micron for all flaming tests and for non-flaming tests at the lowest heating rate (3.2 W/cm^2). Non-flaming tests at higher heating rates show particle size distribution peaks to be near 1.0 micron. These values are typical for all three materials tested. Also, smoke particles generated during flaming combustion are predominantly sooty in nature while particulates generated under non-flaming conditions consist of a complex mixture of liquid and/or solid organic substances. Particulate mass concentration behavior was found to be closely related to sample weight loss rate under both flaming and non-flaming conditions.

Variations in radiant heating rate were observed to have a significant effect on particulate characteristics for non-flaming conditions. Increases in radiant heating rate resulted in larger measured particle sizes and substantially higher particulate mass concentrations for all three materials. Furthermore, time-resolved particle size measurements show that particle sizes tend to vary during non-flaming tests run at high radiant heating rates.

Discussions of these results in relation to the known mechanisms of pyrolysis and combustion of polymeric materials yield general explanations for the measured particle size and concentration behavior observed during this test program. In addition, these results provide important new information, from a practical standpoint, on the physical characteristics of smoke particulates generated by burning polymeric materials. Measurements of smoke particles show that they

are in a size range where a high percentage may be inhaled and then retained within the human respiratory system. The fact that particulate mass concentrations increase substantially with increases in radiant heating rates (for non-flaming tests) is particularly significant in relation to test methods using relatively low radiant heat fluxes. Finally, this particle size and concentration information is necessary in the development of light obscuration theories which would predict the obscuration of vision due to smoke particulates.

LIST OF ILLUSTRATIONS

Figure Page

Figure Page

Figure Page

Figure Page

Figure Page

LIST OF TABLES

CHAPTER I

INTRODUCTION

In recent years, it has become widely accepted that smoke and toxic gases are responsible for the majority of fatalities and much of the property damage attributed to fires in buildings.[1] During the initial phases of most fires, the rate of spread of smoke and toxic gases from the fire site to nearby locations is considerably faster than the spread of the fire itself.[2] The large quantities of smoke that spread in this manner produce physical discomfort and obscure vision, thus preventing occupants from using available escape routes. Victims trapped under such circumstances soon succumb to the toxic effects of the combustion products. In addition, smoke often prevents firemen from locating and then extinguishing a fire, while it also interferes with rescue efforts.

As progress in science and technology has produced a greater variety of more complex materials, the danger of losses in lives and property due to smoke produced in building fires has increased. These new products generate varying quantities of smoke and toxic gases, and thus add a significant "unknown" to the evaluation of the hazards present during building fires. Also there is an increased smoke hazard due to the increasing number of high-rise buildings. Smoke produced in multi-story building fires is often rapidly transported by various mechanisms (e.g., ventilation systems, stack effect, etc.)

to parts of the building remote from the fire. Stairwells and elevator shafts become clogged with smoke, making them unusable for escape purposes, and thus endangering the lives of a greater number of occupants.

Smoke consists of a complex mixture of solid and liquid particles, such as soot, tar droplets, mists, etc., in addition to the gaseous combustion products. Although the particulate matter is not generally considered to be as toxic as the gaseous products, it may have an extremely irritating effect on the eyes and nasal passages resulting in reduced vision, coughing, extreme discomfort, and undesirable synergistic effects. Smoke particles vary in size, although most of them are approximately one micron in diameter or less. Particles of this size are very effective in obscuring vision and are readily transported by gas currents.

Smoke particulates are characterized by size distribution, shape, chemical composition, mass, mass-to-charge ratio, and particle concentration. These physical and chemical characteristics can be linked to the physiological and toxicological consequences of smoke. Particle size and charge influence the depth of penetration of smoke into the respiratory system[3,4], while its solubility and chemical composition are presumably responsible for the toxic effects of the smoke and any synergistic effects of the inhaled gaseous combustion products.

Although available evidence directly relates the chemical and physical characteristics of the smoke to its undesirable effects, very little has been done to date to determine the properties of the

smoke produced by the burning of different materials under different conditions. It is clear, therefore, that additional information is needed on the characteristics of smoke and gaseous combustion products in order to institute effective building code requirements and to develop better test methods for studying smoke generation. The objective of the studies described in the following pages is to help fill the above-mentioned information gap by providing new information on the physical characteristics of smoke produced by burning materials. Measurements of smoke particulate size distributions and particulate mass concentrations have been made while small samples of commonly-used building materials were burned under conditions simulating "real-fire" situations. Changes in smoke characteristics have been studied for samples burned under conditions of flaming and non-flaming combustion in atmospheres having different compositions. Finally, existing hypotheses dealing with the mechanisms of pyrolysis and combustion of polymers have been used to help analyze the results obtained in the above-mentioned experiments. The importance of these results in determining actual fire hazards is also discussed.

Background

A complete description of the smoke particles produced from any burning material can be provided only when the total weight of the material in suspension, its physical and chemical properties, and its state of dispersion are known. The techniques for determining such properties may be divided into two categories: (1) methods which involve withdrawing samples from the suspension for further analysis

by various apparatus, and (2) in situ methods. Reviews of the methods and apparatus used to analyze aerosols are given in Refs. 5 and 6. Particle size and concentration measurements by sampling can be obtained in a wide variety of ways. Cascade impactors, centrifugal separators, electrical mobility analyzers, and light scattering instruments are specifically designed for the determination of particle size data. Particles collected by filters, electrostatic precipitators and impingement samplers may be analyzed to determine size, as well as concentration data. In addition, instrumentation is available for continuous particulate mass concentration measurements (by sampling) using a piezoelectric crystal.

In situ aerosol analysis usually employs some type of optical system for light attenuation and scattering measurements. Optical density, average particle size, index of refraction, and volume concentration are examples of data obtained from such systems.

A number of research programs that are concerned with the determination of the "smoking" properties of various materials, by means of small scale tests, have been, and are currently under way. Small scale tests frequently adopted in building codes are the ASTM E84 Tunnel Test[7], and the ASTM E286 8 foot Tunnel Test[8]. While these tests are principally designed for the evaluation of flame spread characteristics of materials, they are nevertheless used by many codes in the evaluation of the potential smoke particulate production of various building and furnishing materials. Thus, in order to deal more adequately with the problem of smoke production, other small-

scale smoke test chambers have been developed. In such chambers, samples of materials are tested under conditions of either smoldering or flaming combustion. Tests are conducted with and/or without chamber ventilation, and the relative smoke particulate production capability of each sample is determined by the attenuation of a collimated beam of light passing through the smoke.

Two widely used smoke test chambers are the Rohm and Haas XP-2 chamber[9] and the NBS Smoke Chamber[10]. The XP-2 chamber is a closed box, 12" x 12" x 31", in which one inch square, 1/4" thick samples are exposed to a flame. Smoke density is evaluated from light attenuation and the loss of visibility of a standard EXIT sign. The NBS chamber is larger (2 ft. x 3 ft. x 3 ft.) and it uses a larger test specimen (3 in. square, 1/4 in. thick) than the XP-2 chamber. The standard NBS chamber test is conducted under either smoldering or flaming conditions, where the chamber is not ventilated. Relative smoke density is again determined from light attenuation measurements, and is evaluated in terms of the specific optical density[10]. Optical density measurements are advantageous, since they can be related to the visibility of objects seen through smoke; and, in fact, such information is quite often used to compare the relative smoke production capabilities of various materials[11]. Unfortunately, the above-mentioned data cannot, at present, be directly related to other smoke particle characteristics (i.e., particle size, particle concentration, chemical composition, etc.), which are important in the evaluation of the physiological and toxicological effects of smoke. Furthermore, small-scale tests

results obtained in different chambers at different laboratories often do not correlate well with one another; or with results obtained in other related experiments[12].

Modifications to the standard NBS smoke chamber have been made at the Lawrence Radiation Laboratory (LRL)[13,14] and the University of Utah.[15,16] The smoke chamber at LRL has been modified to provide controlled ventilation rates of up to 20 air changes per hour. Test results at LRL provide a large quantity of data on the relative smoking properties of polymers and woods in terms of optical density measurements.[13,14] The NBS chamber at the University of Utah has been modified to allow for continuous monitoring of sample weight.[17] In addition, a variable high-energy flux radiant heat source has been developed and results show the smoking characteristics of materials to be dependent upon radiant heat flux during flaming and non-flaming smoke tests.[18] Once again, the information obtained in these tests has been basically limited to optical density measurements.

The increased use of additives and coatings for building materials has created interest in the effects that such treatments have on their smoking properties. Specifically, there is evidence to indicate that the use of fire retardants in synthetic polymers may tend to increase the amount of smoke produced by such polymers.[19,20] Also, studies of wood coating systems[21] have shown that coated Douglas Fir produces varying quantities of smoke as compared to the wood itself. Notably, none of the coatings tested reduced smoke under conditions of flaming combustion.

Although the number of detailed theoretical studies dealing with the smoking characteristics of polymers is limited to a few, some examples do exist. In an analytical study related to NBS chamber experiments conducted at the University of Utah, Seader and Chien[22] have recently pointed out the need for studies that will provide data on smoke particulate size distribution and concentration. In Japan[23] and Canada,[24] theoretical considerations have led to the definition of a "smoke generation coefficient," for characterizing the smoke production capabilities of materials. This smoke coefficient is used in conjunction with a first-order Arrhenius type reaction rate expression to predict the smoke production rate of a particular material.

Finally, there are a number of investigations deserving mention, which deal with the detailed characteristics of particulates produced during the pyrolysis and combustion of polymers. The U. S. Public Health Service has sponsored studies[25] of particles produced from the pyrolysis of polytetrafluoroethylene (Teflon). This work includes investigation of both physical and chemical characteristics of the particulates, and the toxicological aspects associated with their generation. The physical characteristics, i.e., particle size and shape, were determined by electron microscopy techniques. More recently, the Federal Aviation Administration has sponsored studies in which aircraft cabin materials were studied under "flash fire" conditions.[26] Here, attempts were made to establish the chemical composition of the particulate residue produced during the burning of a flexible urethane foam. Similar work has also been done at the

British Fire Research Station at Borehamwood.[27] At the U. S. Naval Research Laboratory, investigations[28] have established that soot particles generated by burning polyvinyl chloride may act to transport hydrochloric acid. Thus, the penetration of HCL (also produced by burning PVC) into the human respiratory system might then be determined by the size characteristics of the soot particles. Work conducted at the National Bureau of Standards has yielded information on the size and shape characteristics of smoke particles produced from combustion of PVC, red oak (wood) and ABS under flaming conditions.[29] Scanning electron microscope pictures taken of the smoke particles show the general appearance of the particles and provide an estimate of the maximum and minimum particle sizes. Such data give qualitative information on particle characteristics although it does not provide important quantitative information on particle size distributions.

While the above-mentioned research indicates increasing emphasis on the analysis of smokes produced by burning materials, it also points our areas in which additional research is needed. The investigation reported in Ref. 22 clearly points out the need for experimental data on the size distribution and concentration of smoke particles in the development of theoretical models. In addition, size distribution and concentration data are important for toxicological studies related to smoke particulates. Finally, previously developed small-scale test chambers are not able to adequately simulate "real-fire" environments; where materials are burned at high radiative heating rates in high temperature gases of varying compositions. To be meaningful, data

must be obtained under conditions that simulate those observed in actual fires as closely as possible. The research presented in this thesis represents an effort to provide data on smoke characteristics that will meet these needs.

Objectives

The review presented in the previous section indicates that in order to reduce the hazards of combustion products, research is needed in several areas. The research presented here is designed to meet the following objectives:

1. Development of small-scale testing methods that could be used to predict the characteristics of the smoke particulates generated in actual fire situations.

2. Development of an aerosol sampling system to be used in conjunction with small-scale smoke test methods.

3. Determination of particle size distributions and particulate mass concentrations of smokes generated by burning three commonly used building materials under different environmental conditions. The materials to be used are Douglas fir (wood), rigid urethane foam, and polyvinyl chloride plastic.

4. Determination of the effects of changes in atmospheric composition on the smoke particulate characteristics measured during the burning of the above-mentioned materials.

5. Determination of the effects of the types of combustion, i.e., flaming or smoldering, on the smoke particulate characteristics measured during the burning of the above-mentioned materials.

6. In the case of smoldering combustion, determination of the effects of variation in radiant heat flux on the smoke particulate characteristics measured during the burning of the above-mentioned materials.

7. Discussion of measured smoke particle size and concentration characteristics as they relate to current hypotheses dealing with the mechanisms of smoke formation for the materials studied in this program. Such information could possibly be of use in extending the experimental results obtained here to other environmental conditions of interest, and in providing greater insight into the basic mechanisms responsible for the generation of dangerous smoke particulates during actual fires. Also, these results will be discussed in terms of their applicability to the analysis of actual smoke hazards to humans.

CHAPTER II

EXPERIMENTAL PROGRAM

In order to meet the objectives outlined in Chapter I, an experimental test program has been carried out in a new small-scale smoke test facility. The facility consists of two basic components. First, a small-scale smoke test chamber to be called the Combustion Products Test Chamber[30,31], has been constructed for determining the properties of the smoke produced during the combustion of various samples under carefully controlled conditions. Second, an aerosol sampling system has been developed for determination of the physical properties of smoke particulates generated during tests run in the Combustion Products Test Chamber. Measurements of particle size distributions, particulate mass concentrations and sample weight loss characteristics have been made for three commonly used building materials: Douglas fir (wood), polyvinyl chloride, and a rigid urethane foam.

Facilities and Instrumentation

Combustion Products Test Chamber

In this study, a recently developed[30,31] small-scale test chamber has been utilized in determining the physical properties of the smoke produced during the combustion of various samples under carefully controlled environmental conditions. The Combustion Products

Test Chamber (CPTC) incorporates several features designed to make it more versatile than previous smoke-test chambers. The CPTC, shown in Figure 1, consists of two (2) stainless steel shells, and is designed to be continuously ventilated during smoke tests. The outer shell is solid, cubical (4 ft. x 4 ft. x 4 ft.) and equipped with a door for access to the inner shell. Four one-half inch diameter ports for introduction of selected ventilation gases are located on one wall near the floor of the outer chamber.

The perforated inner shell consists of a cylindrical lower section 27 inches in diameter and a conical upper section, approximately 19.5 inches high. A four (4) inch diameter exhaust stack mounted on top of the cone, projects through the top of the outer shell. The inner shell is equipped with a removable, perforated plexiglas window in the lower section, for access to the sample. The sample is mounted in the center of the inner shell two inches above the floor. The sample holder, a modified version of the one used in the NBS chamber[10] is shown in Figure 2. It is supported by a quartz rod, leading to a force transducer for continuous recording of sample weight.

The perforations of the inner shell allow the ventilating gas mixture, entering the plenum between the shells, to slowly and uniformly flow into the immediate surroundings of the test sample. The flow of ventilating gas through the perforated shell prevents absorption and deposition of condensable vapors and solid particles on the surface of the inner shell and forces all combustion products

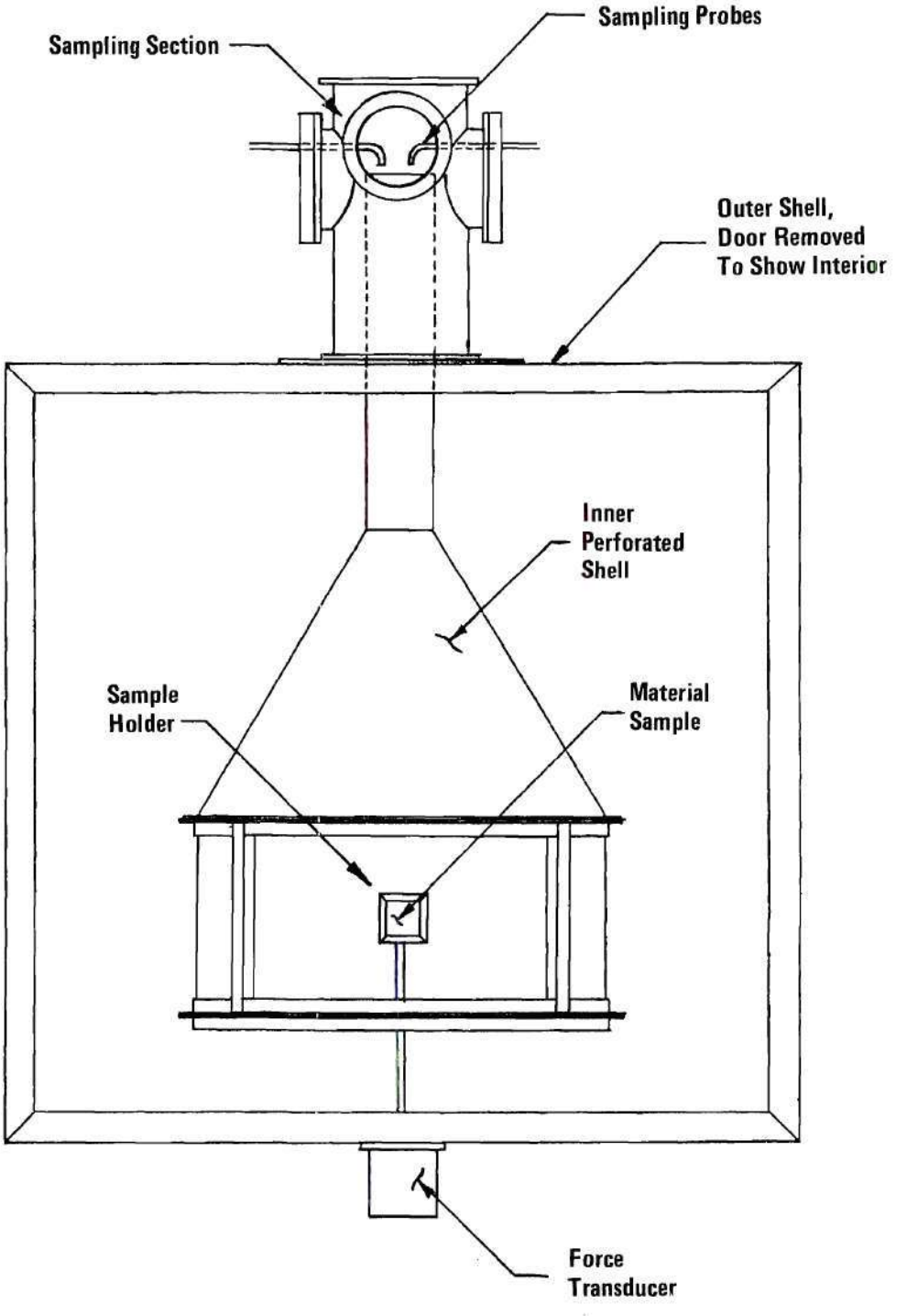

Figure 1. Combustion Products Test Chamber

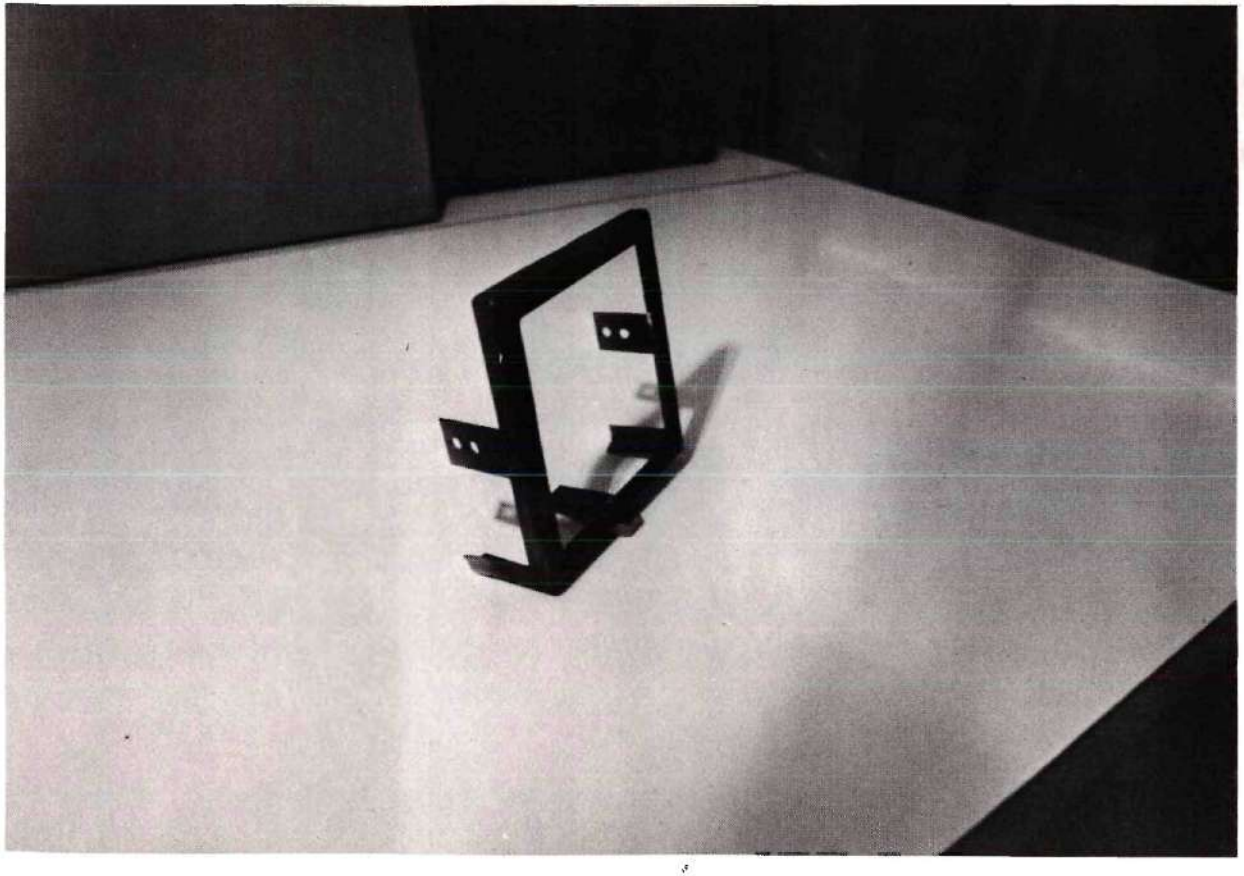

Figure 2. Sample Holder

to flow through the Sampling Section immediately above the chamber. Thus, the gas flow prevents the accumulation of combustion products in the chamber by continuously sweeping them out through a vent above the Sampling Section.

The conditions under which combustion of a sample take place can be varied in three ways:

1. The atmospheric composition in the chamber can be carefully controlled through introduction of selected gases through the four ports mounted in the outer shell. Needle valves and float-type variable area flowmeters are used to control gas flow from high-pressure cylinders adjacent to the outer chamber.

2. Combustion of the sample may be carried out under either flaming or smoldering conditions. The inner shell is equipped with a variable flux radiant heat source, with the capability of providing up to 10 W/cm^2 of radiant energy at the face of the sample being tested. The heat source, shown in Figure 3, consists of four tungsten filament quartz lamps with a flat ceramic reflector (Research Inc., Model No. 4083-5-6-E). The dimensions of the "radiating" area of the heater are approximately 5.25 inches x 4.75 inches. The inner shell is also equipped with a stainless-steel propane pilot burner (Figure 4). The burner consists of a 1/4 inch diameter tube, positioned along the bottom edge, and 1/4 inch away from the face of the sample. The side of the burner adjacent to the sample has been drilled with 25 0.024 inch diameter holes, 1/8 inch center-to-center, extending the width of the sample face. This arrangement provides a band-like flame across the lower edge of the sample. Propane and an air-oxygen mixture

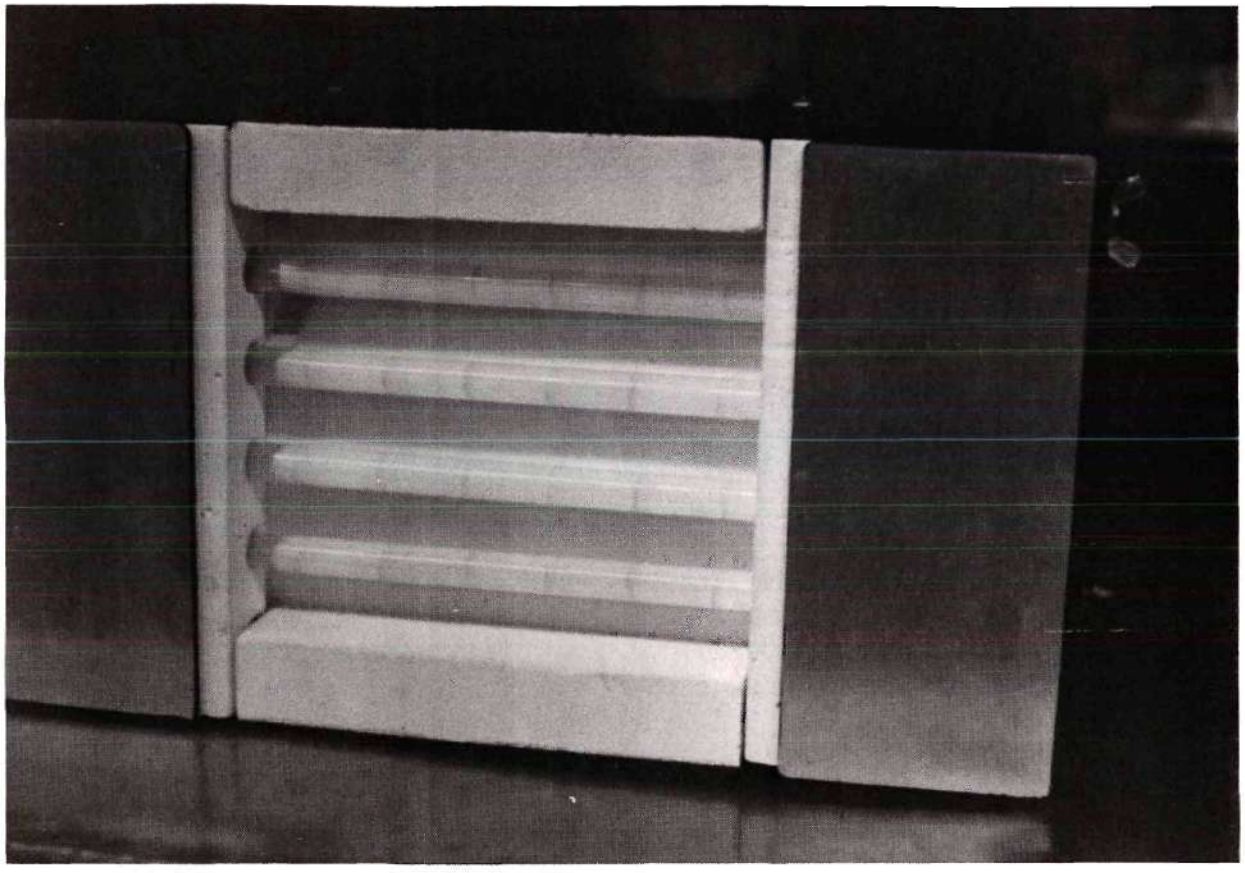

Figure 3. Radiant Heater

Figure 4. Propane Burner

are supplied to the burner from bottles outside the outer chamber, and the flame may be remotely ignited by a spark igniter mounted near the center of the flame strip. During tests involving smoldering conditions, the radiant heater is adjusted to various pre-determined heating rates; while in flaming tests the propane flame is utilized to ignite the flammable products generated by a smoldering sample, also subjected to a preselected radiant heat flux.

3. The variable flux radiant heat source allows the study of sample behavior under a number of radiant heating conditions. By adjusting the voltage input into the heater and the distance between sample and heater, the incident radiant energy at the sample face can be varied over a relatively wide range of heating levels. In this study, the effects of variations in radiant heating conditions have been studied for smoldering combustion only.

Aerosol Sampling System

The sampling section located above the shell is designed to allow samples to be continuously withdrawn from the vent gas flowing from the CPTC. A schematic of the aerosol sampling analysis system is shown in Figure 5. Two stainless steel sampling probes are used to withdraw samples of the combustion products from the sampling section. The sample withdrawn by one of the probes (1/2" O.D.) leads to an Andersen Sampler (Model 21-000)[32], which measures particle size distribution for the size range 0.43 to 11 microns. Part of the sample withdrawn by the second probe (1/4" O.D.) goes to a Whitby Electrical Aerosol Analyzer (Thermo-Systems, Inc., Model 3030)[33,34]

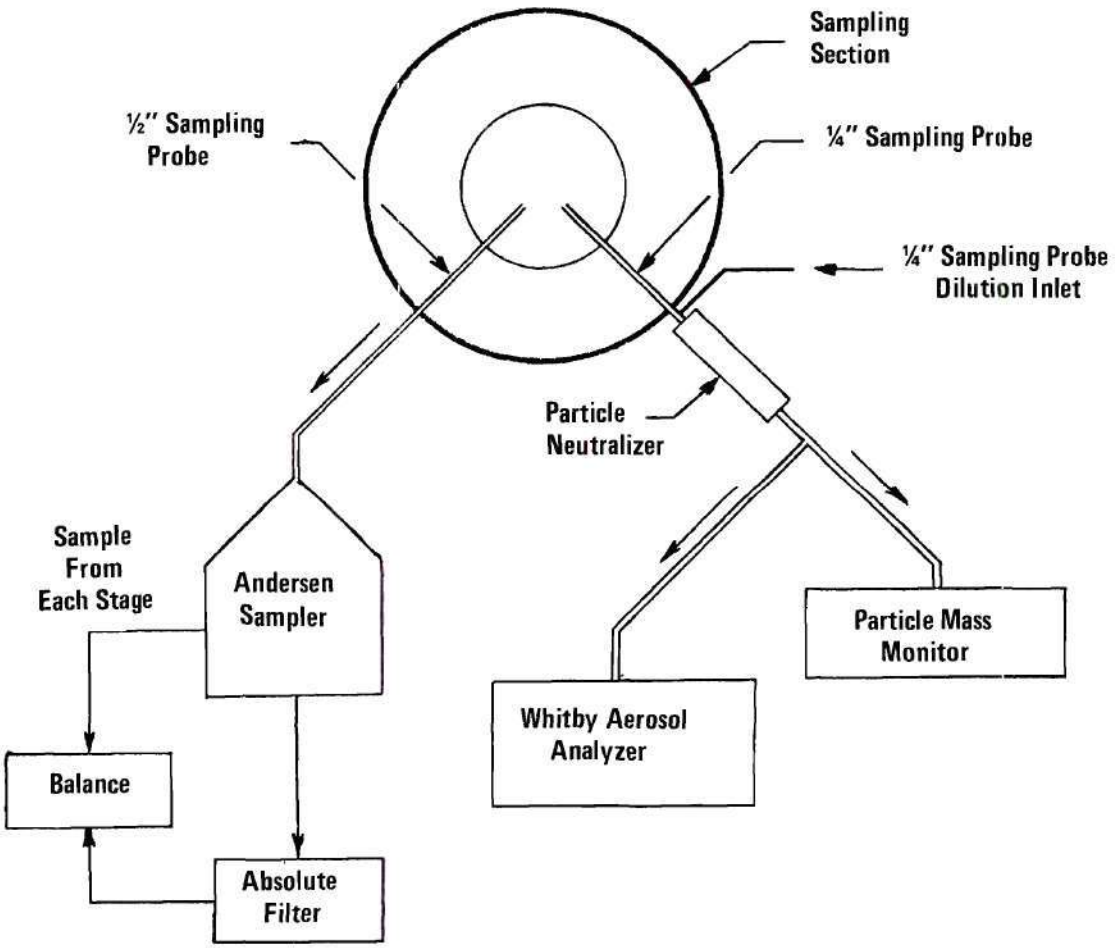

Figure 5. Aerosol Sampling System - Schematic

for particle size distribution determination in the range 0.01 to 1.0 micron. The remaining portion of the second sample is directed into a Mass Monitor (Thermo - Systems, Inc., Model 3200 B)[35,36] which measures the smoke particulate mass per unit volume. The Whitby Analyzer provides size distribution measurements every 1.5 minutes during a test. While the Andersen Sampler (cascade impactor) gives an integrated size distribution for an entire test. Samples of the solid and liquid particles accumulated in the stages of the Andersen Sampler are collected after each test, weighed and then stored for later chemical analysis. Smaller particles (less than 0.43 micron) not collected in the Andersen Sampler are trapped by an absolute filter (Gelman Type A, glass fiber) and are later recovered for further analysis.

The openings of the two stainless steel probes are positioned parallel to the flow passing from the inner shell through the four (4) inch diameter exhaust pipe. After entering each probe, the sample flow undergoes a ninety (90) degree turn and exits through flanges on opposite sides of the sampling section. Flow through the 1/2 inch probe is then directed to the Andersen Sampler for separation by particle size. The flow through the 1/4 inch diameter tube is diluted as soon as it leaves the Sampling Section, where it then passes through a particle charge neutralizer. The dilution is required in order to maintain particle concentrations within the limits required for operation of the Whitby Electrical Aerosol Analyzer and the Mass Monitor. The Electrical Aerosol Analyzer also necessitates use of the particle neutralizer because its operation depends upon the

electrical properties of uncharged aerosols. Finally, after exiting the neutralizer, the aerosol flow in the 1/4 inch probe is split, and separate flows are directed into the Electrical Analyzer and the Mass monitor. Detailed procedures establishing sampling flow and dilution rates are given in Appendix A. Also, it was determined at the outset of the program that isokinetic sampling procedures were not required for the particle sizes under consideration. A discussion of the justification for the sampling procedures used, especially pertaining to isokineticity, is included in Appendix A.

Test Program

The test program has been designed to study the properties of the smoke particulates produced by burning samples of typical construction and furnishing materials under conditions simulating actual fire conditions. The materials that have been studied are Douglas fir (wood), polyvinyl chloride plastic, and a rigid urethane foam. The experimental program followed for each material is outlined in Table 1. During the test program, the following quantities have been systematically varied: (1) the composition of the chamber atmosphere, (2) the type of combustion (i.e., flaming or smoldering), and (3) in the case of smoldering combustion, the intensity of the radiant heat flux received at the sample surface. The data from these experiments could then be analyzed in an effort to determine the similarities and differences between the properties of smoke particulates resulting from the burning of the three materials under identical conditions and the burning of the same materials under different conditions.

Table 1. Test Schedule

Test No.	Ventilation Gas Temperature ^{o}K	Ventilation Gas Composition					Type of Combustion
		$\%N_2$	$\%O_2$	$\%CO_2$	%CO	%He	
1	300	Air		0	0	0	Non-flaming 3.2 W/cm^2
2	300	Air		0	0	0	Non-flaming 6.2 W/cm^2
3	300	Air		0	0	0	Non-flaming 9.2 W/cm^2
4	300	80	10	10	0	0	Non-flaming 3.2 W/cm^2
5	300	80	10	10	0	0	Non-flaming 6.2 W/cm^2
6	300	80	10	10	0	0	Non-flaming 9.2 W/cm^2
7	300	80	5	10	5	0	Non-flaming 6.2 W/cm^2
8	300	Air		0	0	0	Flaming
9	300	80	10	10	0	0	Flaming
10	300	80	5	10	5	0	Flaming
11	300	80	15	2.5	2.5	0	Flaming
12	300	0	15	0	0	85	Flaming

Furthermore, these measurements help determine those variables that have the greatest influence on the characteristics of smoke particulates generated during the combustion of different materials.

The three materials selected for the test program were chosen due to their widespread use in construction and furnishing products, and because of their commercial availability. The results of experiments where such materials are tested can then be interpreted in terms of the actual danger, or relative lack of it, to occupants of buildings during most fires. Wood is the most widely used of the three polymeric materials under consideration, and Douglas fir is extensively used for construction purposes. Wood is composed of three basic polymeric materials: cellulose (50 percent), hemicellulose (25 percent), and lignin (25 percent)[37]. Cellulose and hemicellulose are polymers of glucose, while lignin is an extremely complex polymer which is predominantly aromatic in nature.[38]

Polyvinyl chloride produced by the polymerization of vinyl chloride, is used extensively in automobiles, household items, house siding, flooring, piping and textile coatings.[39] The PVC samples tested here are a standard-impact, rigid plastic manufactured by General Tire. The basic polymer unit for PVC is given by:

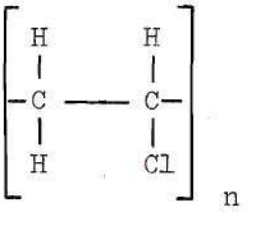

In addition to the pure polymer, PVC usually contains plasticizers for maintaining the desired flexibility (or rigidity), according to the application.[39]

Urethane foams cover a wide class of rigid and flexible cellular materials used in furniture and bedding (flexible), and thermal insulation (rigid).[39] Rigid foams are usually based on branched polyether polyols and either toluene diisocyanate , or a polymeric polyisocyanate.[40] The urethane tested in these studies is a flame retardant expanded rigid foam manufactured by the Dow Chemical Company (Thurane brand). It is a closed cell material prepared for use as thermal insulation and has an average density of 1.9 lb/ft^3. Although, the exact molecular formula is proprietary, it is known that the formulation includes a polymeric polyisocyanate, with functionality of 3 to $3\frac{1}{2}$, and a polyether polyol derived from a phenol formaldehyde resin and propylene oxide.

The gas compositions indicated in Table 1 reflect atmospheric extremes which might be found in actual fire situations. Oxygen concentrations in fires vary from well below 10 percent to near normal levels depending on the stage of fire development and the location within a burning enclosure.[41,42] Carbon monoxide and carbon dioxide concentrations are also found to vary significantly in fires. For example, CO levels have been measured near 3 percent [41,42] and CO_2 levels have peaked above 10 percent (by volume).[43] Clearly, then, there is no established set of atmospheric compositions to be found in building fires, especially given the highly dynamic

conditions involved. Nevertheless, considering the above mentioned data it is believed that the compositions used in this test program represent a reasonable set of conditions for simulation of "real" fire situations. The tests in atmospheres containing helium have been included to simulate fire environments found in hyperbaric chambers.

The types of combustion sustained by test materials, as indicated in Table 1, is also intended to simulate the burning conditions in actual fires. In that regard, smoke is usually considered to be generated under two different conditions: flaming and non-flaming combustion. For the case of non-flaming combustion, or smoldering, smoke particulates are generated by the thermal degradation of materials subjected to radiant heating levels of varying intensities. When the flammable volatiles released during smoldering are subsequently ignited, the smoke particulates are then generated by flaming combustion. In the smoke tests described here, smoke particles are studied for both types of combustion. Finally, full-scale fire tests have found radiative heating to vary significantly, with measured peak radiation levels ranging between 6 W/cm^2 [44] and 20 W/cm^2. [41] The effects of variations in radiant heating rates on smoke particulates generated during non-flaming combustion are also studied for selected appropriate radiative heating conditions.

In a typical smoldering test, a small sample (3 in. square, 1/8-3/8 in. thick, depending upon the material) of the material to be tested is mounted in the sample holder and positioned within the inner shell. After the specified ventilation gas has begun to flow

through the chamber, the variable flux radiant heater is adjusted to radiate the face of the sample at the pre-determined heating rate. When the radiant heater has reached a steady-state operation, a cover positioned over the sample is remotely withdrawn and the continuous sampling of the combustion products is initiated. In all flaming tests, the radiant heater is adjusted to radiate the face of the sample at a heating rate of 2.5 W/cm^2. When the heater has reached steady-state operation, a propane burner is remotely ignited and the continuous sampling of the combustion products is initiated. The sample cover is not utilized during the flaming tests. For a complete description of test methods and procedures, see Appendix B.

CHAPTER III

NON-FLAMING TESTS - RESULTS AND DISCUSSION

In the combustion and thermal degradation of wood and polymers, the generation of gaseous and particulate products falls into two distinct categories corresponding to non-flaming and flaming conditions.[10,22] Therefore for purposes of discussion, the presentation of results in Chapters III and IV are divided into the two categories: non-flaming tests and flaming tests. This chapter contains the results and related discussion of the non-flaming tests outlined in the Test Schedule in Chapter II. Non-flaming combustion, as defined here consists of the thermal degradation of a sample heated by radiation. The subsequent release of products may contain a complex mixture of solid and/or liquid particles which are not necessarily carbonaceous in nature.[10] Thus, smoke properties observed during non-flaming combustion have been found to be markedly different from the carbonaceous or sooty smoke particulates generated during flaming combustion. (10, 14, 22)

All three materials described in Chapter II were tested under each of the conditions outlined in Table 1. Wood samples tested were 1/4 inch thick, urethane samples 3/8 inch thick, and polyvinyl chloride samples 1/8 inch thick. The exposed face of all samples is 3 inches by 3 inches square, and all samples are mounted vertically in the inner shell. In this chapter, measurements of smoke particle size

distributions, smoke particulate mass concentrations and sample weight loss are presented for each of these materials during non-flaming combustion. For details of instrument operation, data reduction methods and data accuracy the reader is referred to Appendix C.

Douglas Fir

Douglas Fir Results

Results from tests of Douglas fir samples under non-flaming conditions are given in Figures 6 through 24. Figure 6 presents a comparison of particle sizes obtained for three heating rates in air, from Andersen Sampler data. The particle weight distributions shown, then, are integrated distributions taken over an entire test. It should be noted that the results for the 9.2 W/cm^2 case are for flaming combustion, as the majority of wood samples tested at 9.2 W/cm^2 (in air) experienced flaming ignition between one and two minutes into the test. Figures 7 and 8 give particle size distributions for particles below the range of the Andersen Sampler from Electrical Aerosol Analyzer measurements. Figure 7 shows a typical volume distribution for small particles during tests run at 3.2 W/cm^2 in air, while Figure 8 shows a significant change in particle size characteristics with time for a test run at the higher heating rate of 6.2 W/cm^2. Note that the volume distribution data taken from Electrical Aerosol Analyzer measurements can be directly compared with weight distribution data from the Andersen Sampler, assuming that the composition of the particles (and thus the density) is

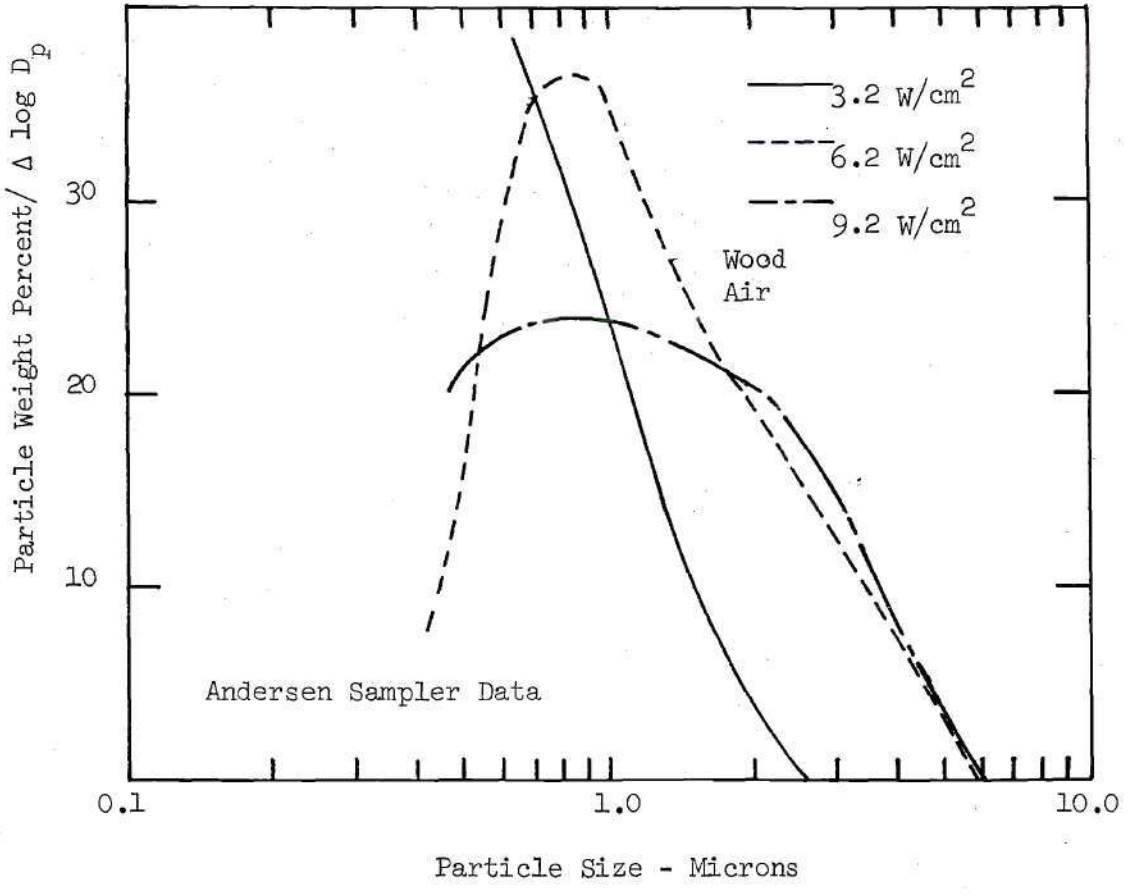

Figure 6. Particle Weight Distribution for Wood Smoke in Air

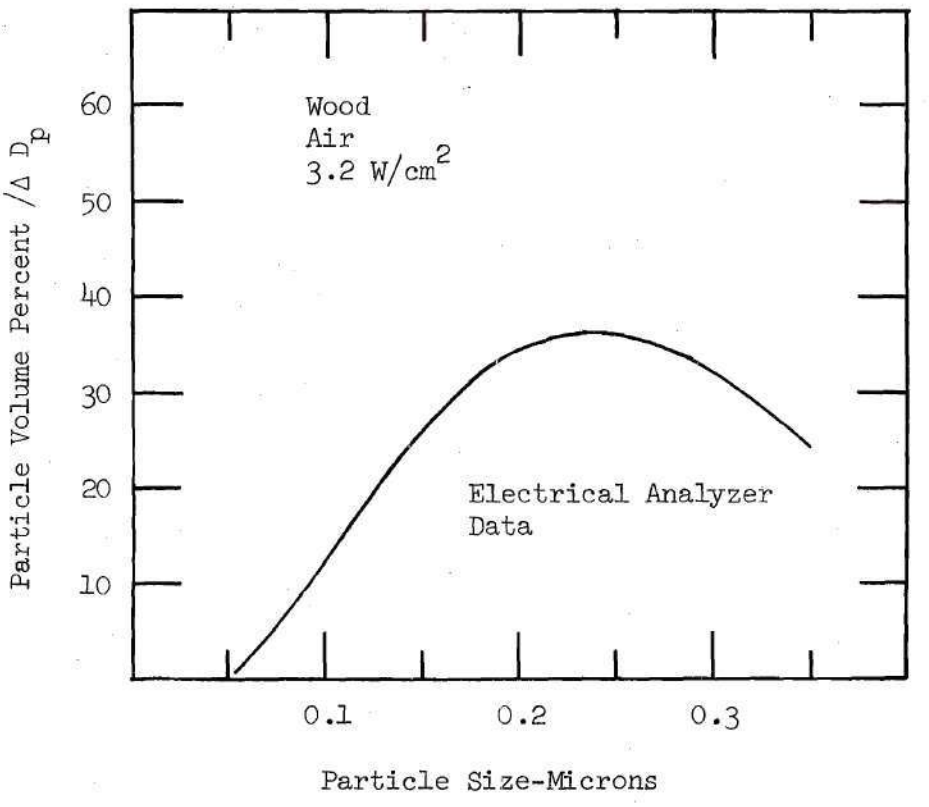

Figure 7. Average Particle Volume Distribution for Wood Smoke Particles Less than .36 Micron - At 3.2 W/cm^2 in Air

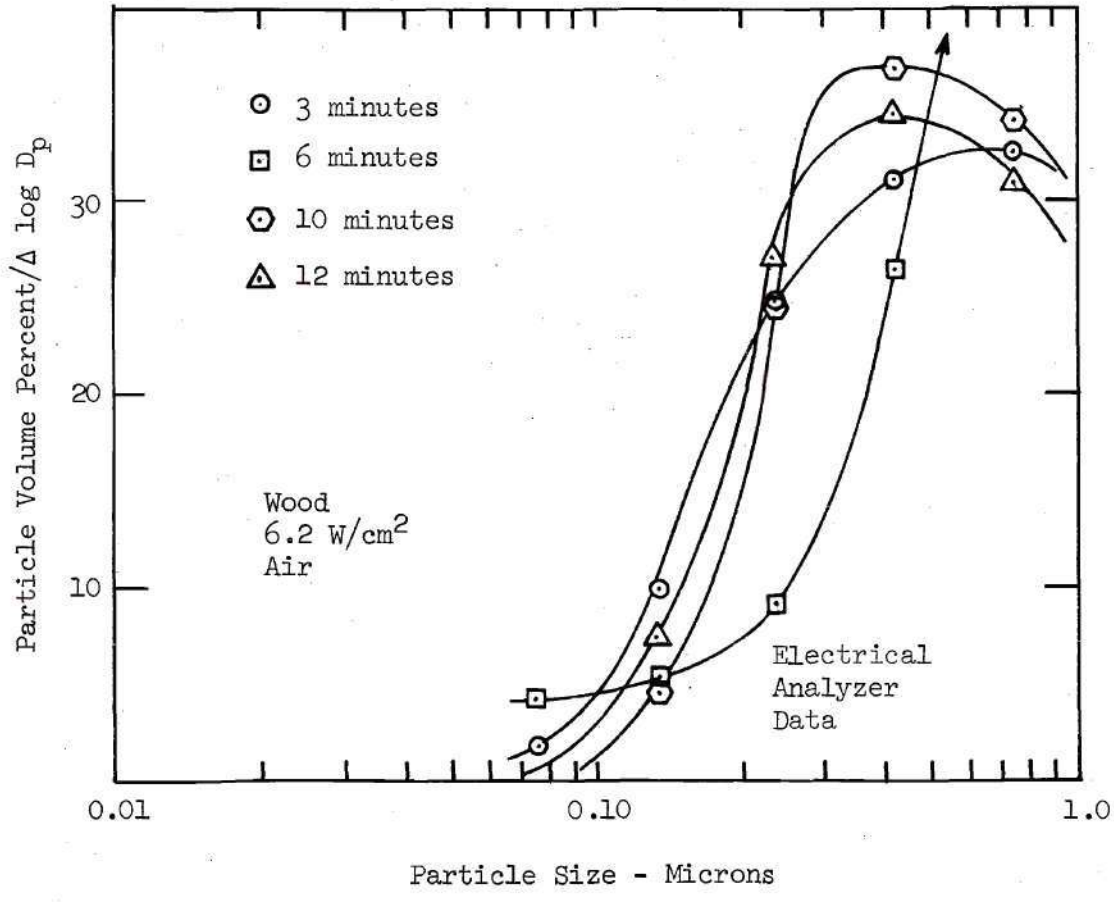

Figure 8. Time Resolved Particle Volume Distribution for Wood Smoke Particles Less than 1.0 Micron - At 6.2 W/cm^2 in Air

relatively homogeneous over the entire range of particle sizes. From visual observations of these particulates collected on the impaction plates of the Andersen Sampler, it was found that the particles do appear to be homogeneous in nature over all particle sizes.

These initial measurements indicate definite smoke particle size dependence on radiant heating rates for the samples of Douglas Fir in air. At the lowest heating rate (3.2 W/cm^2) particle sizes are generally in the range expected for wood pyrolysis; i.e., near 0.5 micron or less.[10] However, at the higher heating rate of 6.2 W/cm^2, a large fraction of the total particulate mass is shifted toward greater particle sizes, as indicated by Andersen Sampler data. An interesting aspect of the results is the variation in particle sizes at the heating rate of 6.2 W/cm^2, where particles appear to peak in size at, or near, 6 minutes into the test. As shown in Figure 13, this peak corresponds to a period of maximum smoke concentration. In the 9.2 W/cm^2 case a considerable amount of soot was formed during the flaming combustion.[22] The appearance of these fine black soot particles is in contrast to the brownish, translucent, tarry droplets predominant in wood smoke produced under non-flaming conditions.

Measurements of smoke particle size characteristics for Douglas Fir in different atmospheres are presented in Figures 9 through 12. Figure 9 gives a comparison of particle size characteristics at the two higher heating rates in an atmosphere containing only 10 percent oxygen. Notably, ignition did not occur at 9.2 W/cm^2 in this atmosphere,

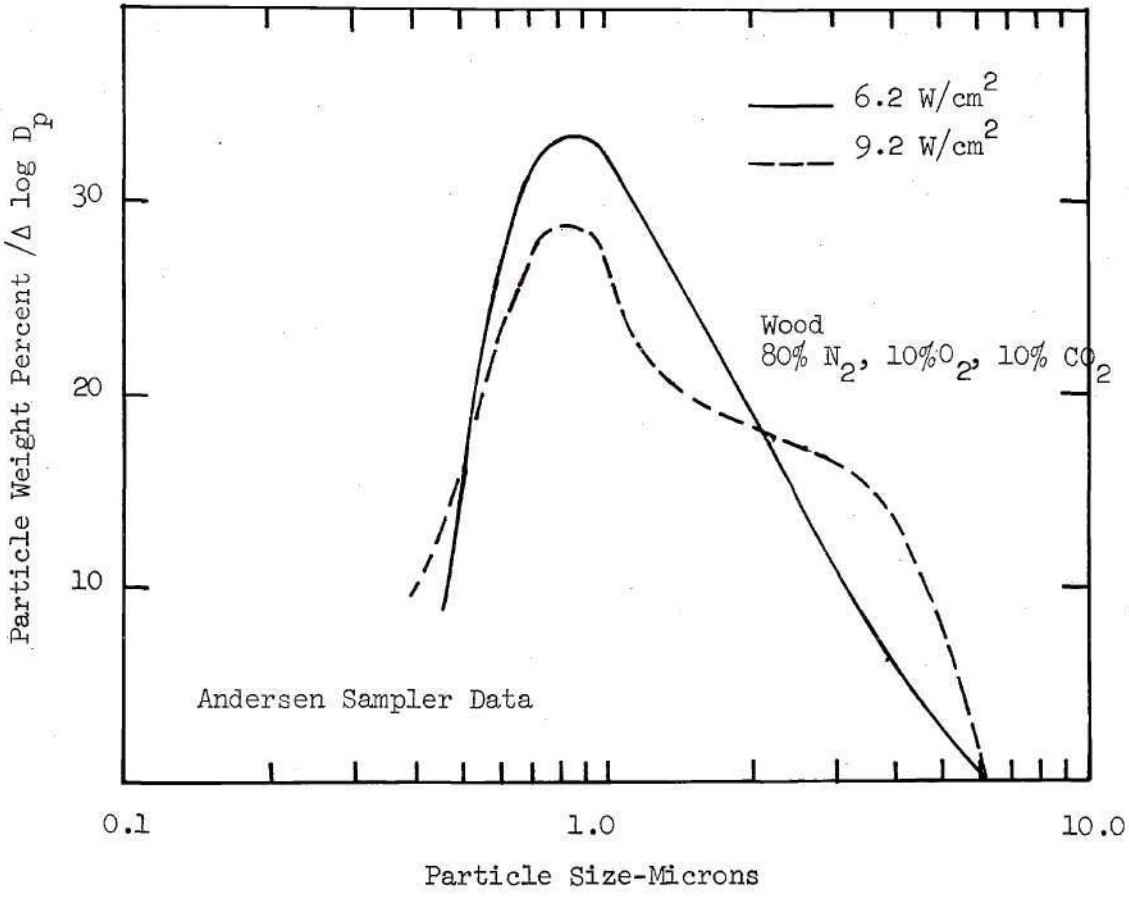

Figure 9. Particle Weight Distribution for Wood Smoke in 80% N_2, 10% O_2, 10% CO_2

as it did for the same heating rate in air. Figure 10 shows the average volume distribution of particles at the lowest heating rate (3.2 W/cm^2) in the same atmosphere of 10 percent oxygen. The time resolved particle volume distribution in Figure 11 again indicates variations in particle sizes during tests run at 6.2 W/cm^2. Similar data was presented for non-flaming conditions in air. Finally, comparisons of particle size characteristics in three atmospheres can be taken from Figure 12.

Generally, the results obtained in oxygen depleted atmospheres show the same trends as indicated earlier for tests run in air. The data shows a general increase in particle sizes as heating rate increases; especially as the heating rate is increased from 3.2 W/cm^2 to 6.2 W/cm^2. Furthermore, while the Andersen Sampler gives size distributions for the total mass of particulates generated, it is again interesting to note the fluctuation in particle size distribution throughout a test at 6.2 W/cm^2. Comparison of Andersen Sampler data for the three atmospheres at 6.2 W/cm^2 provides further evidence that the non-flaming smoke particle size characteristics for wood are relatively insensitive to changes in atmospheric composition. Only minor differences in the respective curves for each atmosphere are indicated.

Particulate concentrations and sample weight loss data are presented in Figures 13 through 17. Figures 13 and 15 demonstrate the fact that the measured maximum particulate mass concentrations were substantially greater at the higher heating rates in both air and an oxygen depleted ventilation gas mixture. Furthermore,

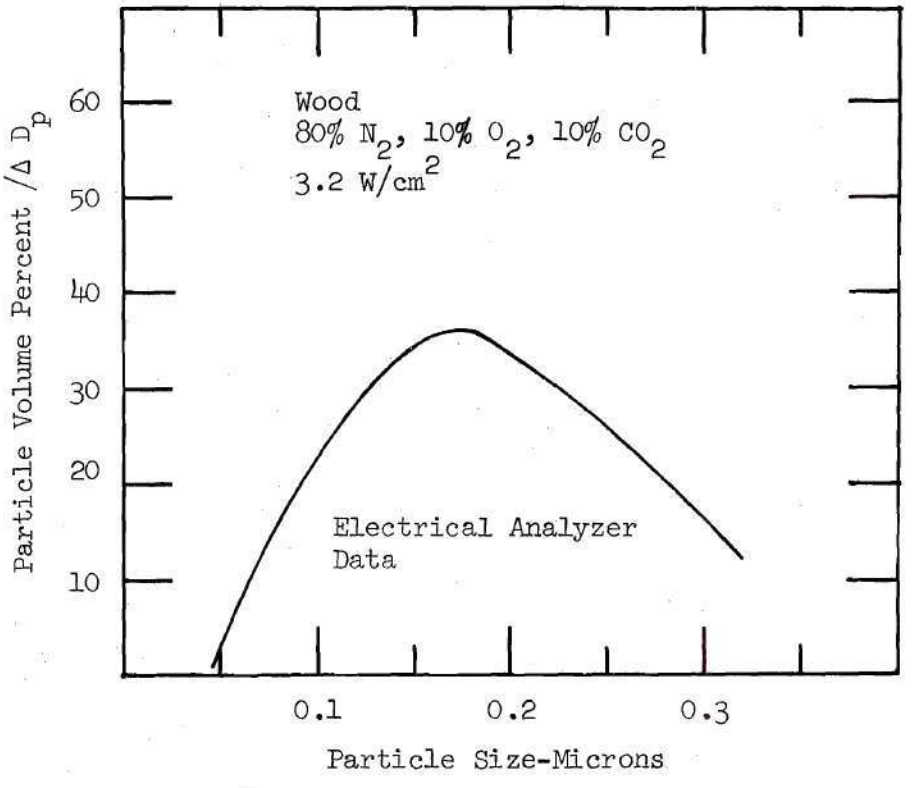

Figure 10. Average Particle Volume Distribution for Wood Smoke Particles Less than 0.36 Micron - At 3.2 W/cm^2 in 80% N_2, 10% O_2, 10% CO_2

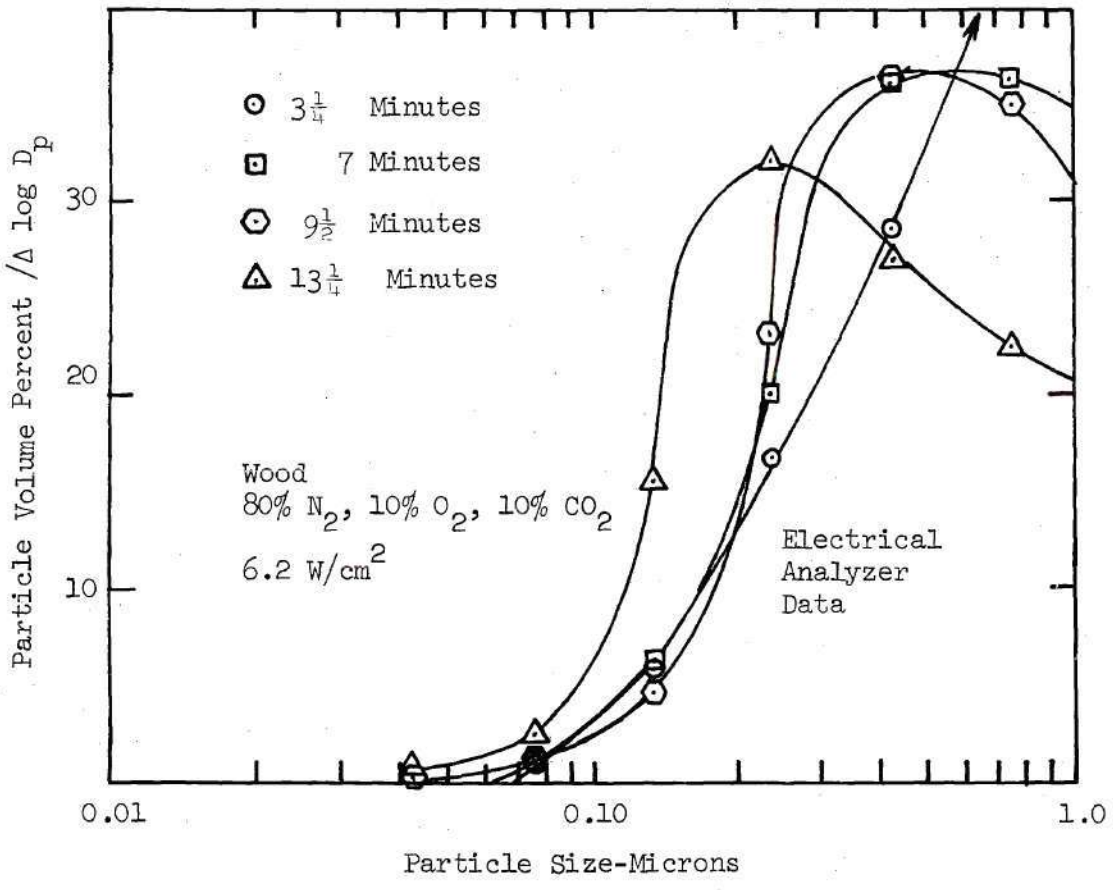

Figure 11. Time Resolved Particle Volume Distribution for Wood Smoke Particles Less than 1.0 Micron - At 6.2 W/cm^2 in 80% N_2, 10% O_2, 10% CO_2

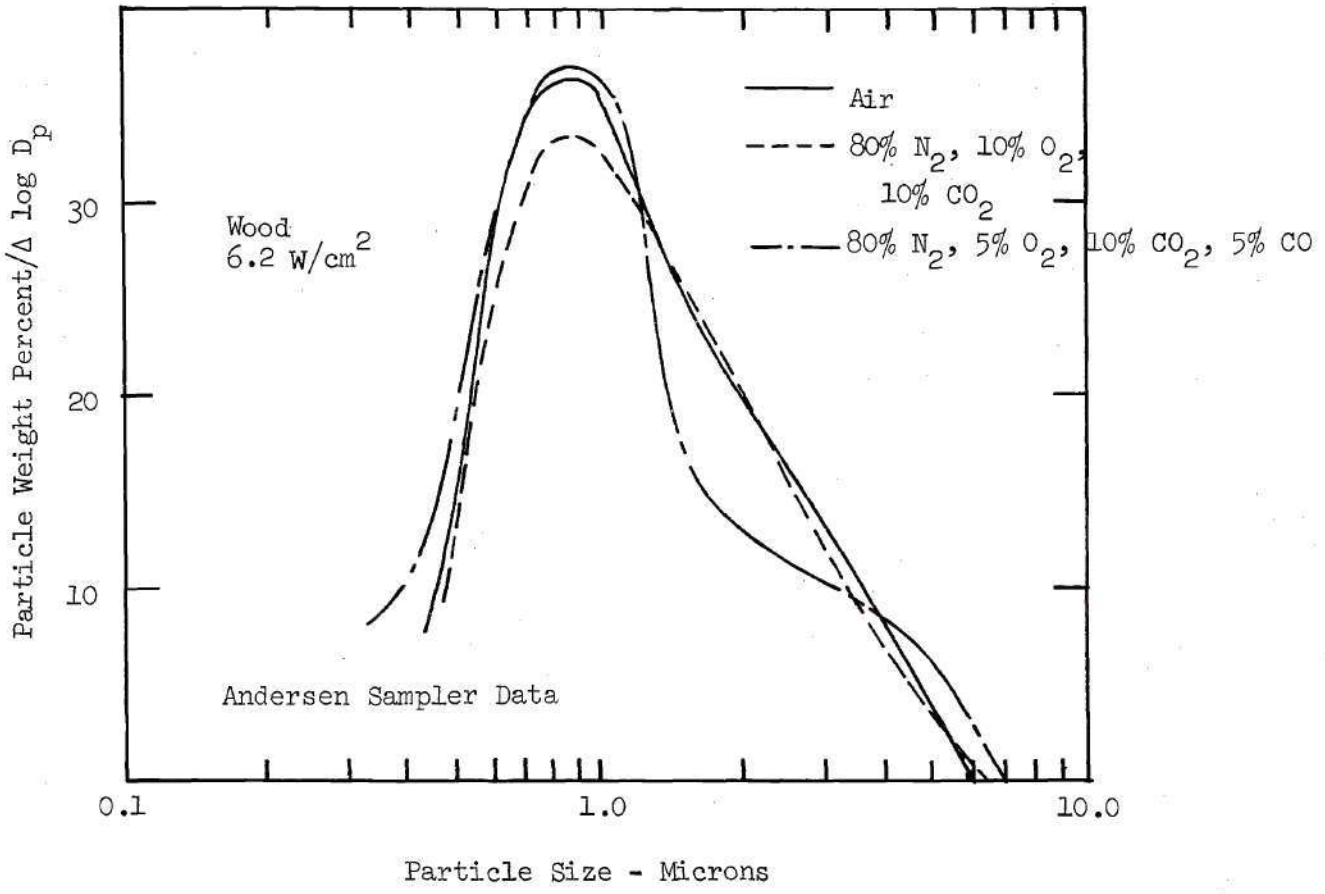

Figure 12. Comparison of Wood Smoke Particle Size Characteristics in Three Atmospheres

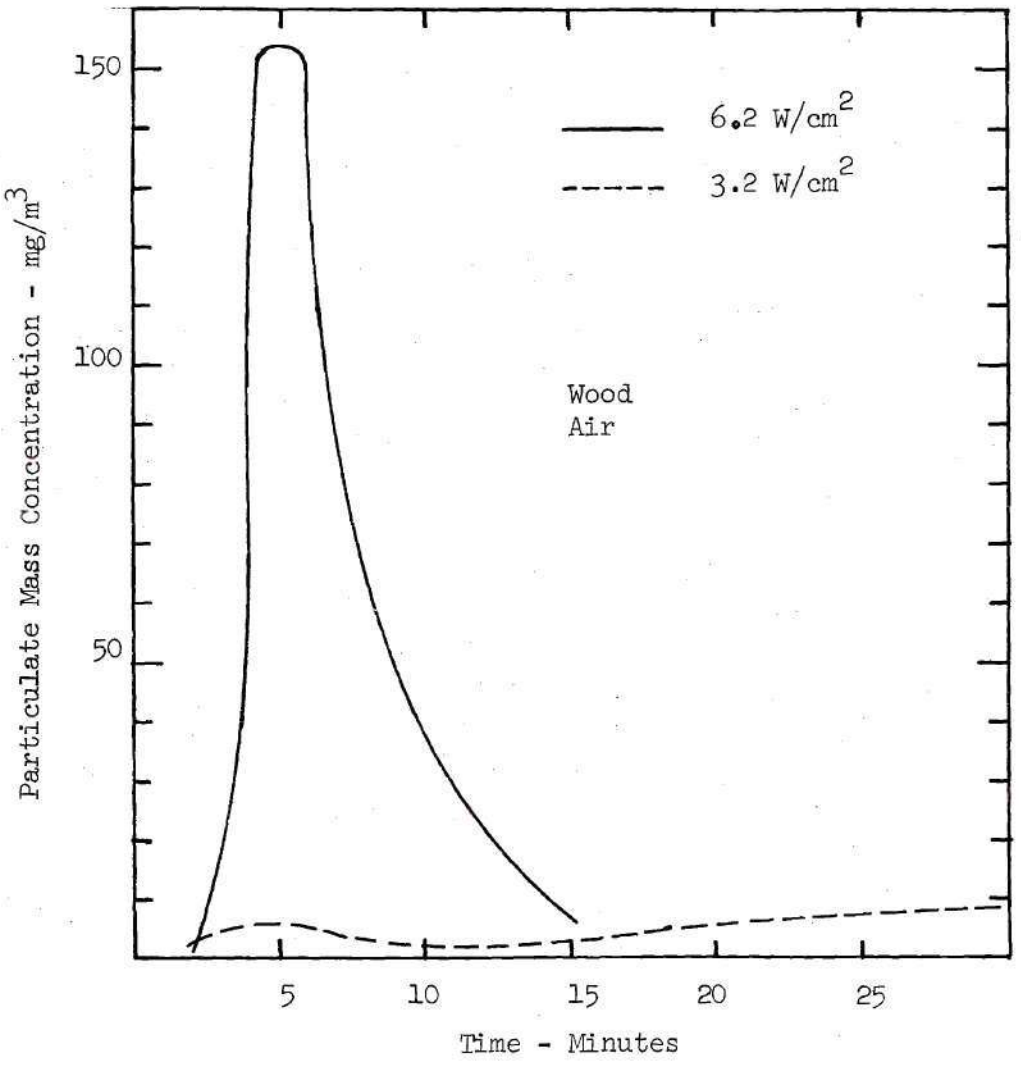

Figure 13. Comparison of Wood Smoke Concentration at Different Heating Rates - In Air

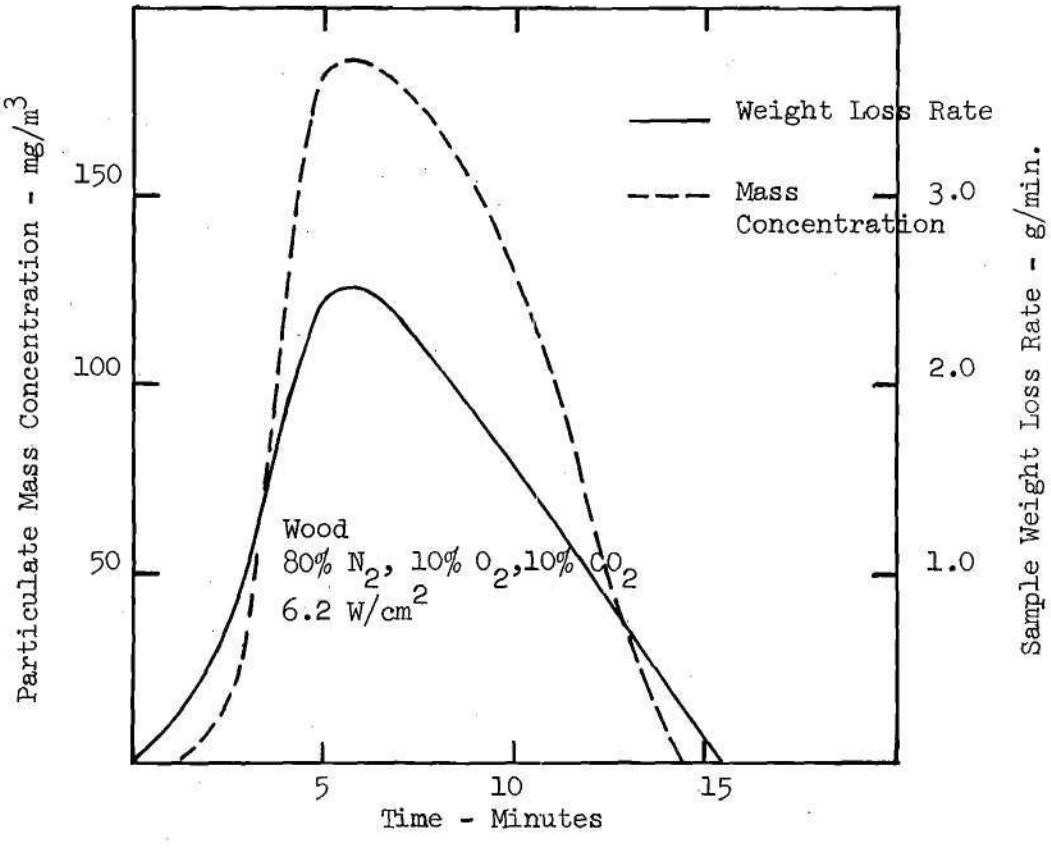

Figure 16. Comparison of Sample Weight Loss Rate with Particulate Concentration for Wood - At 6.2 W/cm^2 in 80% N_2, 10% O_2, 10% CO_2

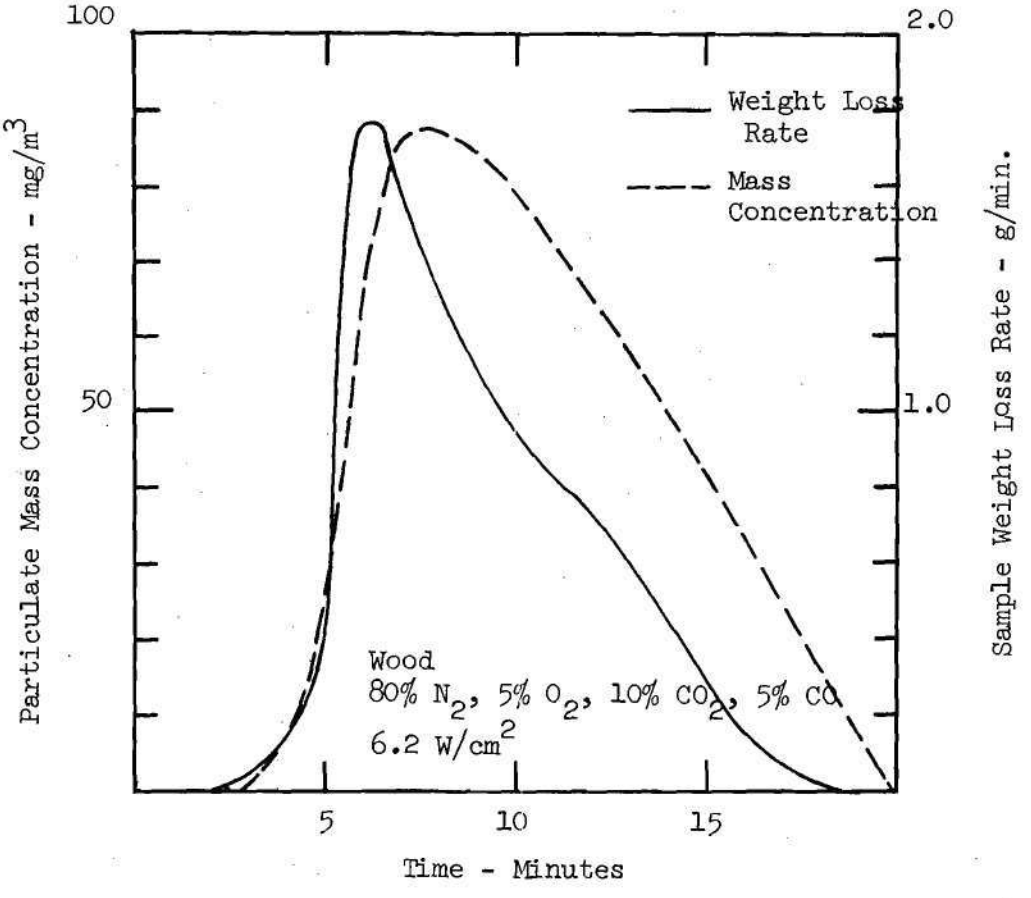

Figure 17. Comparison of Sample Weight Loss Rate with Particulate Concentration for Wood - At 6.2 W/cm^2 in 80% N_2, 5% O_2, 10% CO_2, 5% CO

correlations between sample weight loss rate and particulate mass concentration are evident in Figures 14, 16 and 17. They show that particulate concentrations are closely related to the rate at which the smoldering sample is losing mass during a test. The above-mentioned data also shows little difference in particulate concentration and sample weight loss characteristics due to changes in atmospheric compositions.

CPTC Ventilation Rate Effects. Since the nucleation, growth and agglomeration processes which take place during the formation of smoke particulates can be affected by the surrounding chemical and thermal environment[45], it follows that the ventilation rate used during smoke tests might influence particle sizes measured at the Sampling Section. For this reason, non-flaming tests of wood irradiated at 6.2 W/cm^2 were run at two CPTC ventilation rates in addition to the standard 15 CFM rate indicated in Table 4. The results of these tests are presented in Figures 18, 19 and 20. Figure 18 compares Andersen Sampler data for the three ventilation rates. It shows little difference in particle size characteristics between vent rates of 10 CFM and 15 CFM, but does show somewhat larger particle sizes at the ventilation rate of 20 CFM. Figures 19 and 20 seem to support this finding, since the larger particle sizes are dominant over a greater (in time) fraction of the test run at 20 CFM, than at tests run at 10 CFM and 15 CFM.

Sample Thickness Effects. Although wood sample thicknesses of 1/4 inch have been widely used in this study and others (such as the

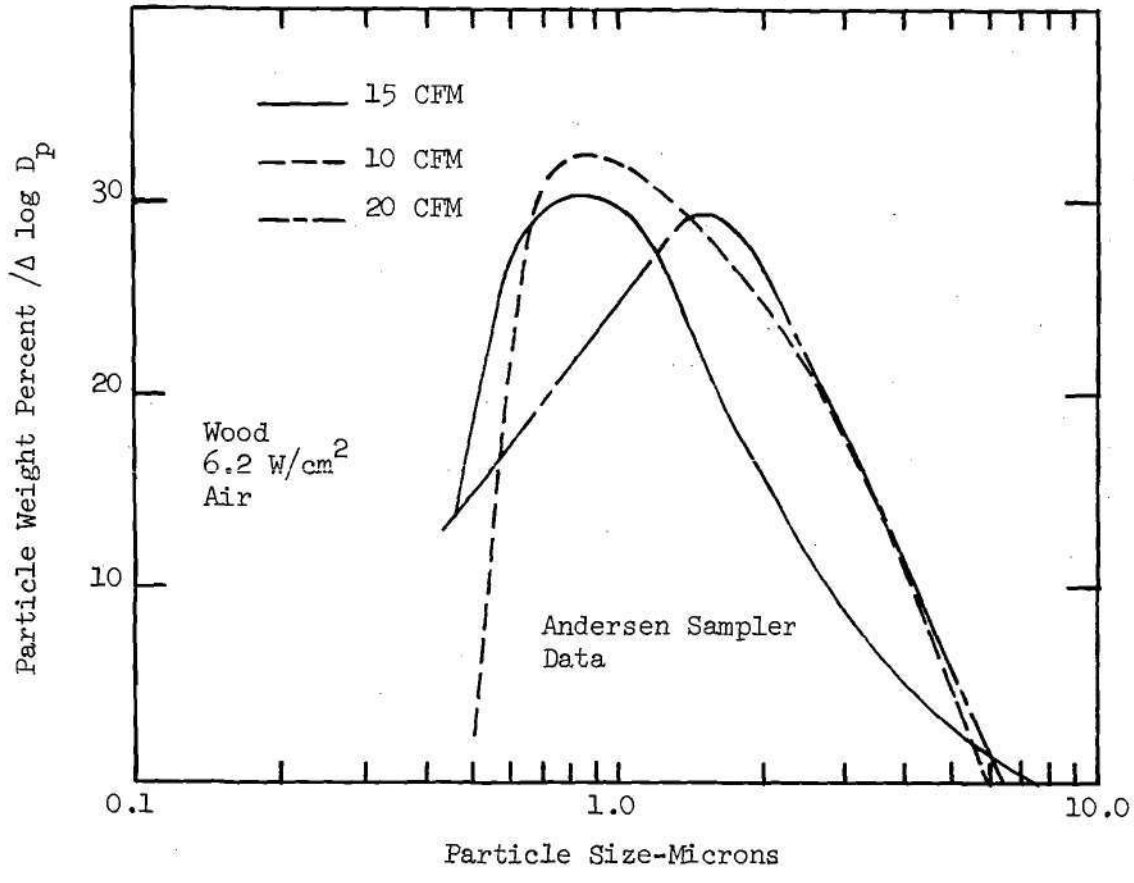

Figure 18. Comparison of Wood Smoke Particle Size Characteristics at Three CPTC Ventilation Rates - At 6.2 W/cm^2 in Air

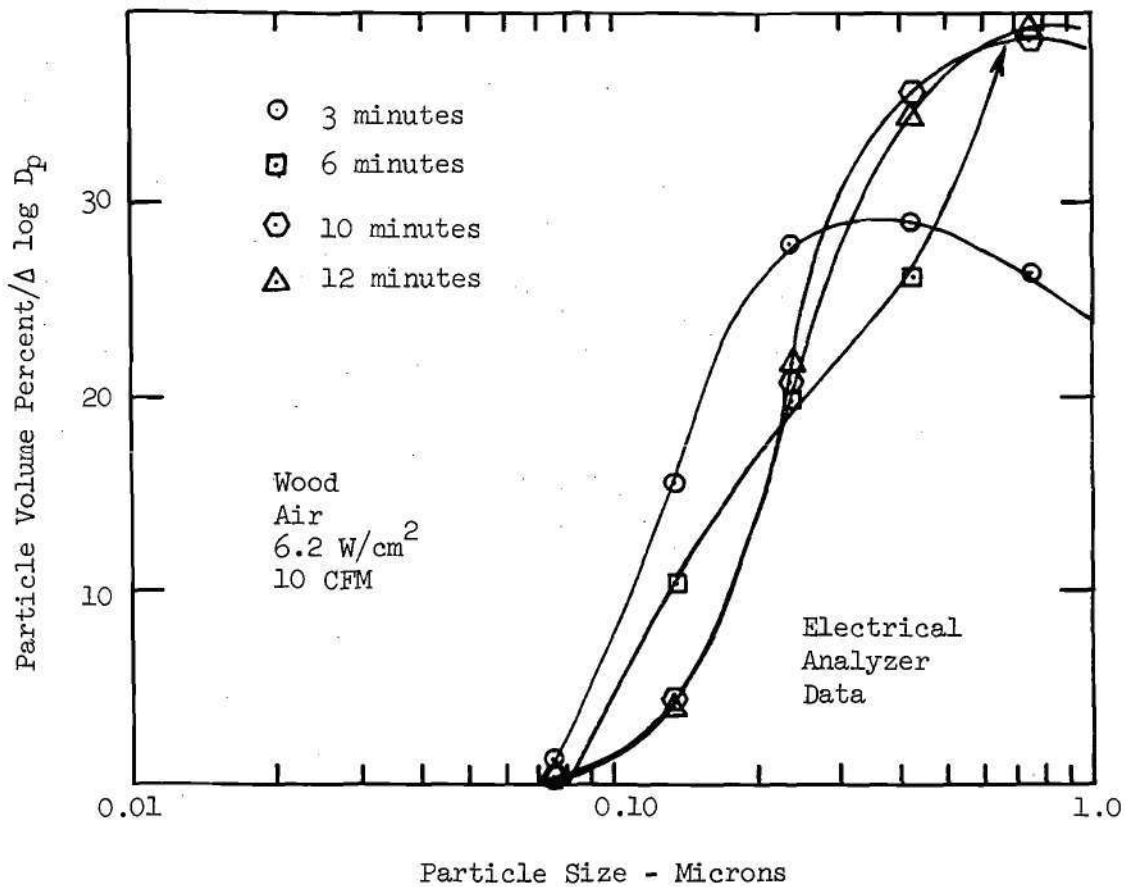

Figure 19. Time Resolved Particle Volume Distribution for Wood Smoke Particles When CPTC Vent Rate is Decreased - At 6.2 W/cm^2 in Air

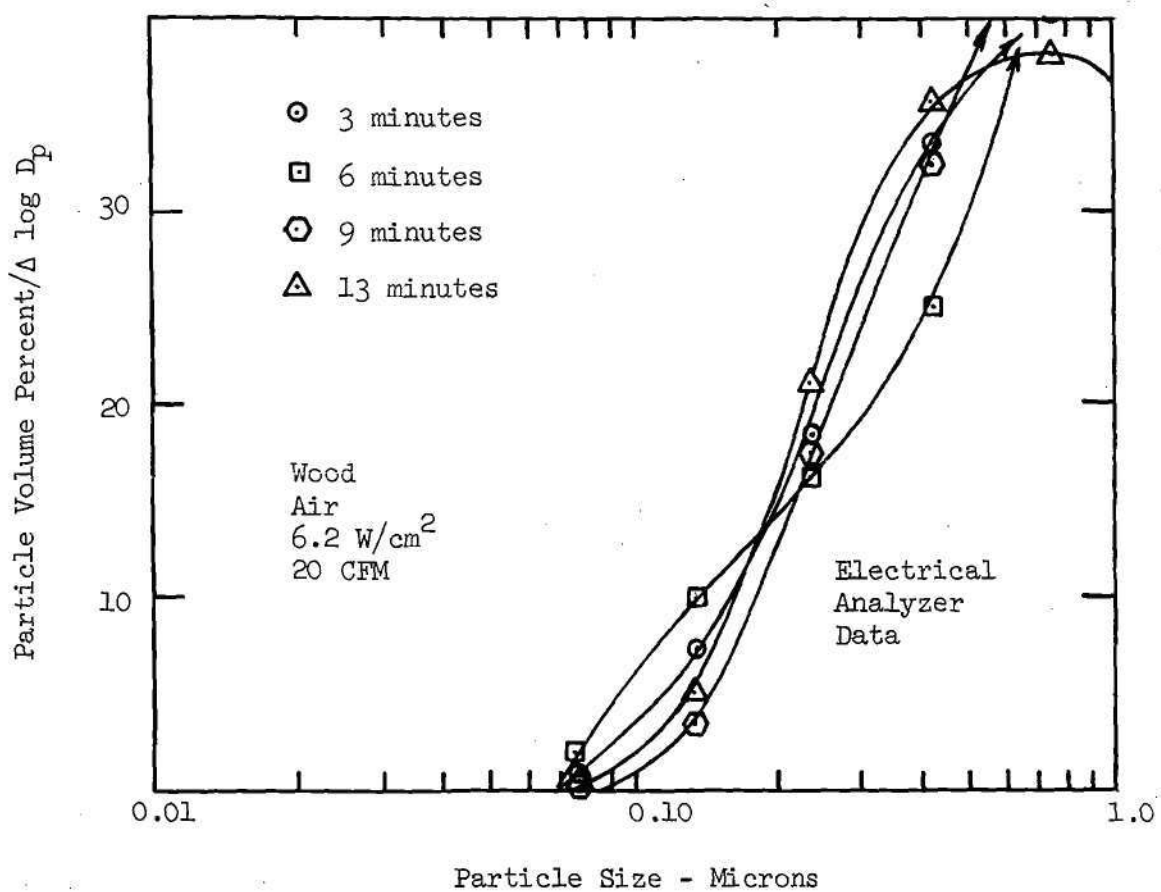

Figure 20. Time Resolved Particle Volume Distribution for Wood Smoke Particles When CPTC Vent Rate is Increased - At 6.2 W/cm^2 in Air

NBS smoke tests[10,11], many other sample thicknesses are of great importance from a practical standpoint. Furthermore, it is important conceptually to know what effect changes in sample thickness might have on the particulate characteristics measured here. In recognition of these facts, a limited study of 1/2 inch thick wood samples was carried out during this program. The results are presented in Figures 21, 22 and 23. Figure 21 shows only a slight difference in the integrated particulate weight distribution between sample thicknesses of 1/4 inch and 1/2 inch, which have been irradiated at 6.2 W/cm^2 in air. Furthermore, the fluctuation of particle size characteristics indicated in Figure 22 is similar in trend to results obtained for 1/4 inch samples. The only substantial difference in the smoke-producing characteristics of 1/4 inch and 1/2 inch thick wood samples is shown in Figure 23. This data shows the 1/2 inch thick sample producing high mass concentrations of particulate for a longer time period. In fact, relatively high concentrations of smoke were still observed when the test of the 1/2 inch thick sample was terminated.

Comparison with Optical Measurements. Simultaneous in situ optical measurements at the Sampling Section level have been made during these smoke tests for purposes of comparison with the Aerosol Sampling System data. Particle size data is determined from continuous measurements of scattered blue light at forward angles of 5° and 15°. The ratio of forward-lobe scattered intensities for those two angles then yields the volume-surface mean diameter, D_{32}:

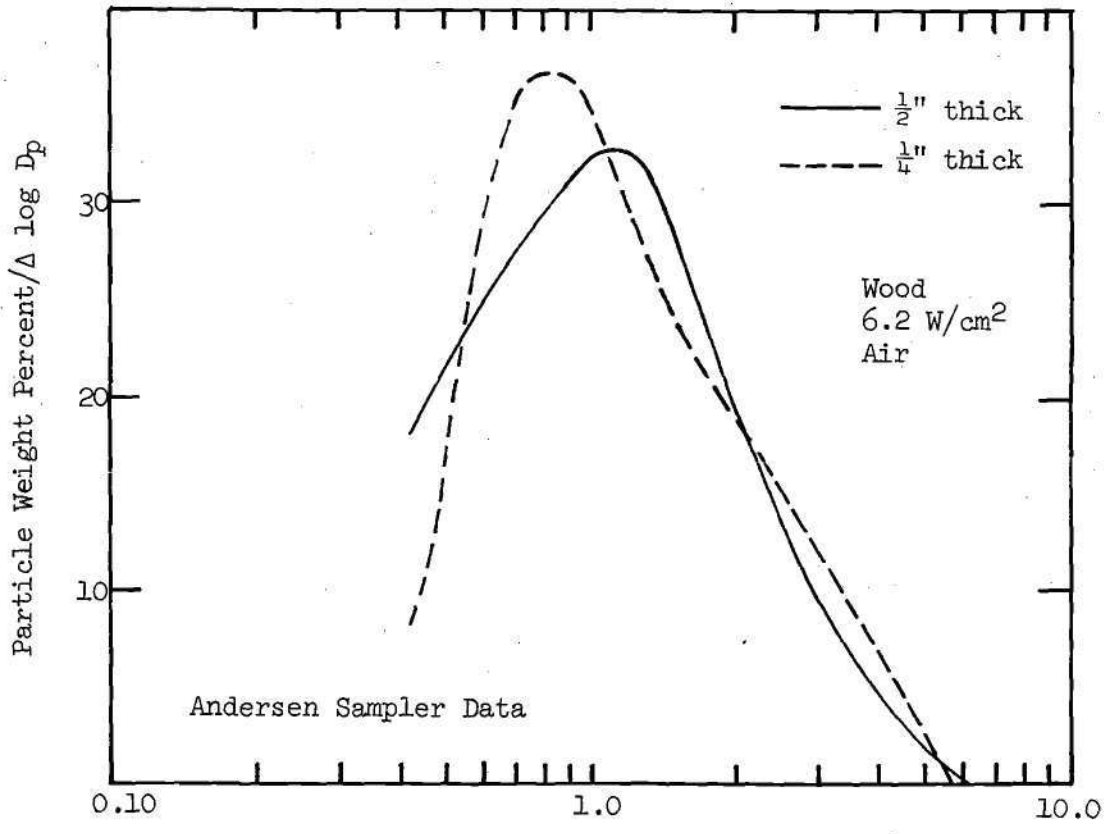

Figure 21. Comparison of Wood Smoke Particle Size Characteristics for Samples of Different Thickness - At 6.2 W/cm^2 in Air

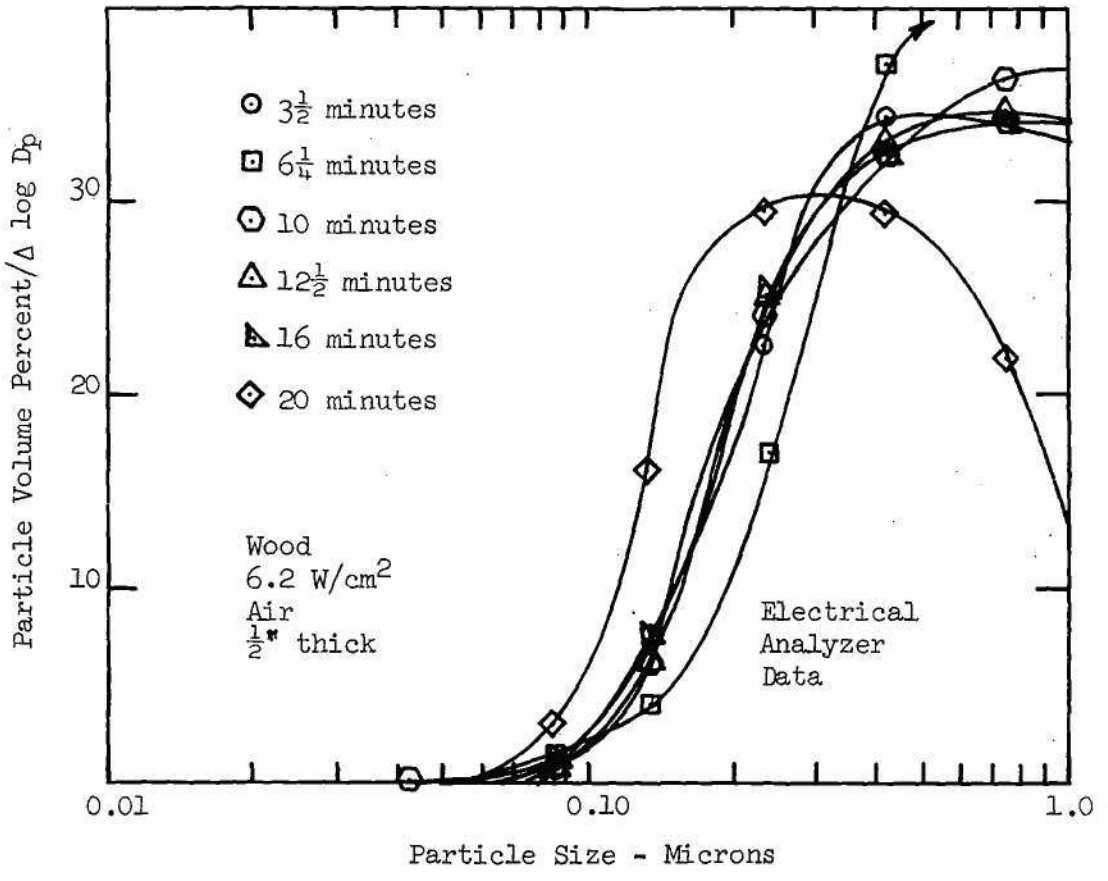

Figure 22. Time Resolved Particle Volume Distribution for Wood Smoke Particles When Sample Thickness is Increased - At 6.2 W/cm^2 in Air

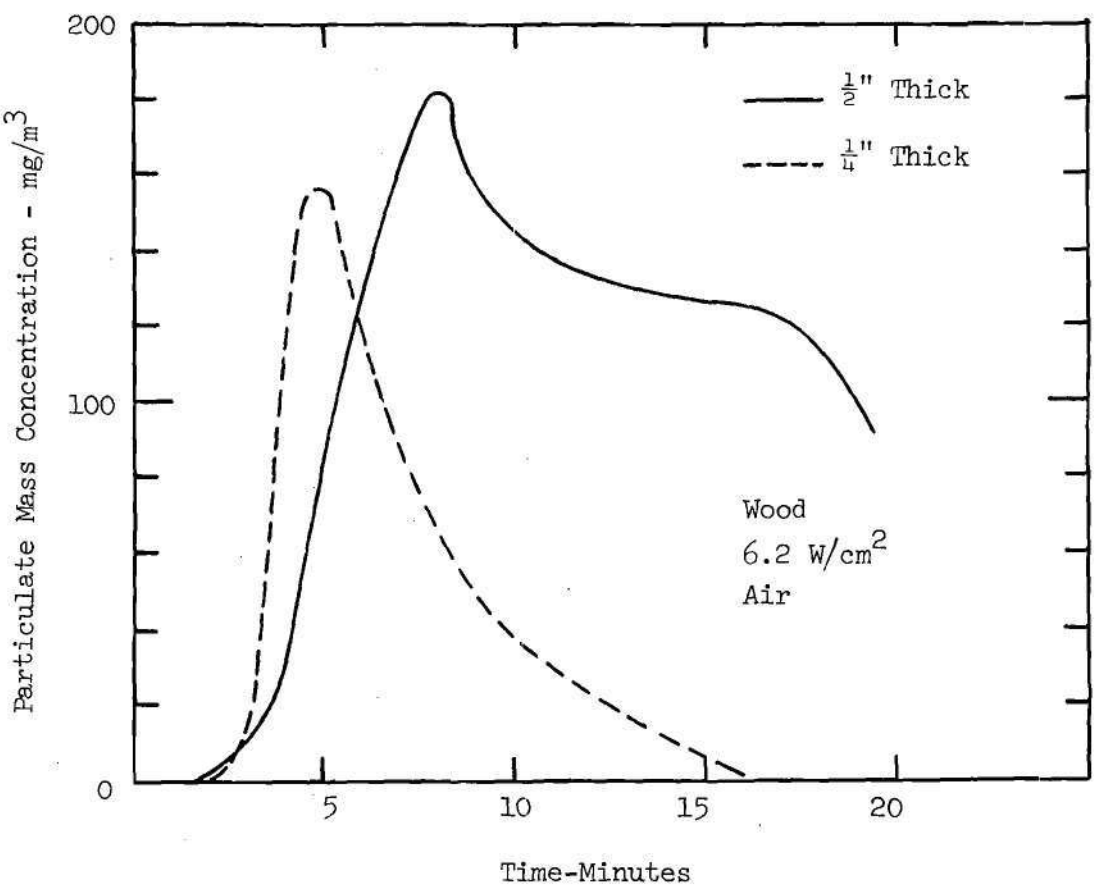

Figure 23. Comparison of Wood Smoke Concentration for Different Sample Thicknesses - At 6.2 W/cm^2 in Air

$$D_{32} = \frac{\int_0^{D_\infty} N(D)\ D^3\ dD}{\int_0^{D_\infty} N(D)\ D^2\ dD}$$

When D_{32} is determined by the ratio of scattered light at two forward angles, the results have been found to be nearly independent of the shape of the size distribution function and relatively insensitive to particle refractive index and concentration. The average particle size, D_{32}, is then determined as a function of time during the smoke tests. Complete details of the optical measurement system can be found in Reference 46.

Figure 24 presents an example of optical particle size data for wood irradiated at 6.2 W/cm^2 in air. The particle size fluctuations shown in Figure 24 compare favorably with the time-resolved size distributions presented in Figure 8. In addition, the volume-surface mean, D_{32}, has been calculated from the Andersen Sampler data, and plotted on Figure 24 for purposes of comparison. Clearly the data from the Aerosol Sampling System compares favorably with measurements made by the in situ optical methods for this case.

Discussion of Douglas Fir Results

The results just presented will be interpreted from two important points of view. First, they should be discussed in terms of the complex mechanisms responsible for smoke generated by burning materials. In this manner, proposals for altering those processes to reduce hazards during fire situations, might eventually be formulated. Secondly, it is important to know the physiological and

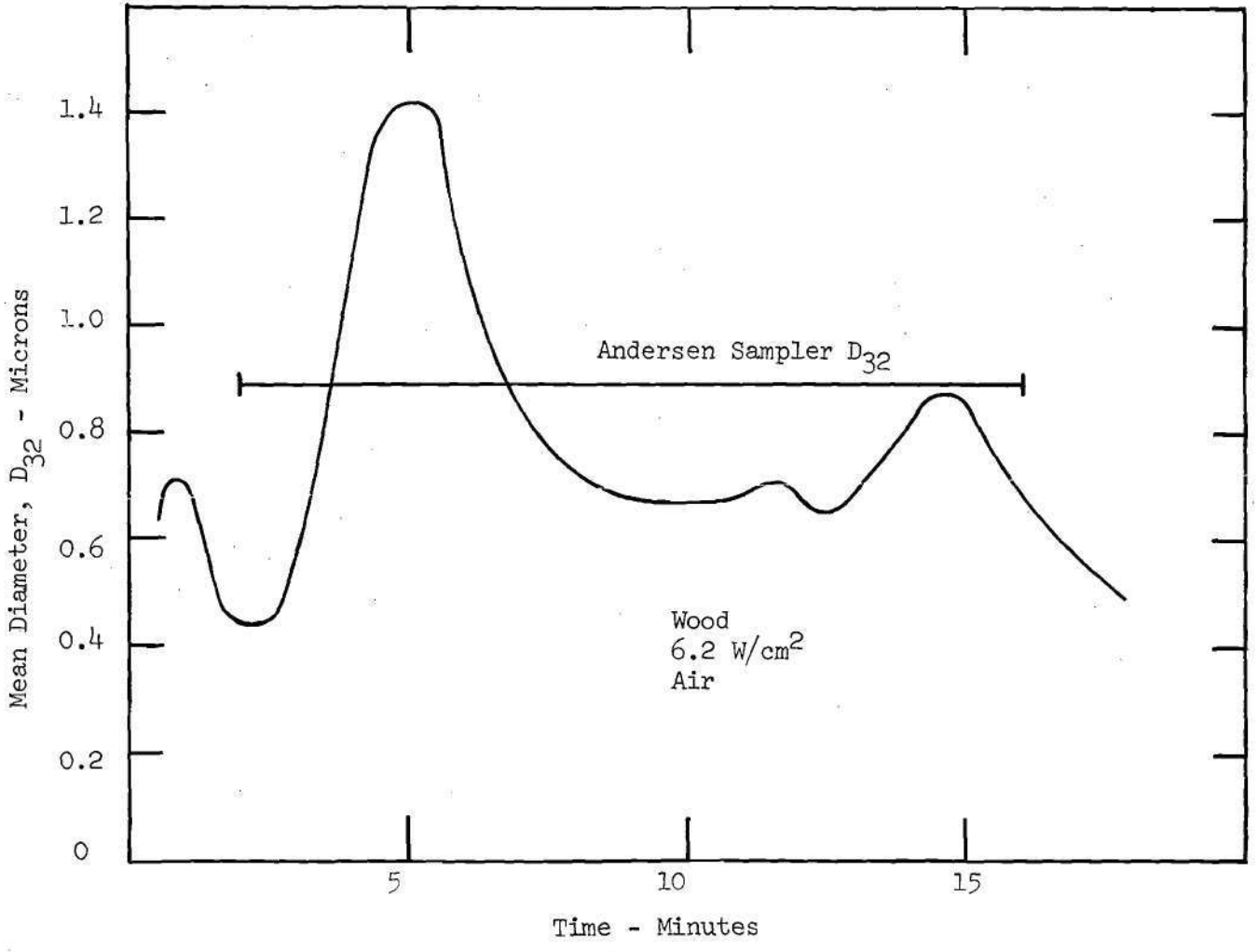

Figure 24. Time Resolved Average Particle Size, D_{32}, for Wood Smoke Particles - at 6.2 W/cm^2 in Air

toxicological consequences of smoke produced by materials in widespread use today. The results presented in this section for Douglas Fir provide new and important information which may be used in determining potential hazards to humans exposed to smoke particulates.

The formation of particulates generated in any combustion process is a complex sequence of nucleation, growth and agglomeration.(45) The problem is further complicated here by the fact that wood is composed of three different constituents which break down separately into many reaction products during the thermal degradation process. In fact, each component decomposes one after another as the temperature of the sample increases.(47) Hemicellulose breaks down usually between 200°C and 260°C, and would be expected to produce few condensable tars and liquids as compared to cellulose and lignin.(47) Cellulose evolves water initially and pyrolytic chain scission of the cellulose macromolecules takes place between 240°C and 350°C. The points at which random breaks in the macromolecules occur, and the manner in which these breaks are initiated will determine the subsequent reactions and corresponding reaction products.(47) High boiling point tars from the pyrolysis of cellulose have been attributed in part to aromatization and aromatic condensation of reaction products to form higher molecular weight resinous substances.(47) Lignin may also account for the presence of tarry aromatic compounds in the pyrolysis of wood, due to its highly aromatic nature.(47)

The initial combined reaction products of hemicellulose, cellulose and lignin undergo polymerization and condensation reactions,

in addition to further pyrolytic reactions. Polymerization and condensation then account for the high-boiling tars, waxes and resinous substances found presumably in particulate form in the "smoke" produced during the thermal degradation of wood.[47] The complexity of these processes is emphasized by the fact that more than 200 compounds have been identified in the liquid products of destructive distillation of wood.[48] Furthermore, it is difficult to "approximate" wood by its most abundant constituent, cellulose, since the predominant liquid product of the decomposition of cellulose, levoglucosan, is found only in small quantities in the liquid products of wood pyrolysis. Inorganic impurities often found in wood tend to reduce or prevent the formation of levoglucosan.[47]

The actual formation of tarry particles or droplets as discussed above can thus be characterized by a complex series of pyrolytic reactions, polymerization, condensation and agglomeration to yield the particulates characterized by the measurements presented here. Moreover, it is not clear whether particles are formed within the sample (in the solid phase of the pyrolysis zone or in the char), or are condensed upon cooling as gaseous products leave the sample surface. Given the wide range of molecular weights and volatilities of the compounds present in the tarry smoke,[48] it seems possible that droplets are formed within the sample (near the pyrolysis zone) and when cooling takes place as the condensable products flow away. Figure 25 provides a graphic representation of the pyrolyzing wood sample with regions of possible particulate formation indicated.

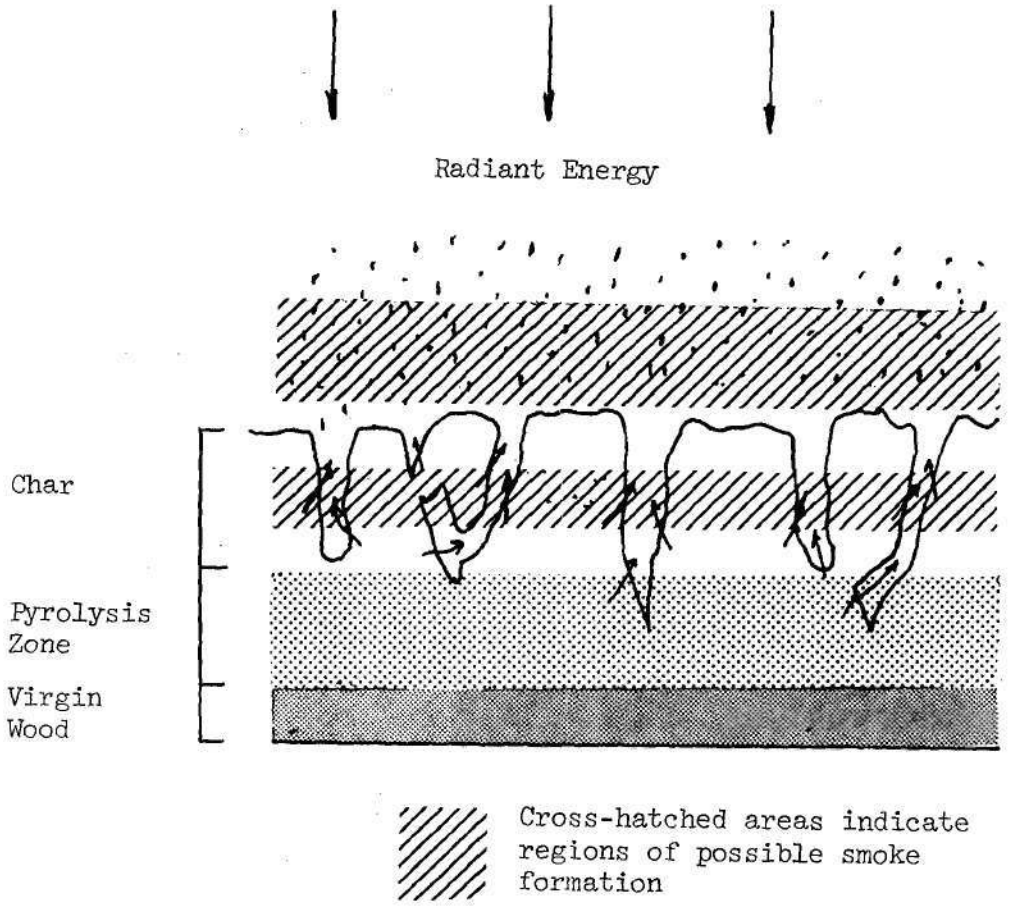

Figure 25. Cross Section of a Pyrolyzing Wood Sample

Particle size characteristics as presented earlier show variations in particle sizes with changes in radiant heating levels for non-flaming combustion. Generally, particle sizes are seen to increase with increase in heating rate. Also, the increase in particle sizes coincides with the higher particulate mass concentration levels measured at the higher heating rates. Accordingly, particle size differences may then be determined by the relative mass loss rate of samples, since the concentrations of condensable species for nucleation and subsequent growth and agglomeration are directly controlled by the rate at which the sample decomposes. Furthermore, at higher heating rates, macromolecules may be torn apart in large fragments and carried away before secondary decomposition can take place.(47) This could tend to augment nucleation and then particle growth by way of collisions with larger, more complex molecular species.

Particle size variations during a single test can also be explained in this manner, since the heat flux received at the pyrolysis zone moving through a sample continuously decreases as a test proceeds. As the pyrolysis wave moves into the sample, an insulating char grows in thickness, and thus acts to decrease the rate of decomposition and generation of reaction products. Additionally, in later portions of tests at higher heating rates, most of a sample has been reduced to char, leaving little virgin material for further decomposition. Therefore, with the concentration of condensable species thus decreasing, it is reasonable to expect measured particle sizes to be decreasing during later periods of the test. This is shown to be

the case in Figures 8 and 11.

Variations in CPTC ventilation gas compositions had no discernible effect on particle size characteristics during non-flaming combustion, as compared to tests run in air. Although variations in oxygen concentrations would be expected to affect oxidation reactions and possibly overall reaction kinetics, it is apparent that such effects are negligible in so far as the physical characteristics of particulate generation are concerned. Also, the particulate formation process may take place prior to significant mixing with oxygen.

Although a change in sample thickness produced only slight changes in particulate characteristics, those changes are consistant with previous conclusions drawn from data for 1/4 inch thick samples. For the 1/2 inch thick sample, the particulate mass concentration level remained at a high level throughout the test primarily due to the greater mass of material to be pyrolyzed. Consequently, particle sizes were larger throughout the test, as compared with the results from 1/4 inch thick samples. Also, the overall particle weight distribution from Andersen Sampler data is shifted toward larger particle sizes as would be expected from the time-resolved measurements.

Variation in CPTC ventilation rates shows only slight dependence on the relative cooling rates encountered by the aerosol as it is carried out of the chamber. The larger particles measured at the highest vent rate could be explained by more advanced particle growth due to more rapid cooling of the products at that vent rate. Otherwise, this effect does not significantly change particle size

characteristics. Furthermore, new data[49] is available that provides pertinent information on smoke particulates at concentrations and sizes approximating the concentrations and particle sizes measured at the Sampling Section. These data on the aging of smoke[49] indicate that there should be little change in the particle size distribution of the smoke aerosol due to agglomeration during the time it takes the smoke to travel from the sample face to the Sampling Section. Thus, it may be concluded that the ventilation gas rates utilized tend to quickly dilute and preserve aerosol properties from the time the particles leave the vicinity of the sample face. Consequently, the measured particle size characteristics are probably determined within the sample (pyrolysis zone or char layer), or at least at the surface of the sample face. In any event, the evidence indicates that little change takes place in particle size characteristics after the combustion products leave the domain of the sample.

As previously mentioned, the particulate mass concentrations generated during non-flaming tests of wood varied considerably with heating rate. This is consistant with a number of experimental and theoretical studies,[50,51,52] where the mass loss of wood samples has been described by Arrhenius rate equations. Thus, the higher sample temperatures expected at higher heating rates would then give rise to higher mass loss rates. Furthermore, the data shows that the particulate concentration is then closely related to the rate at which the smoldering sample is losing mass during the test. The greatest difference between maximum particulate mass concentrations

is evident between heating rates of 3.2 W/cm^2 and 6.2 W/cm^2. The fact that maximum particulate mass concentrations do not substantially increase between 6.2 W/cm^2 and 9.2 W/cm^2 may be due to more secondary pyrolytic breakdowns and oxidative reactions of tarry substances at the higher temperatures.

The results reported here provide important new information on the properties of wood smoke produced under non-flaming conditions, in terms of three practical considerations. First, the correct measurement of particle sizes is found to be important because the observed particle sizes are in a range where ingestion and retention in the human respiratory system may be high. For particle sizes near one micron, Davies shows that up to 75 percent of particulates may be retained in the respiratory tract and lungs of a human.[53] Thus, if these particles are toxic in nature, or when combined with the volatile combustion products are responsible for toxic synergistic effects; then their retention within the respiratory system becomes extremely important. Also, Stone[28] has shown that toxic gases may be absorbed on the surface of particles, and then carried into the respiratory system. Secondly, the fact that higher heating rates result in the much greater quantities of smoke is significant in relation to test methods developed for determining the smoking properties of materials. Frequently, the most widely accepted smoke test methods, e.g., the NBS Smoke Test Method[10], use relatively low radiant heat fluxes as compared to heating rates possible in actual fires. The results reported here suggest that for wood under

non-flaming conditions, smoke production varies considerably with heating conditions; and thus materials should be tested for their behavior under higher heat flux levels. The relative acceptability of materials would then be determined under more realistic conditions. Finally, this data may be used in a theory such as the one developed by Seader and Chien,[22] to help determine the ability of a burning material to obscure vision. In that study, the specific optical density can be predicted once particle size characteristics are known.

Urethane

Urethane Results

Results from tests of the rigid urethane foam under non-flaming conditions are given in Figures 26 through 36. The data is discussed in the same manner as previously presented for wood under non-flaming conditions. Figure 26 gives a comparison of particle sizes obtained for three heating rates in air, from Andersen Sampler data. In contrast to wood, spontaneous ignition did not occur during any tests of urethane at 9.2 W/cm^2. Figures 27 and 28 give particle size distributions below the range of the Andersen Sampler. Figure 27 shows a typical particle volume distribution from tests run at 3.2 W/cm^2. While particle sizes remained relatively stable during tests at 3.2 W/cm^2, the time resolved data shown in Figure 28 shows that particle sizes varied substantially during tests run at 6.2 W/cm^2.

The trends indicated in these results for urethane are similar to those shown for wood under non-flaming conditions. Definite smoke particle size dependence on radiant heating rates is again

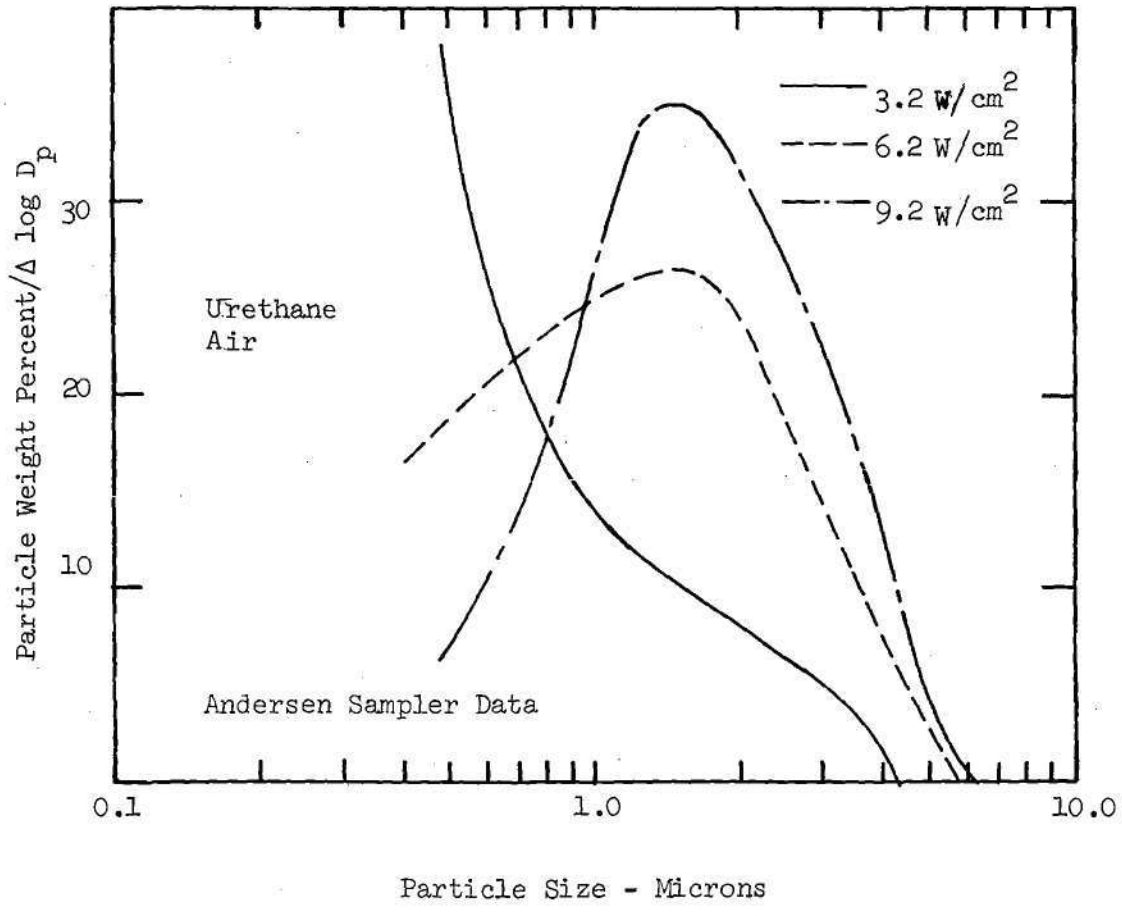

Figure 26. Particle Weight Distribution for Urethane Smoke in Air

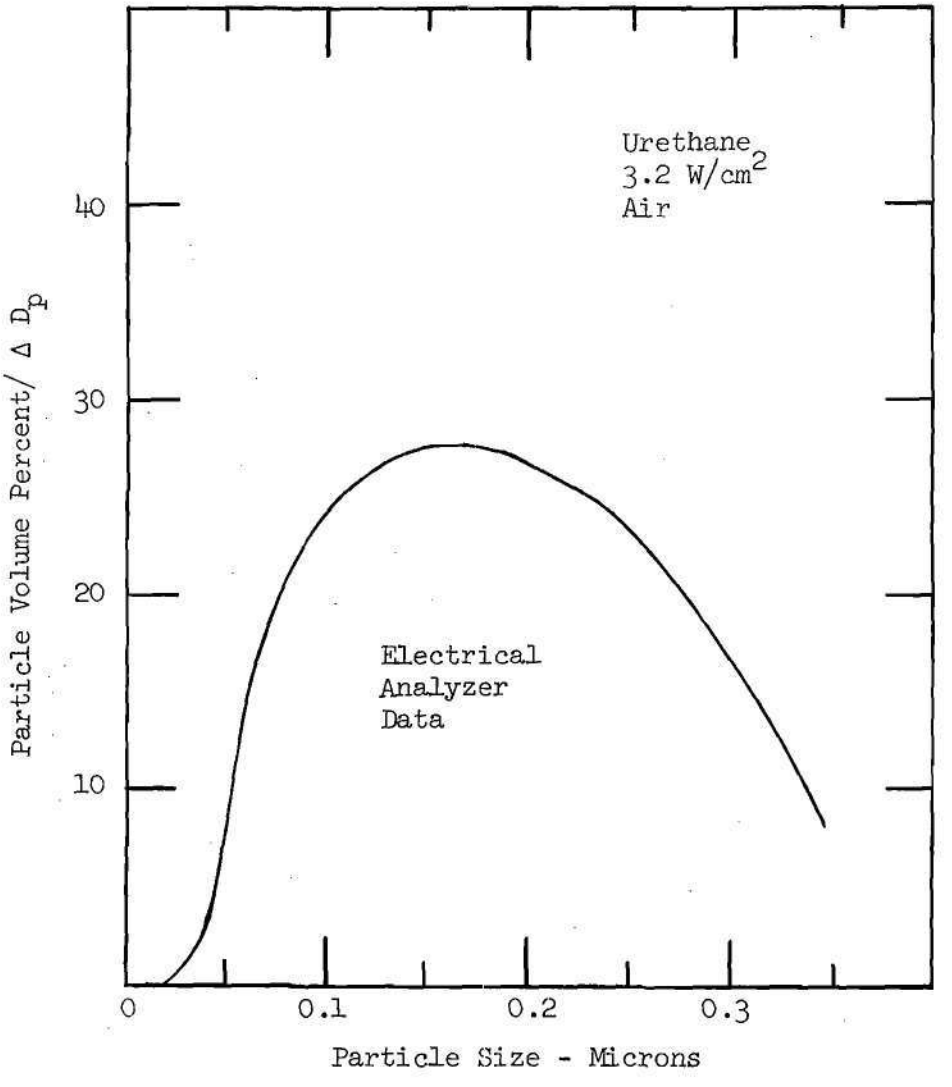

Figure 27. Average Particle Volume Distribution for Urethane Smoke Particles Less Than 0.36 Micron - At 3.2 W/cm^2 in Air

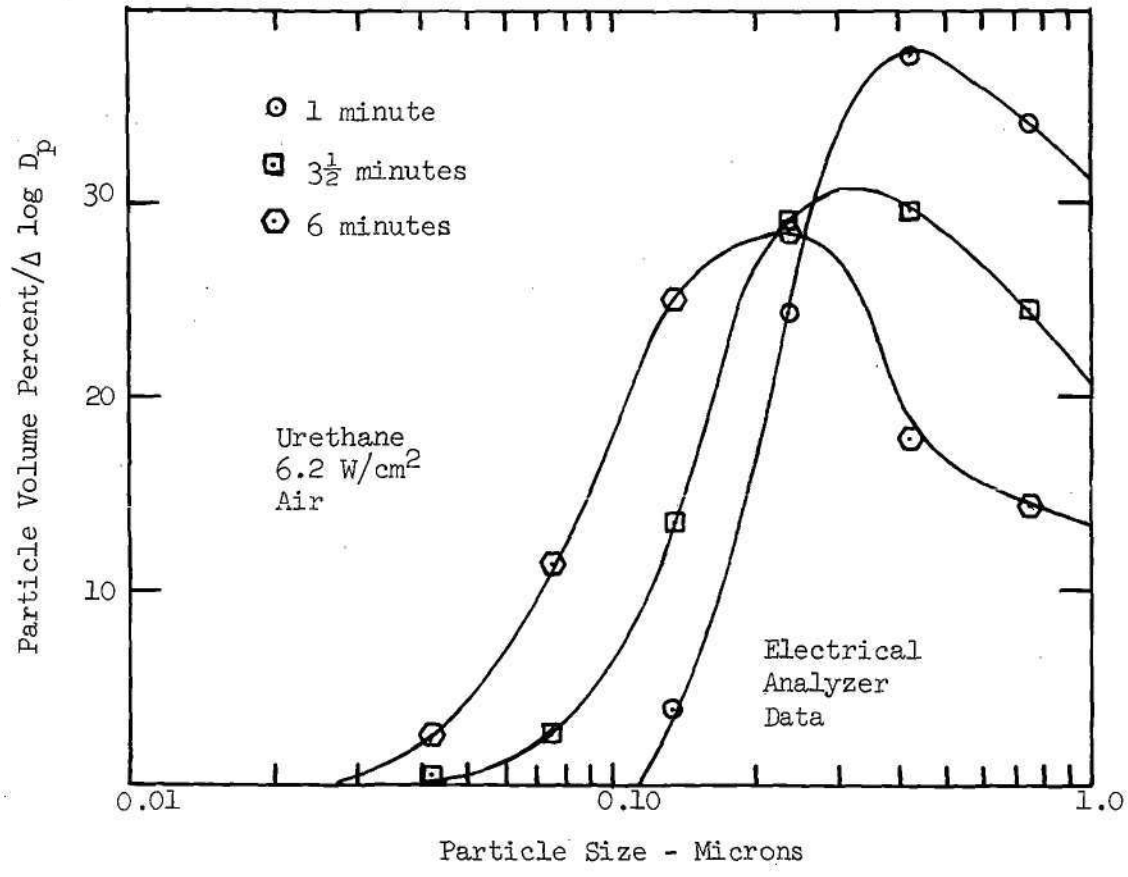

Figure 28. Time Resolved Particle Volume Distribution for Urethane Smoke Particles Less Than 1.0 Micron - At 6.2 W/cm^2 in Air

indicated, where there is substantial difference in particle size characteristics between tests run at 3.2 W/cm^2 and those run at 6.2 W/cm^2 and 9.2 W/cm^2. The particle sizes measured at 3.2 W/cm^2 seem to be nearly the same as those measured under the same conditions for wood, while particle sizes at 6.2 W/cm^2 and 9.2 W/cm^2 are somewhat larger than those found for non-flaming wood smoke; i.e., slightly greater than one (1) micron. Again, the time resolved data at 6.2 W/cm^2 show interesting particle size variations as the test proceeds, with maximum particle sizes corresponding to periods of maximum smoke concentrations. The smoke particles collected on the stages of the Andersen Sampler were found to consist of the yellow-orange, solid residue frequently found in studies of pyrolyzing urethane foams,[26,27] in addition to a tarry liquid fraction.

Figures 29 through 32 show the results of non-flaming urethane tests run in atmospheres different from air. Figures 29 and 30 compare particle sizes measured at the three heating rates in 80 percent N_2, 10 percent O_2, 10 percent CO_2, while Figure 31 shows particle sizes changing in time in an atmosphere containing only 5 percent oxygen. Particle sizes from the three atmospheres at 6.2 W/cm^2 are then compared in Figure 32. Notably, the results of tests with several atmospheres show qualitatively similar trends for all atmospheric compositions tested. The data shows the familiar particle size dependence on heating rate for all of the gas compositions. In addition, changes in particle size distribution with time during tests at the higher heating rates is observed in each case. Quantitative comparison of

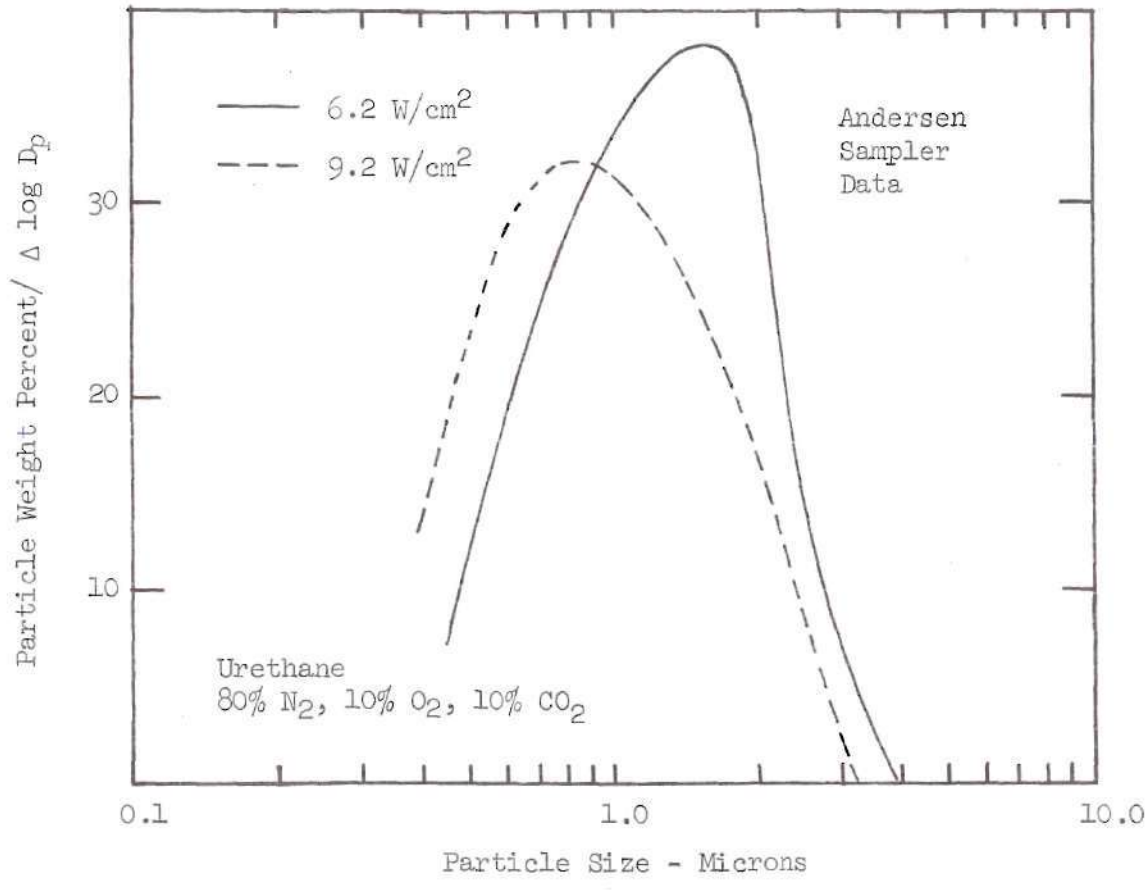

Figure 29. Particle Weight Distribution for Urethane Smoke in 80% N_2, 10% O_2, 10% CO_2

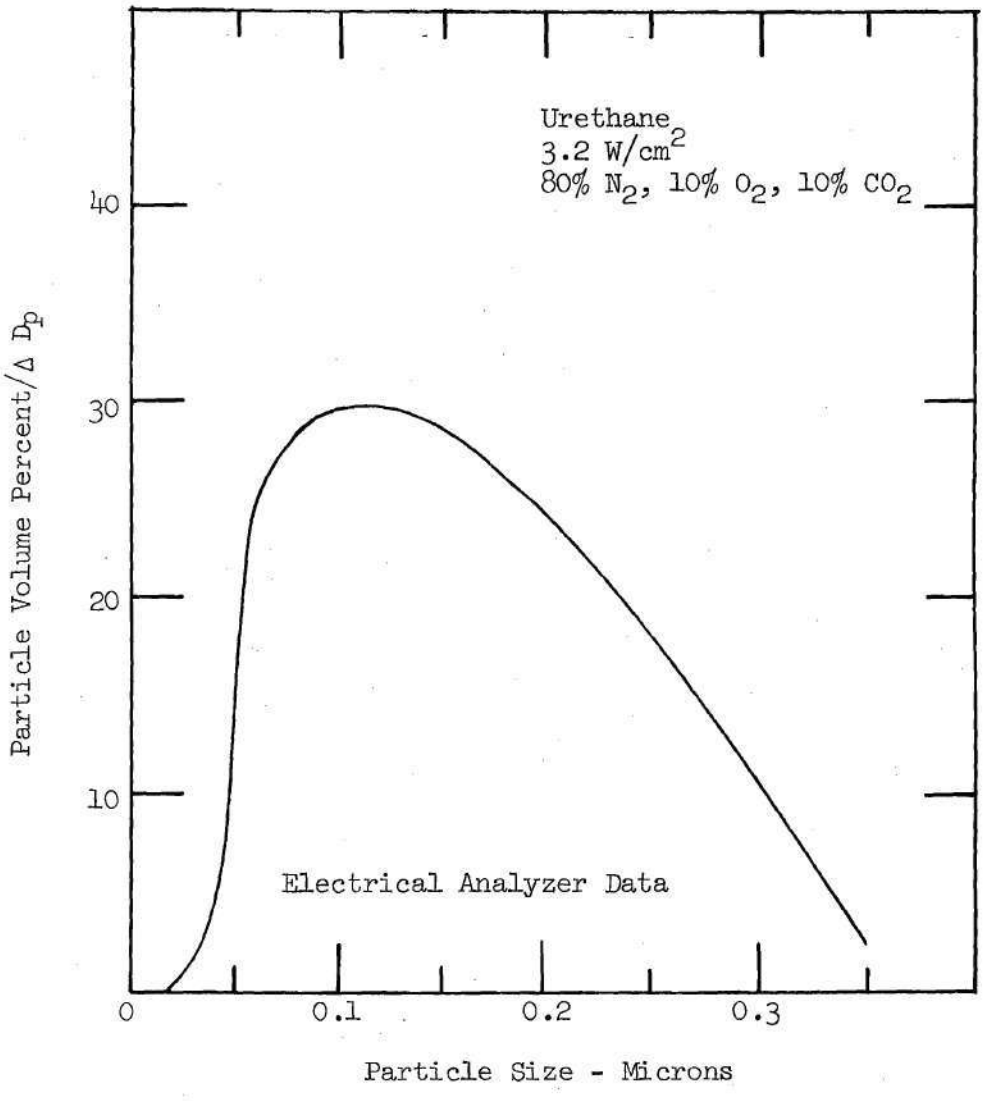

Figure 30. Average Particle Volume Distribution for Urethane Smoke Particles Less Than 0.36 Micron - At 3.2 W/cm^2 in 80% N_2, 10% O_2, 10% CO_2

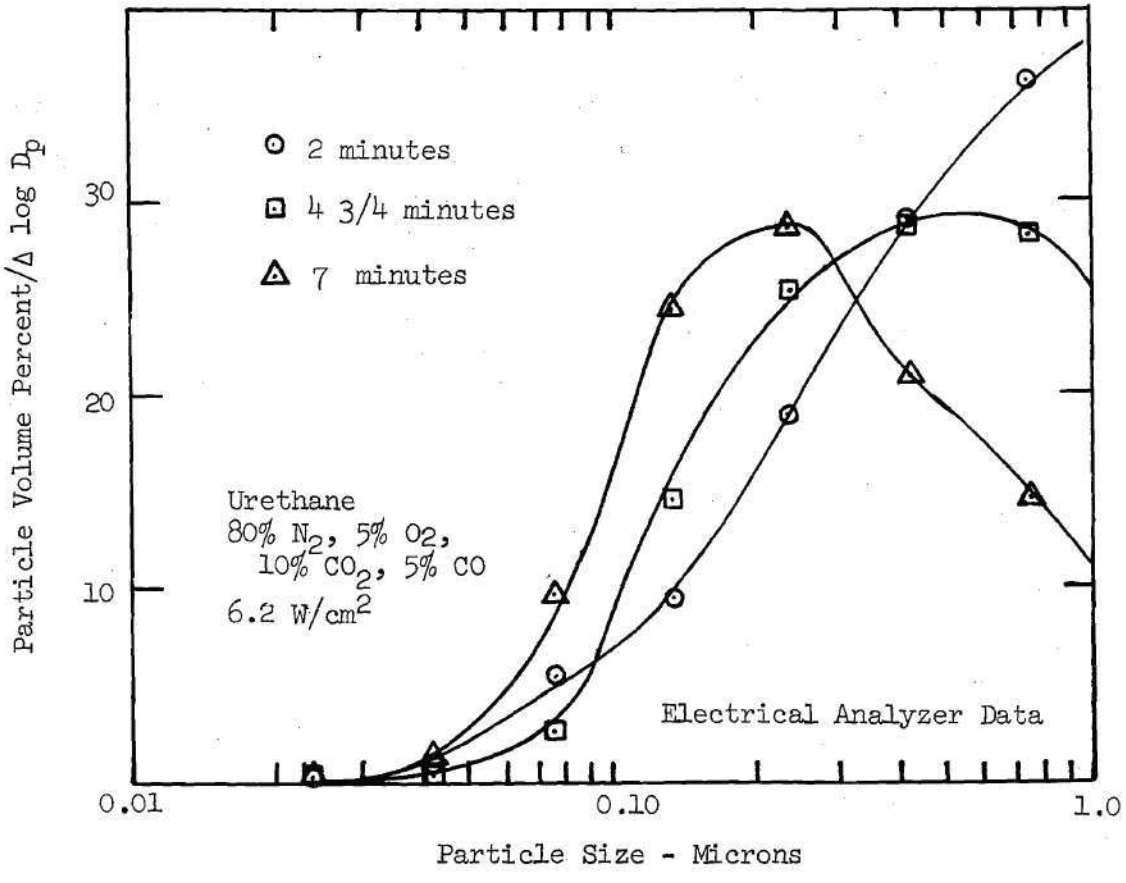

Figure 31. Time Resolved Particle Volume Distribution for Urethane Smoke Particles Less Than 1.0 Micron - At 6.2 W/cm^2 in 80% N_2, 5% O_2, 10% CO_2, 5% CO

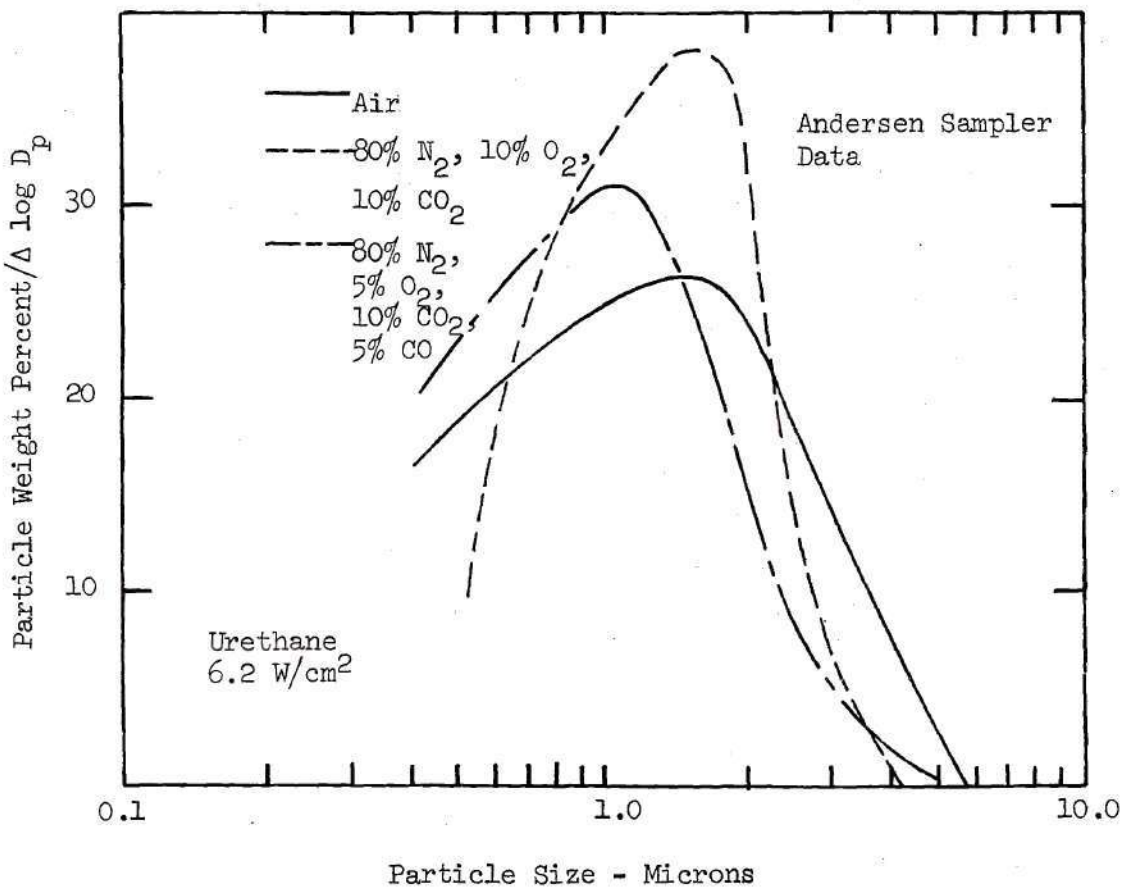

Figure 32. Comparison of Urethane Smoke Particle Size Characteristics in Three Atmospheres

particle sizes at 6.2 W/cm^2 shows differences in the characteristic curves for the three atmospheres. However, no clear trend is evident as, for example, oxygen concentration varies; and the majority of the volume fraction for each curve falls within the same particle size range. Thus, the differences noted for the curves in Figure 32 cannot be attributed to changes in atmospheric composition within the accuracy of these measurements.

Particulate concentrations and sample weight loss data are presented in Figures 33 through 36. Here it should be noted that urethane tests were substantially shorter at the higher heating rates than wood or PVC tests since the density of the foam is considerably lower than the density of the other two tested materials. Thus urethane samples (approximately 1.5 gm in weight) were consumed more rapidly than wood or PVC samples (approximately 25 gms in weight) under the same conditions. Figures 33, 34 and 35 show the expected increase in maximum particulate mass concentration with increase in radiant heat flux. In addition, correlations between sample weight loss rate and particulate mass concentration are again evident in Figures 34 and 36. Note that observed time lags between sample weight loss rates and measured particulate mass concentrations, as in Figure 34, correspond to the travel time from the sample to the Mass Monitor. Finally, these weight loss and smoke concentration data do not appear to be influenced by changes in atmospheric compositions.

Discussion of Urethane Results

The results of the tests of urethane foam under non-flaming conditions are especially relevant, in as much as this particular

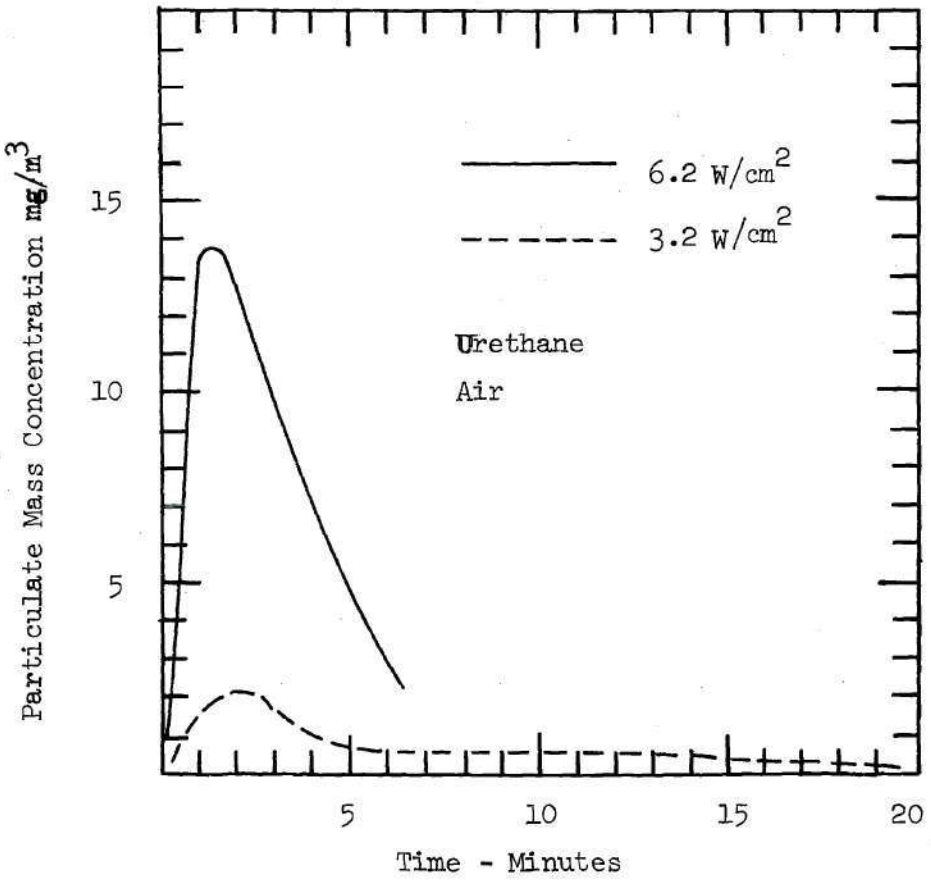

Figure 33. Comparison of Urethane Smoke Concentration at Two Different Heating Rates - In Air

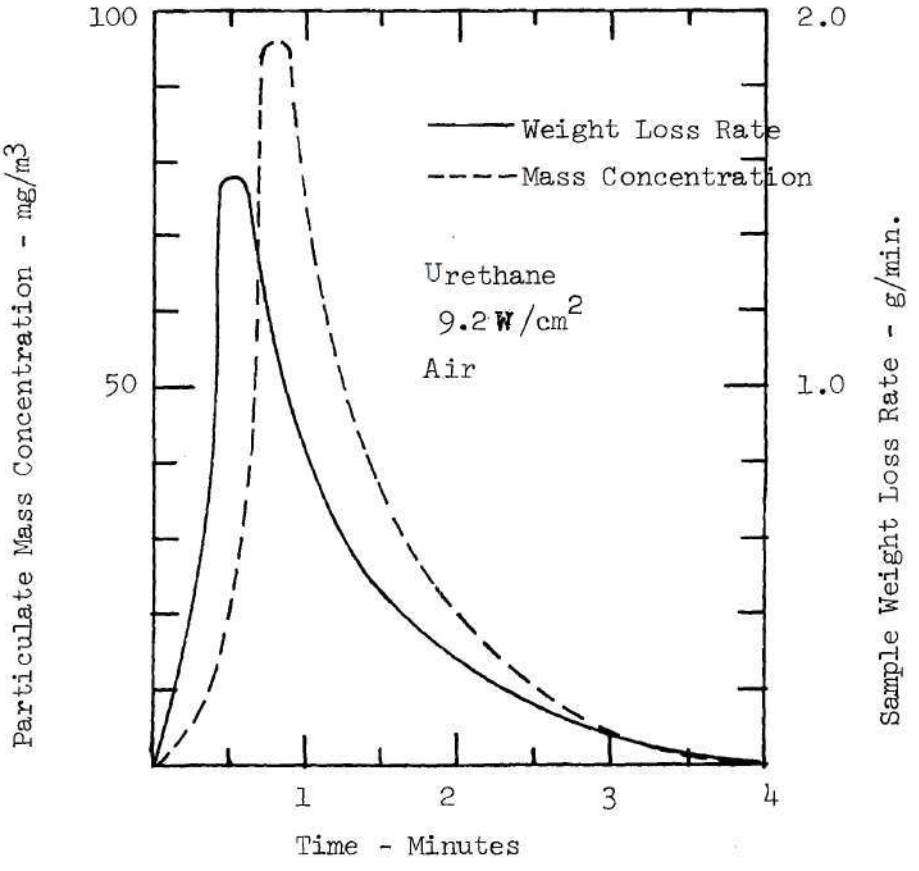

Figure 34. Comparison of Sample Weight Loss Rate with Particulate Concentration for Urethane - At 9.2 W/cm^2 in Air

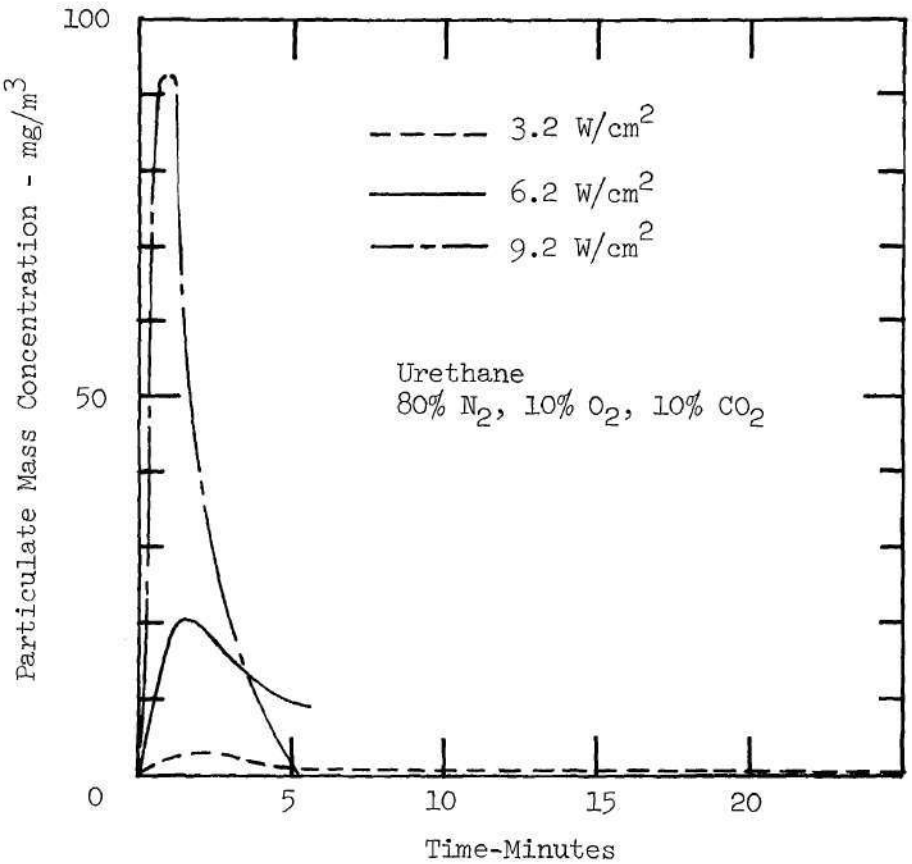

Figure 35. Comparison of Urethane Smoke Concentrations at Different Heating Rates - in 80% N_2, 10% O_2, 10% CO_2

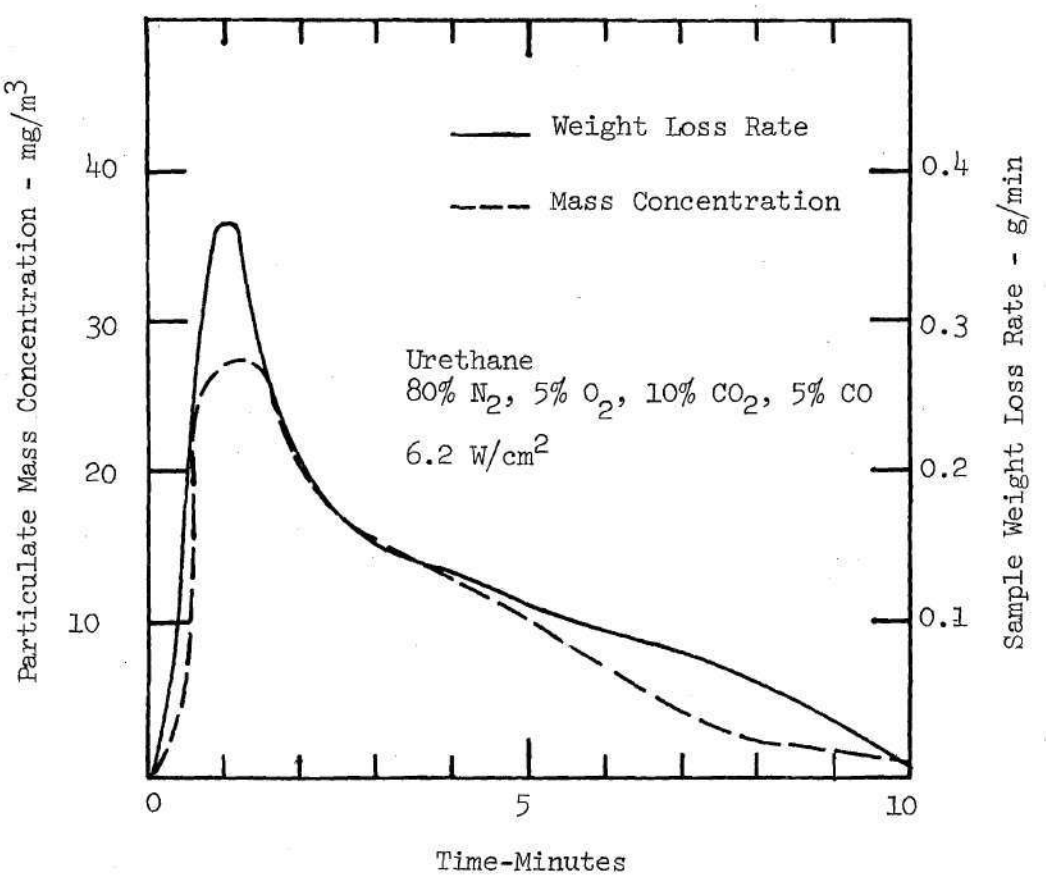

Figure 36. Comparison of Sample Weight Loss Rate with Particulate Concentration for Urethane - At 6.2 W/cm^2 in 80% N_2, 5% O_2, 10% CO_2, 5% CO

foam, along with others with a similar intended use, is flame retardant in nature. Thus, such foam may undergo considerable decomposition without flame under actual fire situations. Furthermore, it has been established that flame retardant foams produce greater "quantities" of smoke than non-flame retarded foams under the same conditions.[19,20] Although relatively little is known about the actual formation of particles from the decomposition of urethane foams, certain facts do provide a framework within which these results may be discussed. Additionally, the results provide new information relevant to the physiological and toxicological effects of urethane smoke on humans.

As previously mentioned, the smoke particles produced from pyrolyzing urethane samples consist of a yellow-orange solid residue commonly found in various tests of the burning characteristics of urethanes,[26,27] and a tarry liquid fraction. It is currently believed that the solid particles consist primarily of the polymeric isocyanate portion of the urethane structure that has been evolved during heating.[26,27] In addition, fragments of the polymer itself might also be included in the solid fraction. These investigators have found that polyether urethane foams produce the yellow-orange smoke at temperatures between 200°C and 300°C, leaving the polyether polyol behind as residue. Of particular note here is the fact that the remaining residue is virtually nitrogen free, because most of the nitrogen is carried away as part of the yellow-orange smoke (i.e., the polymeric isocyanate). The polyether polyol residue is then left to decompose at higher temperatures to produce a complex mixture of

volatile hydrocarbons and oxygenated species.[27] These products are presumably responsible for the tarry fraction in urethane smoke. The yellow-orange solid residue is stable up to 800°C, as shown in the decomposition schematic given by Woolley,[27] and presented in Table 2.

The formation of the particles eventually measured by the aerosol sampling system proceeds then by nucleation, growth and agglomeration of complex polymeric molecules of high molecular weights, both liquid and solid. Again, however, it is not clear exactly where the primary particulate formation process takes place. The stability of the yellow-orange smoke at temperatures up to 800°C introduces the possibility that the solid particles appear very near the pyrolysis zone, since no appreciable "cooling" is necessary for the particles to exist in solid form at high temperatures.

As previously observed in results of non-flaming wood tests, the particle size distribution data taken for non-flaming urethane smoke also correlates well with heating rate and thus, particulate mass concentration and sample weight loss rate. In fact, the particle sizes tend to increase more dramatically between heating rates of 3.2 W/cm^2 and 6.2 W/cm^2, than the similar increase recorded for wood. Particle sizes are then controlled to some degree by the mass loss rate of the sample, since a similar dramatic increase in mass loss rates is observed between those heating rates. An increase in sample mass loss creates greater concentrations of species which tend to augment the nucleation, growth, and agglomeration of particles consisting of complicated, high molecular weight species. The large

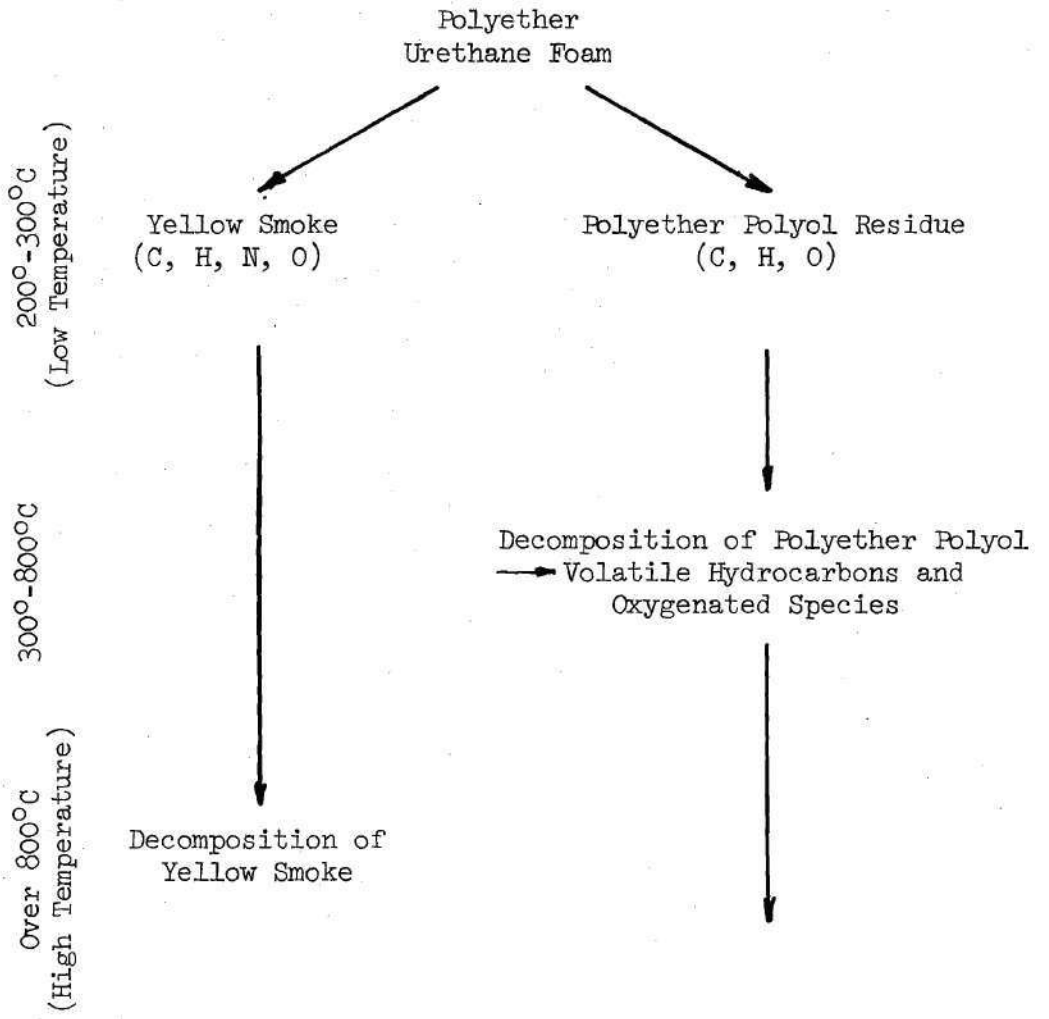

Table 2. Decomposition Schematic for Urethane Foam (from Woolley(27))

polymeric macromolecules that condense in this manner may also contribute to the larger sizes measured for urethane as compared to particle sizes measured for wood. Variations in particle sizes during tests, as indicated in Figures 28 and 31, are attributable to two factors mentioned previously. The char layer first insulates interior portions of the sample from the heat source, and then depletion of virgin material available for decomposition both act to decrease the mass loss rate and thus the specie concentrations that tend to condense in the form of particles. This is the same type of mechanism for particle size variations during non-flaming tests that was previously postulated for wood smoke.

Sample mass loss and particulate mass concentration data for the rigid urethane foam are consistent with data taken for wood samples and the expected behavior of a low density foam under extreme heating conditions. At high heating rates, the sample decomposes rapidly, producing a sharp increase followed by a rapid decrease in particulate mass concentration as the sample is quickly consumed. Maximum particulate mass concentrations are found to sharply increase with each increase in radiant heating level. This result is in contrast to the results for wood in 80 percent N_2, 10 percent O_2, 10 percent CO_2, which show no definitive increase in maximum particulate mass concentrations between 6.2 W/cm^2 and 9.2 W/cm^2, although the mass loss rate does increase. This difference in behavior between the two materials may be attributed to the fact that the solid yellow-orange urethane smoke is more stable at higher

temperatures than the tarry substances predominant in non-flaming wood smoke.

The physical properties reported here for smoke produced by the decomposition of a rigid urethane foam are certainly important in the evaluation of smoke hazards to humans during building fires. The points made in the discussion of non-flaming wood results are also applicable to urethane smoke. Specifically, although particle sizes produced by the smoldering urethane are somewhat larger than those measured for wood at higher heating rates, available evidence[53] still indicates that up to 75 percent of the particles may be retained in the respiratory tract and lungs when inhaled by a building occupant. If the particles are toxic in nature, or if toxic gases are absorbed on the particles, then the danger to a person is increased. These data also emphasize the need for standard test methods to include higher radiant heating rates, since significant changes in smoke concentrations did take place when heating levels were varied.

Polyvinyl Chloride

PVC Results

Test results from PVC samples burned under non-flaming conditions are given in Figures 37 through 51. Figure 37 shows particle weight distributions for three heating rates in air, as determined from Andersen Sampler data. Due to high mass concentrations of particulates produced by PVC, and the tendency of these particles to clog the stages of the Andersen Sampler, the 1/2 inch probe pump was operated in 3 minutes-on, 3 minutes-off cycles during tests at

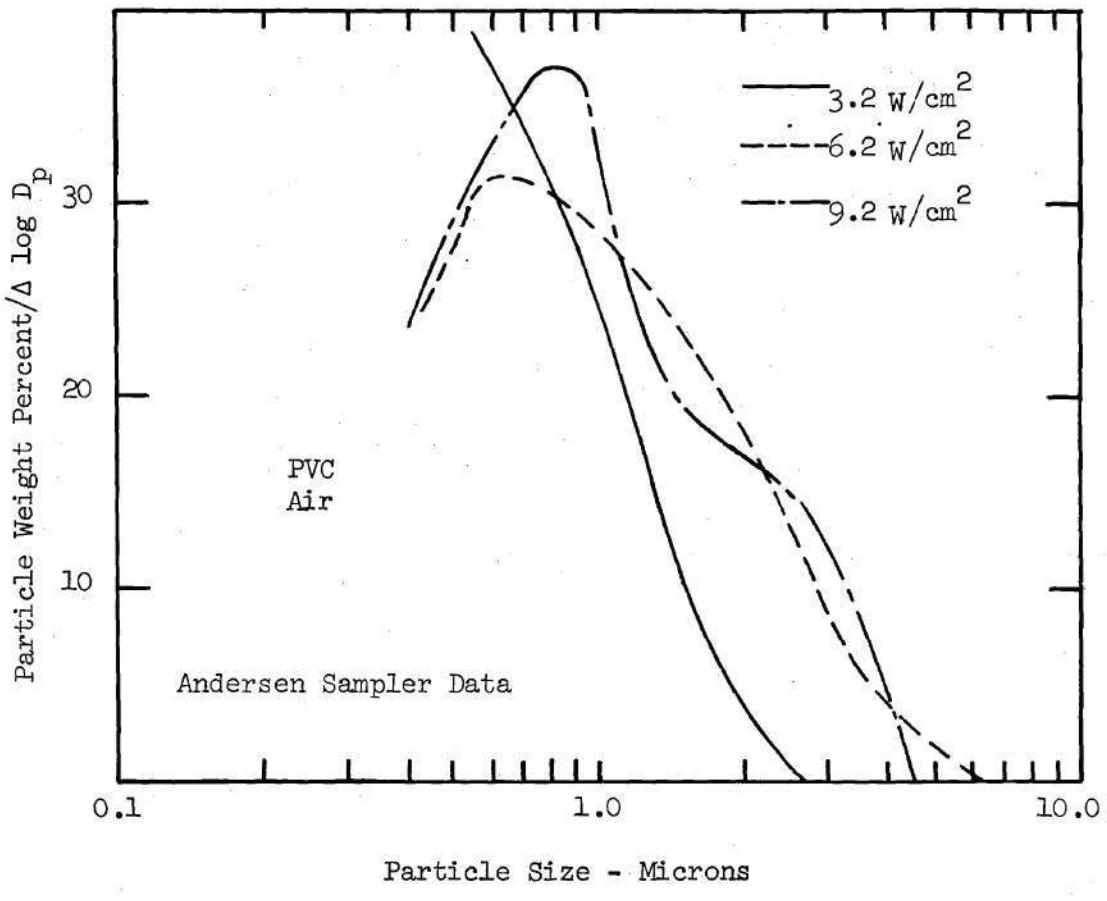

Figure 37. Particle Weight Distribution for PVC Smoke in Air

6.2 W/cm^2 and 9.2 W/cm^2. Also, no spontaneous ignition took place during tests of PVC at the high heating rates. Figure 38 provides information on particle sizes below the range of the Andersen Sampler at the lowest heating rate. Particle sizes remained relatively stable for tests of PVC at 3.2 W/cm^2, and Figure 38 gives a typical distribution for particles less than 0.36 micron in size. At higher heating rates, particles sizes were found to vary during tests. This is shown in Figure 39 from data taken by the Whitby Electrical Aerosol Analyzer.

The trends indicated in the results presented for smoldering PVC in air are similar to those presented earlier for wood and urethane. Particle size increases coinciding with increases in heating rates are evident from both instruments recording size distribution data. The most significant increase is again found to be between 3.2 W/cm^2 and 6.2 W/cm^2, corresponding to the substantial increases in particulate mass concentrations to be discussed later. Time-resolved particle volume distributions show that particle size characteristics seem to vary quite widely at 6.2 W/cm^2, where the possibility of a bi-modal size distribution is indicated late in the test. Generally, however, particle sizes increase over the first half of the test, and then decrease thereafter. The appearance of the PVC smoke particulates, when collected on the Andersen Sampler impaction plates, is characterized by a solid blackish-green deposit mixed with a tarry liquid fraction.

The results of particle size measurements for non-flaming PVC tests in oxygen depleted atmospheres are shown in Figures 40 through

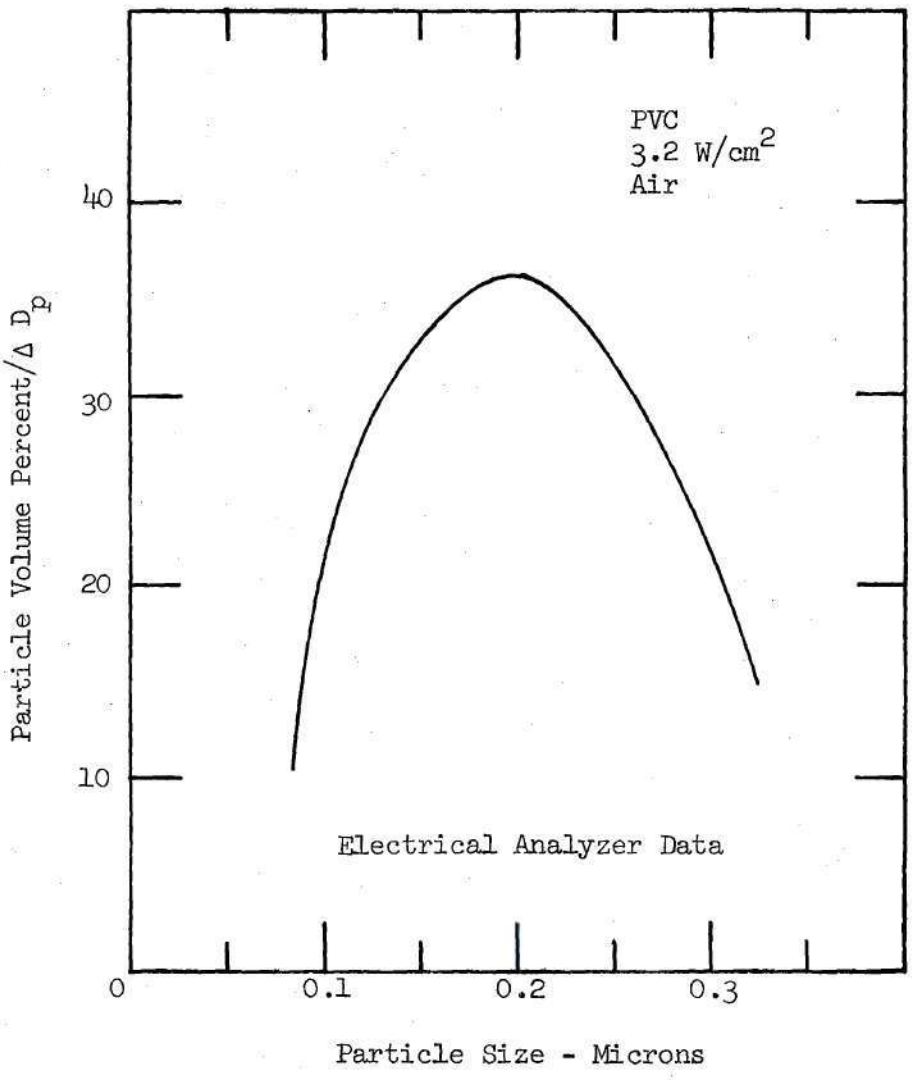

Figure 38. Average Particle Volume Distribution for PVC Smoke Particles Less Than 0.36 Micron - At 3.2 W/cm^2 in Air

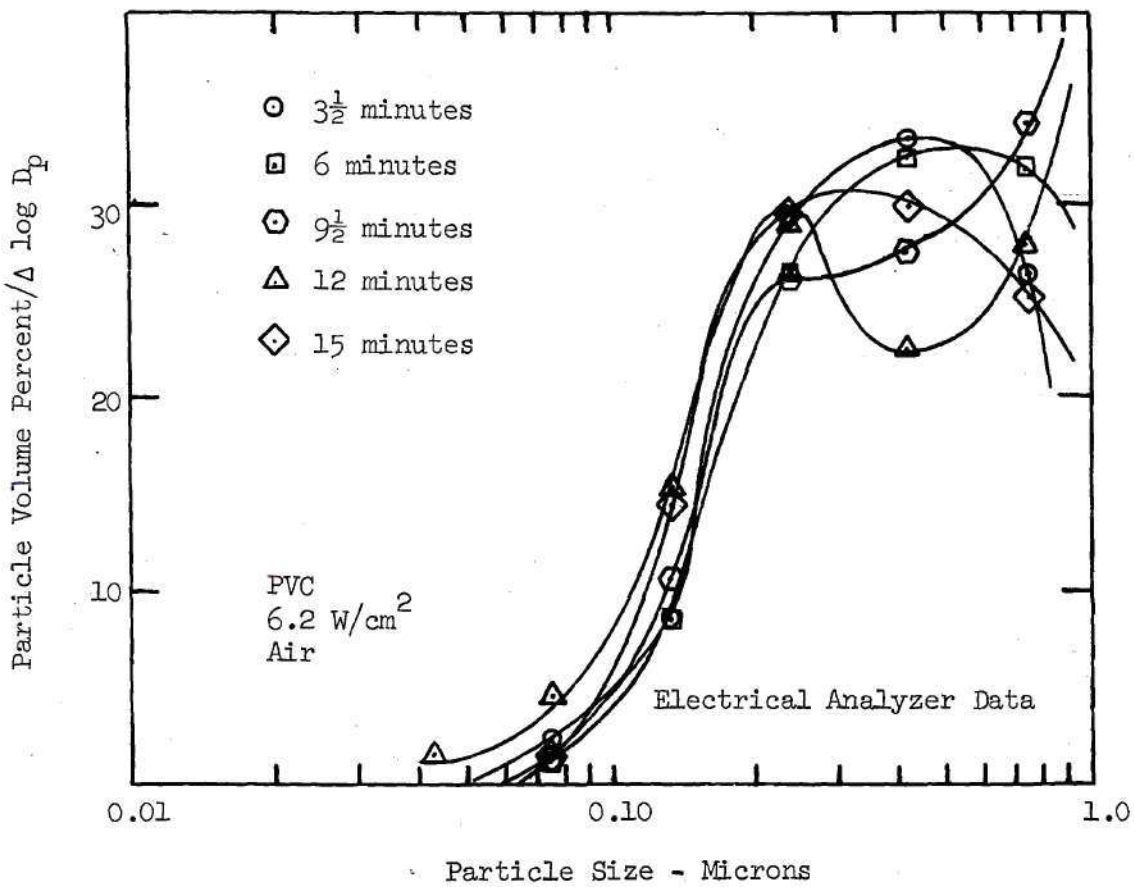

Figure 39. Time Resolved Particle Volume Distribution for PVC Smoke Particles Less than 1.0 Micron - At 6.2 W/cm^2 in Air

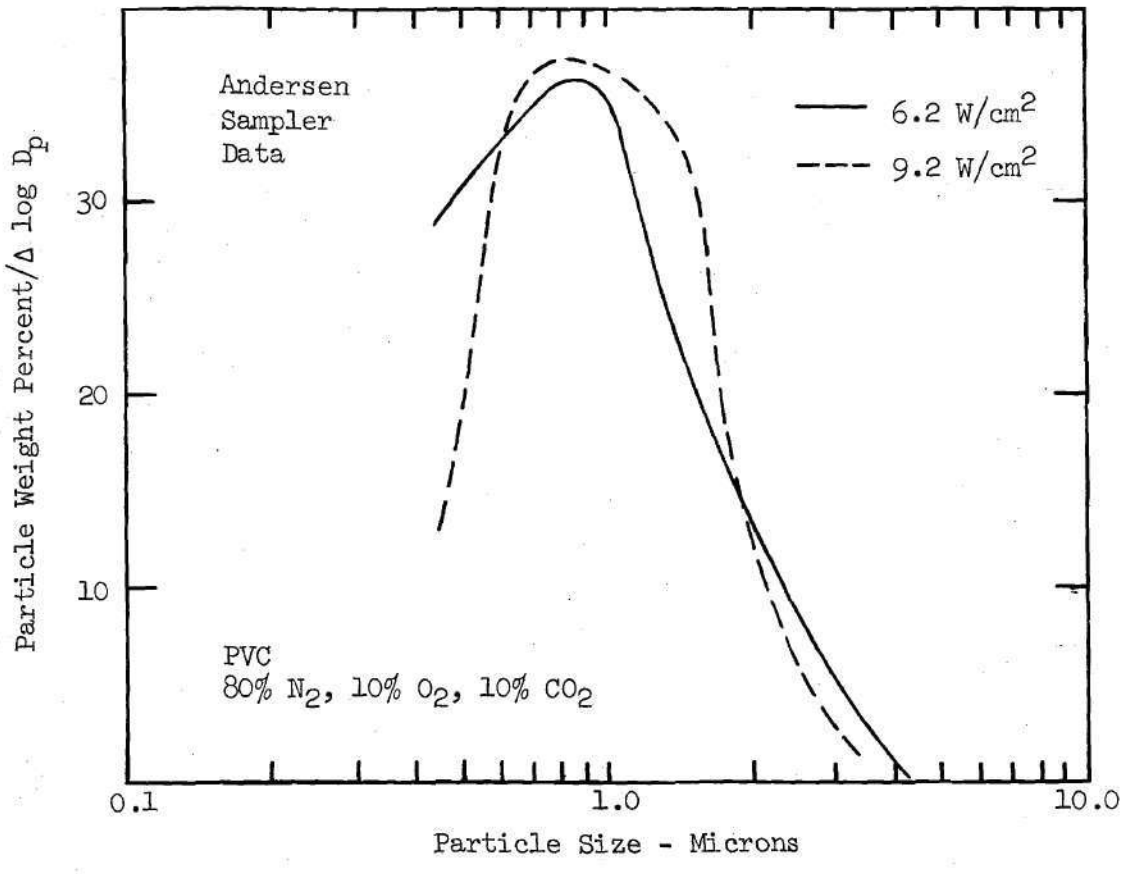

Figure 40. Particle Weight Distribution for PVC Smoke in 80% N_2, 10% O_2, 10% CO_2

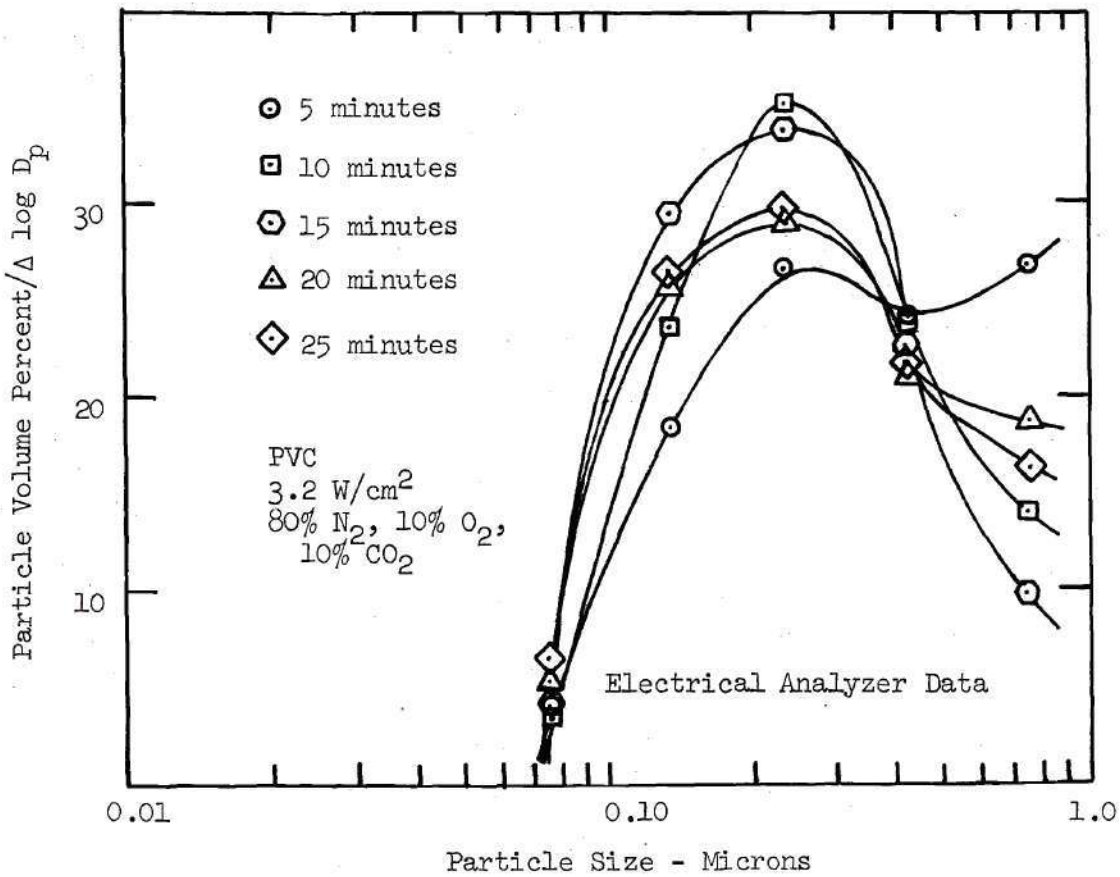

Figure 41. Time Resolved Particle Volume Distribution for PVC Smoke Particles Less Than 1.0 Micron - At 3.2 W/cm^2 in 80% N_2, 10% O_2, 10% CO_2

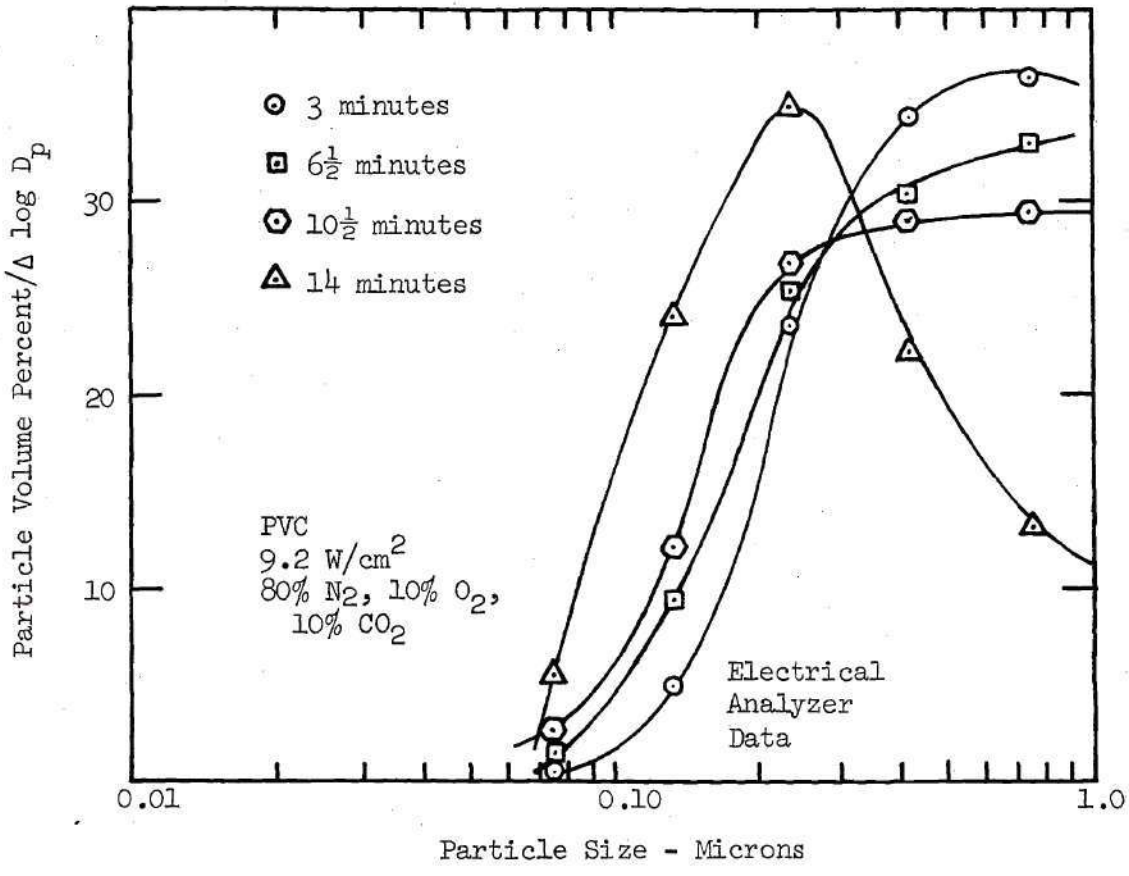

Figure 42. Time Resolved Particle Volume Distribution for PVC Smoke Particles Less Than 1.0 Micron - At 9.2 W/cm^2 in 80% N_2, 10% O_2, 10% CO_2

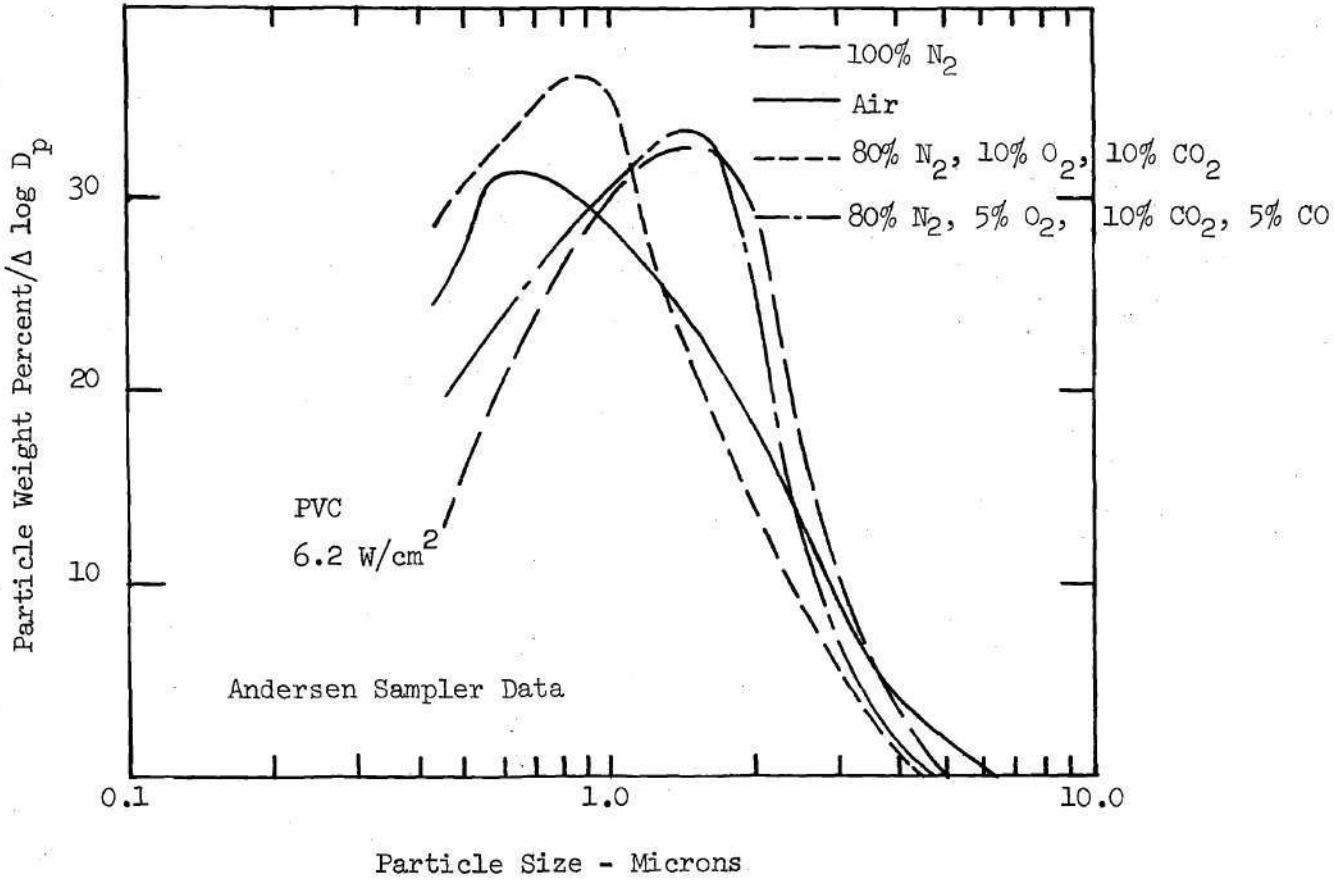

Figure 43. Comparison of PVC Smoke Particle Size Characteristics in Four Atmospheres

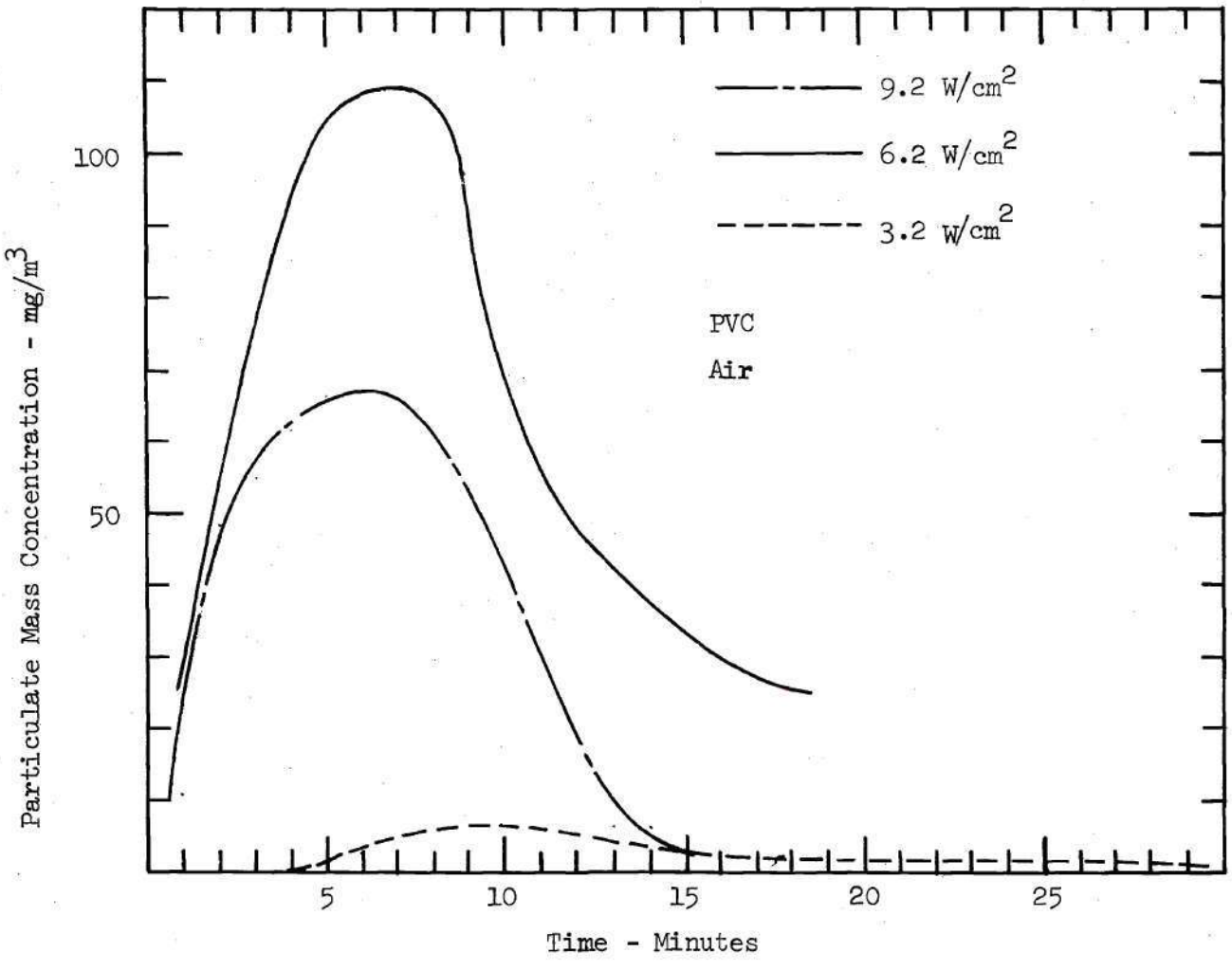

Figure 44. Comparison of PVC Smoke Concentration at Different Heating Rates in Air

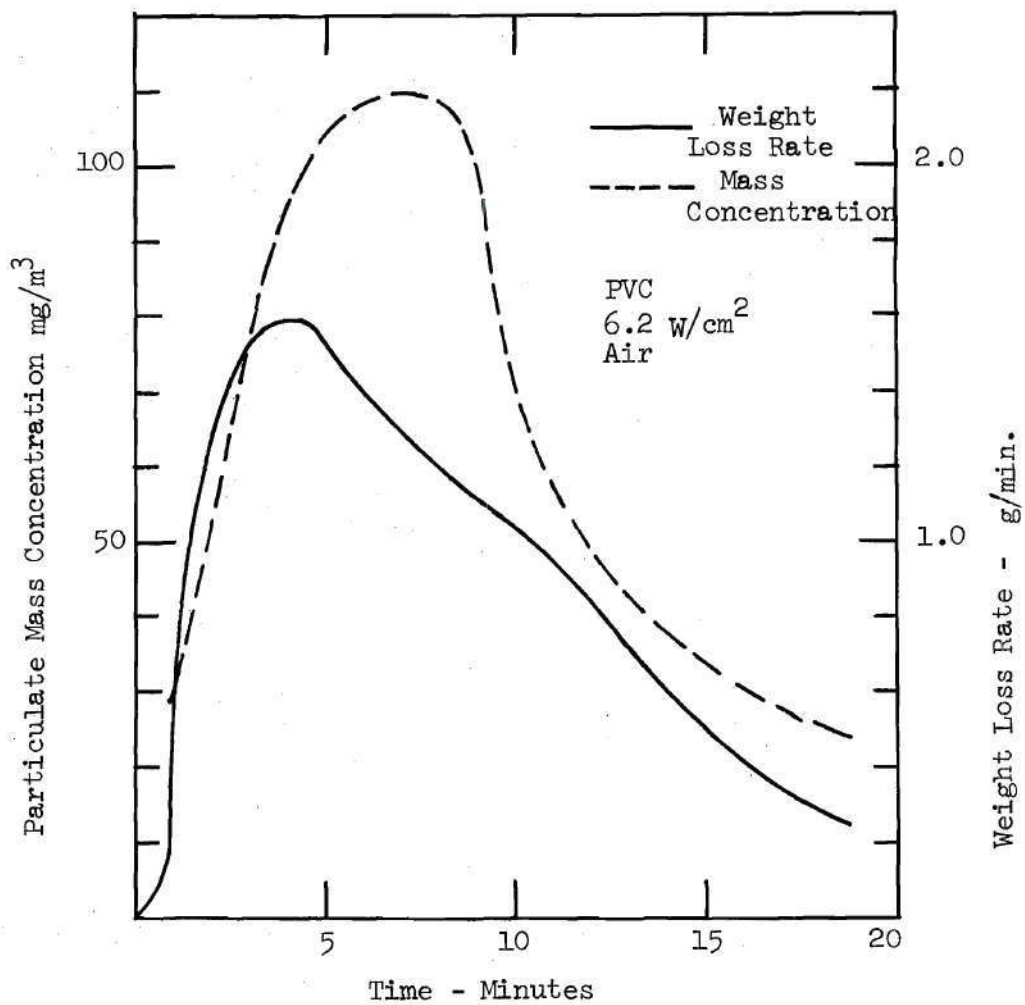

Figure 45. Comparison of Sample Weight Loss Rate with Particulate Concentration for PVC - At 6.2 W/cm^2 in Air

from 3.2 W/cm^2 to 6.2 W/cm^2, and maximum mass concentrations of the same order of magnitude for heating rates of 6.2 W/cm^2 and 9.2 W/cm^2. Correlations between sample weight loss rate and particulate mass concentration are again shown in Figures 45, 47 and 48. Particulate concentrations are thus closely related to the rate at which the smoldering sample is losing mass during tests at all three heating rates and all three atmospheric compositions. A slight decrease in maximum particulate mass concentration is indicated at 6.2 W/cm^2, when the oxygen concentration is decreased from 20 percent to 5 percent.

CPTC Ventilation Rate Effects. In order to determine whether or not CPTC ventilation rates affect the smoke particulate size characteristics measured for non-flaming PVC tests, ventilation rates were varied below and above the vent rate indicated in Table 4. As mentioned previously, such vent rate changes may affect the cooling rate and concentration time history of the combustion products generated during a test, and thus alter the nucleation, growth and agglomeration processes which determine particle sizes. Figure 49 compares integrated smoke particulate weight distributions at three CPTC ventilation rates in air. It shows fluctuations in particle size characteristics with the most noticeable difference indicated at the lowest CPTC ventilation rate. That is, measured particle sizes are somewhat larger at the CPTC vent rate of 10 CFM, as compared to vent rates of 15 CFM and 20 CFM. Figures 50 and 51 give time resolved particle volume distributions for tests at CPTC ventilation rates less than and greater than the "standard" vent rate of 15 CFM.

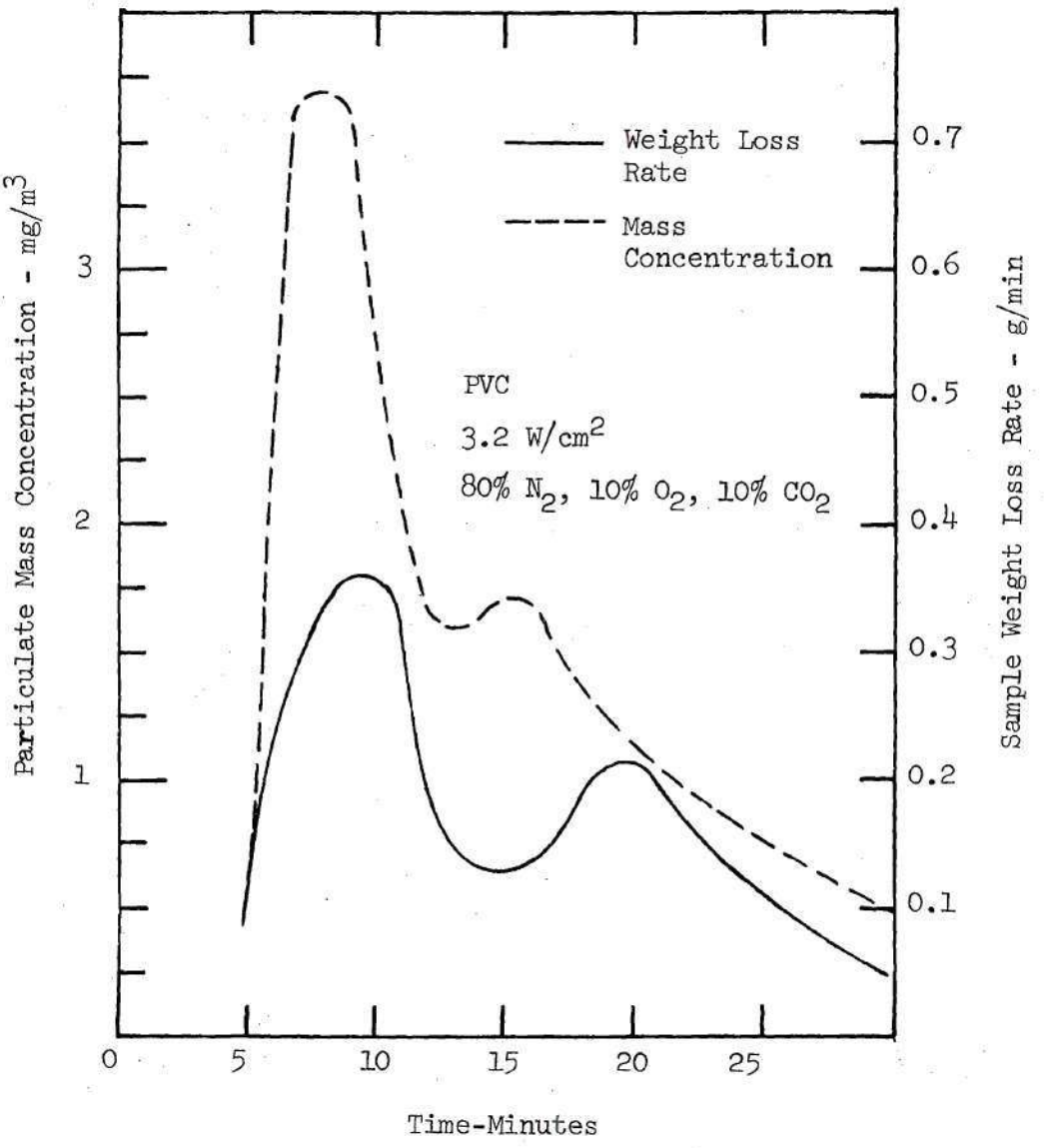

Figure 47. Comparison of Sample Weight Loss Rate with Particulate Concentration for PVC - At 3.2 W/cm^2 in 80% N_2, 10% O_2, 10% CO_2

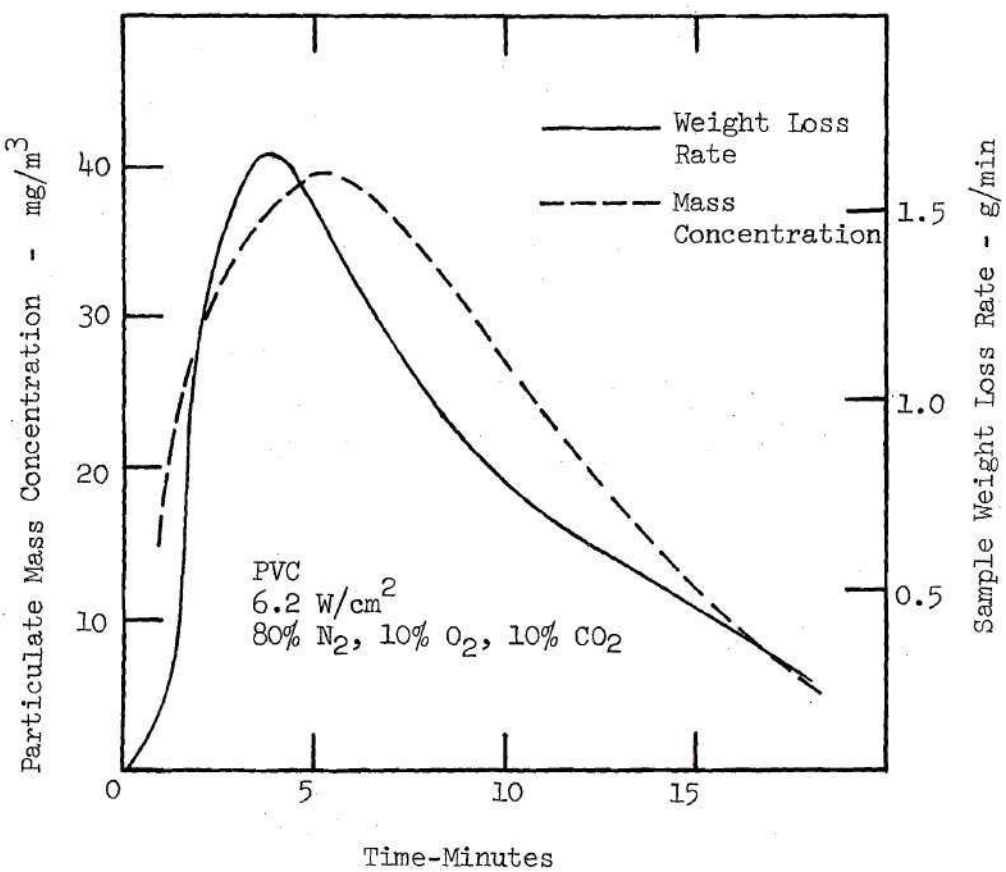

Figure 48. Comparison of Sample Weight Loss Rate with Particulate Concentration for PVC At 6.2 W/cm^2 in 80% N_2, 10% O_2, 10% CO_2

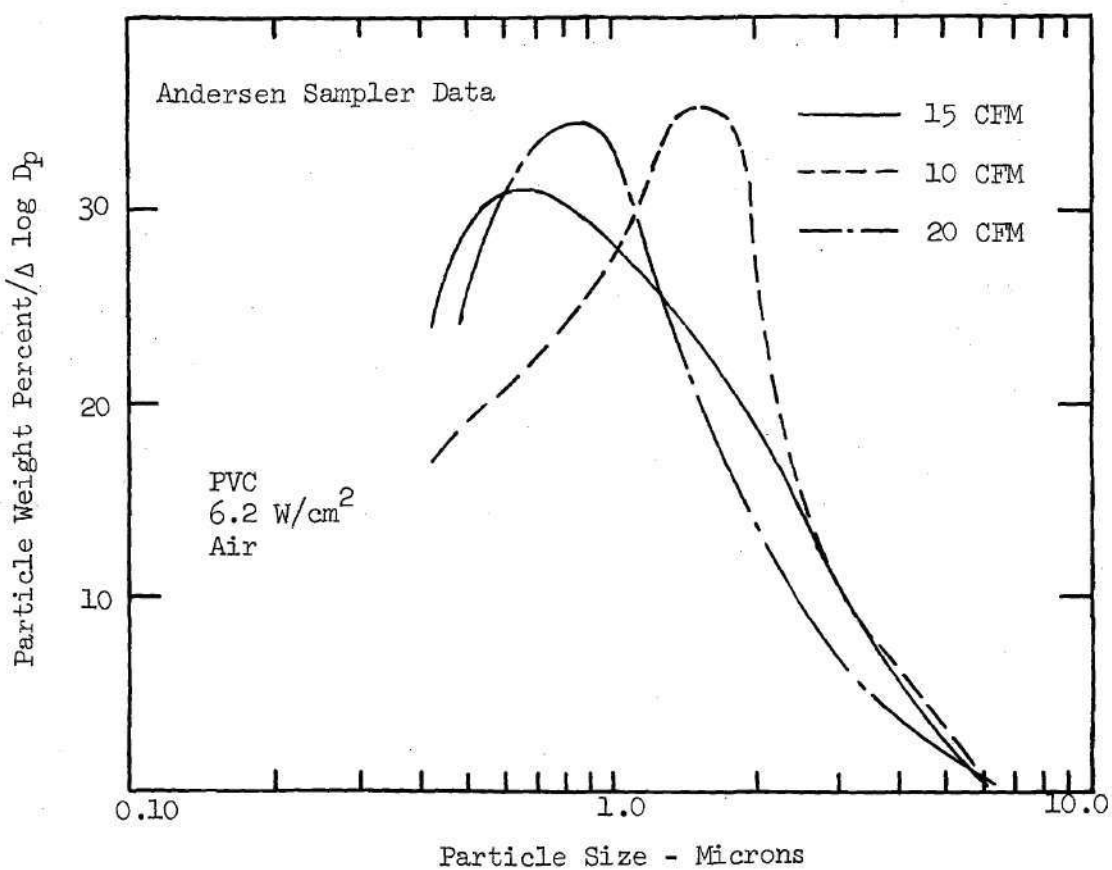

Figure 49. Comparison of PVC Smoke Particle Size Characteristics at Three CPTC Ventilation Rates - At 6.2 W/cm^2 in Air

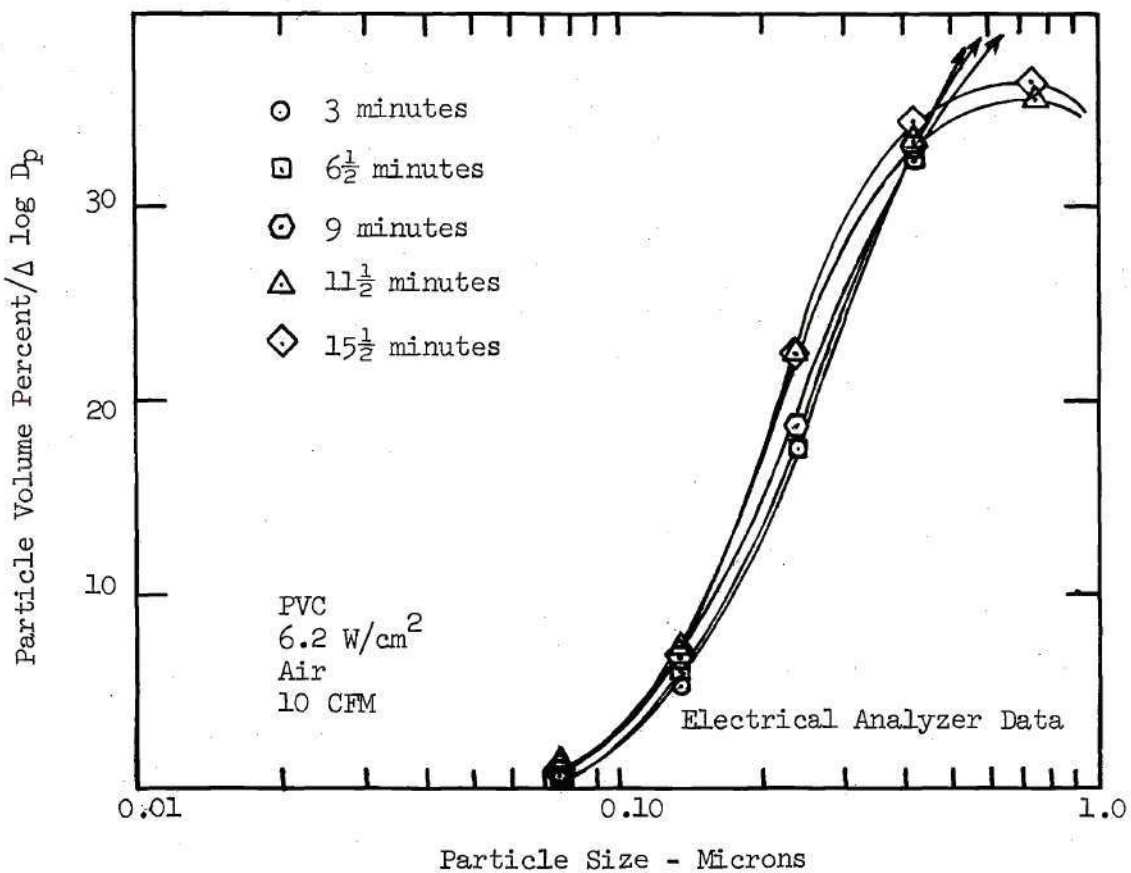

Figure 50. Time Resolved Particle Volume Distribution for PVC Smoke Particles When CPTC Vent Rate is Decreased - At 6.2 W/cm^2 in Air

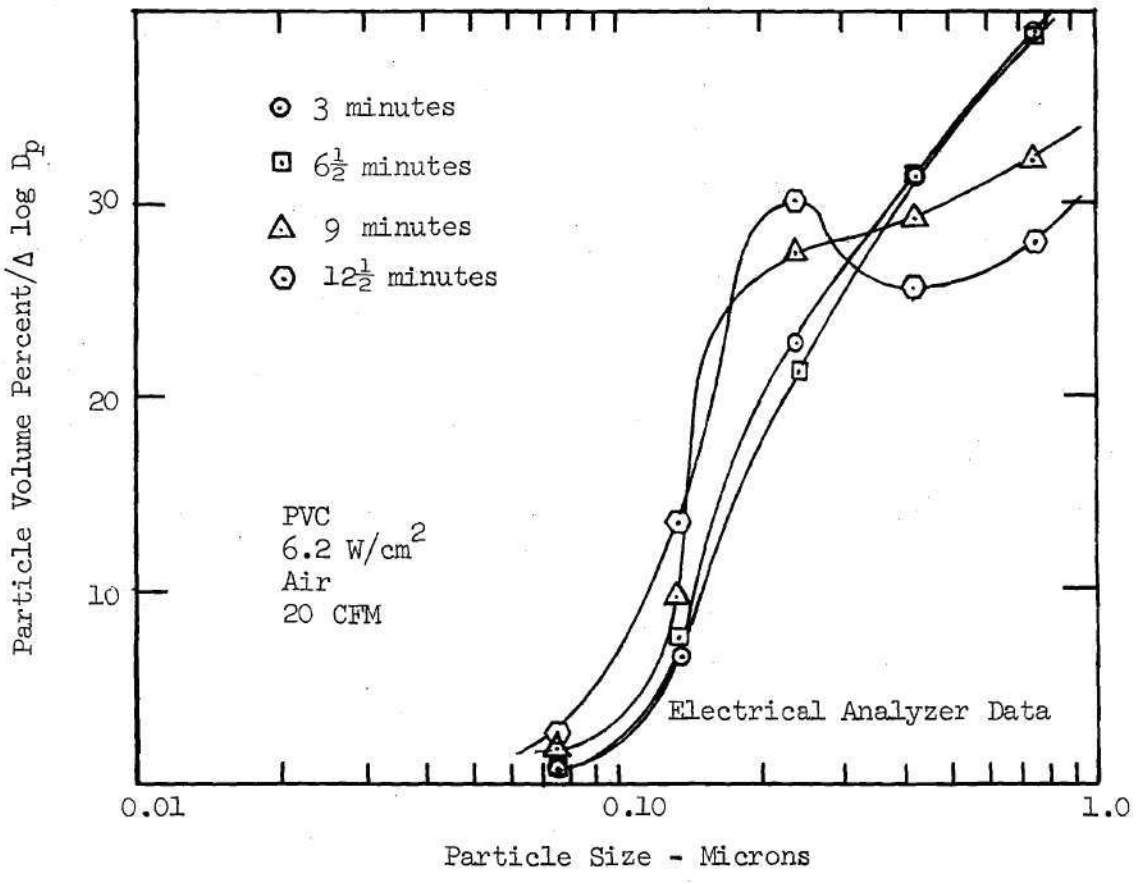

Figure 51. Time Resolved Particle Volume Distribution for PVC Smoke Particles When CPTC Vent Rate is Increased - At 6.2 W/cm² in Air

They show that particle sizes vary during the test, where the indicated trends are consistent with integrated particle weight distribution data.

Discussion of PVC Results

The thermal degradation of polyvinyl chloride has been the object of many investigations in which the mechanisms of degradation have been studied. In particular, interest has revolved around the thermal behavior of PVC exposed to temperature extremes experienced during normal use,[54] and its tendency to produce toxic gases under the extreme conditions imposed by building fires.[55] However, in-depth studies of PVC degradation have generally been limited to the decomposition region of PVC below 300°C, where most data concerns dehydrochlorination mechanisms, and not the production of liquid and solid products of decomposition. Nevertheless, there are relevant data available which aid in the interpretation of the results presented here. Additionally, these results provide new information which is important in evaluating the smoke hazards from smoldering PVC.

The sequence of reactions which eventually produce the complicated smoke particulates generated in the Combustion Products Test Chamber is initiated by the elimination of hydrochloric acid from the polymer chain. There have been a number of proposed theories describing dehydrochlorination and the following explanation is the one most widely accepted at this time.[54,56,57] Given the following polymer chain:

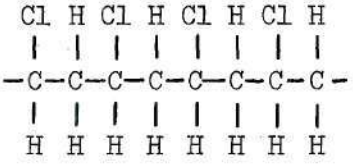

a hydrogen chloride molecule is evolved by any of a number of "initiating" mechanisms, and then succeeding HCl molecules are eliminated down the chain in a "zipper-like" process. There is no concensus as to the location of initiation points in the chain, although the likely possibilities include structural irregularities, chain end groups, irregularities within the chain, and extraneous impurities.(54)

The actual process by which the HCl molecules are lost down the chain is open to question. Winkler(57) and Stromberg(58) have proposed radical chain mechanisms, and Winkler's mechanism will be briefly reviewed for illustrative purposes. The first step involves an attack on a methylene hydrogen preferentially:

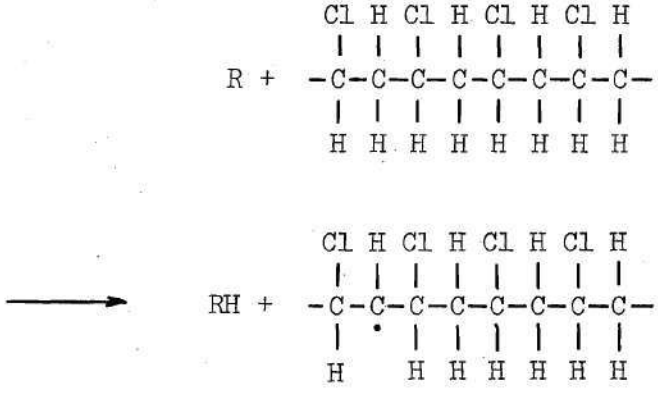

This PVC macroradical then stabilizes itself by rearrangement and the elimination of a free chlorine atom as follows:

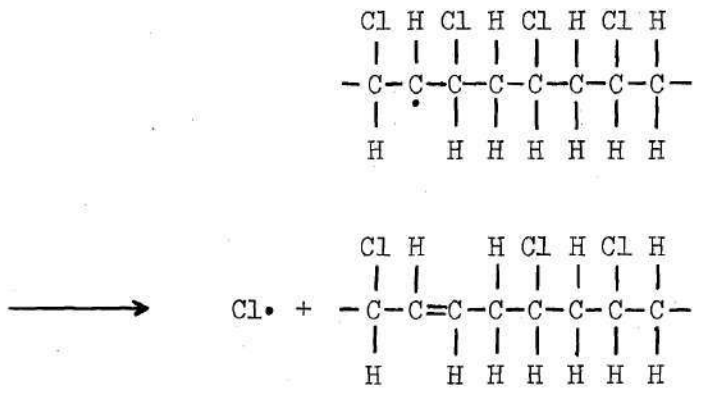

The free chlorine atom then abstracts the neighboring methylenic hydrogen atom to give

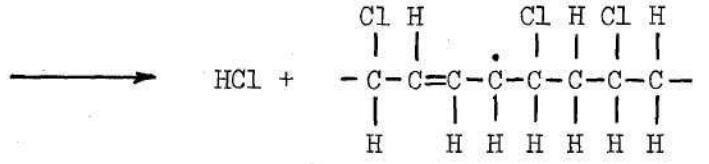

Again, the macroradical stabilizes itself:

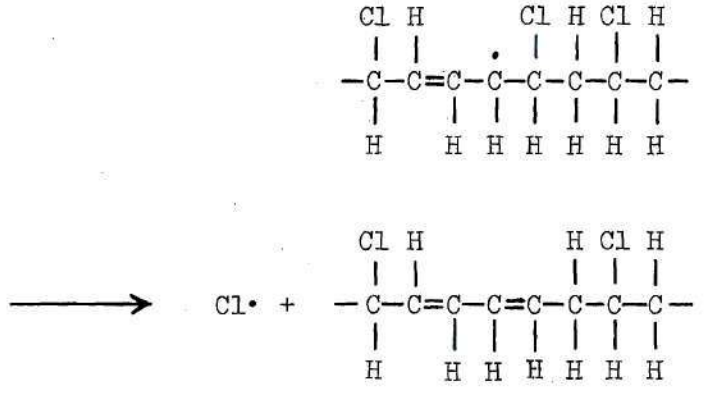

This process thus continues to develop the long chain polyene system, until termination takes place. Termination could then be brought about, for example, by the reaction of one of the radical species involved in the process with any other specie that may be present in

the degrading PVC.

The products other than HCl that have been identified during the thermal degradation of PVC provide evidence that the above-mentioned polyene system is unstable at high temperatures. Consequently, rearrangement and product elimination takes place to produce a more stable structure.[55,59] For example, benzene, toluene, xylenes and naphthalene have been identified frequently in the volatile products of pyrolyzing PVC.[55,59] This would indicate a tendency by the polyene system to form the stable six-membered rings found in cyclic and polycyclic aromatic hydrocarbons.[55,59] Furthermore, initial chemical analyses of smoke particulates generated in the tests described here, have found further evidence of aromatization of the polyene system in the identification of phenanthrene.[46]

In addition to the smoke particulates generated from the polyvinyl chloride polymer itself, it is likely that chemical additives also contribute to smoke produced by smoldering PVC. Specifically, the previously mentioned chemical analysis of smoke particulates generated by burning PVC in the CPTC, has identified dioctyl pthalate as another constituent of the total particulate fraction of the combustion products. Dioctyl pthalate is a commonly used plasticizer used in PVC plastics, and its clear oily appearance may account for some of the liquid constituents found in sampled PVC smoke particulates.

The above-discussed mechanisms for the thermal degradation of PVC provide interesting hypotheses relating to the formation of pyrolysis products, although a number of questions remain unanswered.

Most importantly, there appears to be little available data on the degradation of PVC, kinetic or otherwise, beyond the initial dehydrochlorination process. For example, the generation of the aromatic hydrocarbons which have been identified in the volatile and particulate products of PVC degradation has not yet been characterized in detail. Furthermore, it is not clear whether such reactions occur in the solid phase or gas phase in the pyrolysis zone, or as the products move away from the pyrolysis zone. With such information, the nucleation and growth processes of the particles could be analyzed in more detail.

The dependence of particle sizes on radiant heating rate is the most important aspect of the particle size measurements presented earlier; especially the increases shown between heating rates of 3.2 W/cm^2 and 6.2 W/cm^2. Time resolved particle volume distributions show clearly that the larger particles are generated during periods of highest particulate mass concentrations. Apparently, the non-flaming PVC smoke behaves in a manner typical of all three materials tested in this program, whereby higher particulate mass concentrations seem to contribute to the growth of particles. Furthermore, particle sizes appear to be established generally prior to dilution by ventilation gases, since variation in CPTC vent rates have relatively little effect on particles, except at the lowest CPTC vent rate. At the vent rate of 10 CFM, further agglomeration apparently occurs in transit from sample to Sampling Section. In conclusion, the higher heating rates contribute to higher particulate mass concentrations,

which in turn augment the nucleation, growth and agglomeration of particles, probably in a region near the pyrolysis zone; and thus sizes are then determined before particles are substantially diluted by the chamber ventilation gases.

Particle size variations evident during tests at the higher heating rates can be explained by the development of a char layer as tests proceed. In fact, as the char layer forms, volatile products within the sample expand, and a considerable "bulge" develops at the tested sample face. This creates a bubble of char structure which may expand up to one inch in front of the original sample face. As this char layer develops, it tends to insulate interior portions of the sample from the radiant heat and thus the mass loss rate decreases as less heat reaches the pyrolysis zone. The resultant decrease in condensable species is then indicated by lower particulate mass concentrations and smaller particle sizes later in the test.

Variations in oxygen concentrations have been found to have a significant affect on the dehydrochlorination of PVC.[54,55,57,59] Measured reaction rates have shown that dehydrochlorination proceeds in proportion to the 0.5 power of oxygen concentration.[60] However, there is other evidence to indicate that the formation of products other than HCl is basically thermal in nature, and not generally affected by oxygen concentrations.[55,59] Variations in atmospheric compositions in these tests of smoldering PVC indicate some possible changes in particle sizes due to oxygen depletion. Although there is no clear explanation for this behavior at this time, it does

appear that the combined effect of many reactions other than dehydrochlorination probably tends to minimize the effects of variations in oxygen concentration on smoke generated by smoldering PVC. Also, observed changes attributed to variations in atmospheric composition are not appreciable, considering the problems associated with PVC smoke measurements mentioned earlier in this chapter and in Appendix C.

Maximum particulate mass concentrations measured for smoldering PVC were heavily dependent on radiant heating rate, especially for the increase between 3.2 W/cm^2 and 6.2 W/cm^2. This can be attributed to the higher temperatures created at higher heating rates, as previously discussed for similar results obtained for wood and urethane. Also, this particulate mass concentration information provides additional evidence that smoke particulates are produced in direct relation to the mass loss rate of the burning material for the range of test conditions used here. The double peaks observed in Figure 47 are probably due to irregularities in char formation observed in tests at 3.2 W/cm^2. During a test the char "bulge" appeared to grow in two distinct stages characterized by an initial growth (up to 1/4") earlier during a run, followed by further expansion (up to 3/4") later during the run. Variations in atmospheric compositions produced no definitive changes in particulate mass concentration behavior or sample weight loss rates. This seems to confirm the earlier finding that the dehydroclorination reaction (which depends heavily on oxygen concentration) is probably not the controlling factor in the overall

reaction kinetics of PVC smoke generation, as studied here.

Since particle size characteristics for non-flaming PVC smoke are similar to those measured for wood and urethane under the same conditions; then, previous remarks relating to the importance of these results in establishing physiological and toxicological smoke hazards are still quite valid. That is, substantial quantities of the smoke particles generated under the conditions studied here can be retained in the human respiratory system. The toxicity of these particulates, and any possible synergistic effects with inhaled gaseous combustion products then become of utmost importance. Furthermore, the rates of production of these particulates vary considerably, suggesting that smoke tests of PVC materials should include several radiant heating rates for adequate determination of the smoking hazards of such materials. This fact is also consistent with the results obtained from wood and urethane tests under non-flaming conditions.

CHAPTER IV

FLAMING TESTS - RESULTS AND DISCUSSION

This chapter continues the presentation of results and related discussion of smoke tests run in the Combustion Products Test Chamber. Here, data from the flaming tests indicated in Table 1 will be presented in the same manner as the results of non-flaming tests in Chapter III. Each of the three materials was tested in the atmospheric compositions shown in Table 1, and the standard sample thicknesses were again 1/4 inch for wood, 3/8 inch for urethane and 1/8 inch for PVC. For the case of flaming combustion, the samples are continuously irradiated at 2.5 W/cm^2 radiant flux, and the flammable products of thermal degradation are ignited by a propane pilot burner. The particles generated in this manner have previously been found to consist primarily of carbon particles or soot;[10,22] which is in contrast to the characteristics of smoke particulates generated during smoldering combustion (see Chapter III). As in non-flaming tests, measurements of smoke particle size distributions, smoke particulate mass concentrations and sample weight loss have been made in all flaming tests.

Douglas Fir

Douglas Fir Results

Figures 52, 53 and 54 give particle size characteristics for flaming tests of wood in air. Particle sizes for most flaming tests

were generally within the range of the Electrical Aerosol Analyzer; i.e., less than one micron. This fact, in addition to the decreased particulate mass concentrations (to be discussed later), precluded accurate measurements using the Andersen Sampler due to insufficient particulate deposition on the impaction plates. The time resolved data shown in Figures 52, 53 and 54 show relatively little variation in particle sizes as tests proceed. These data also allow comparison of ventilation rate effects, where CPTC vent rates were first decreased and then increased over the standard vent rate of 15 CFM. It should be noted that at the lowest ventilation rate, the sample flame was extremely erratic and unstable in comparison to the relatively stable, sustained flaming conditions observed at 15 CFM and 20 CFM.

The above-mentioned data shows consistently smaller particle sizes for wood smoke generated under flaming conditions than for wood smoke generated under non-flaming conditions. Furthermore, particle size characteristics remain relatively stable throughout flaming tests in air at all three ventilation rates tested. The appearance of the particulates collected on the absolute filter and impaction plates is that of soot particles mixed with a small amount of a tarry liquid. Thus, the particulates from flaming combustion are composed of solid and liquid fractions. Finally, the unstable flame observed at the lowest CPTC ventilation rate indicates a potential sensitivity to oxygen concentrations near the surface of the burning sample.

Figure 55 presents particulate mass concentration and sample weight loss data for wood flaming in air. Both curves show two

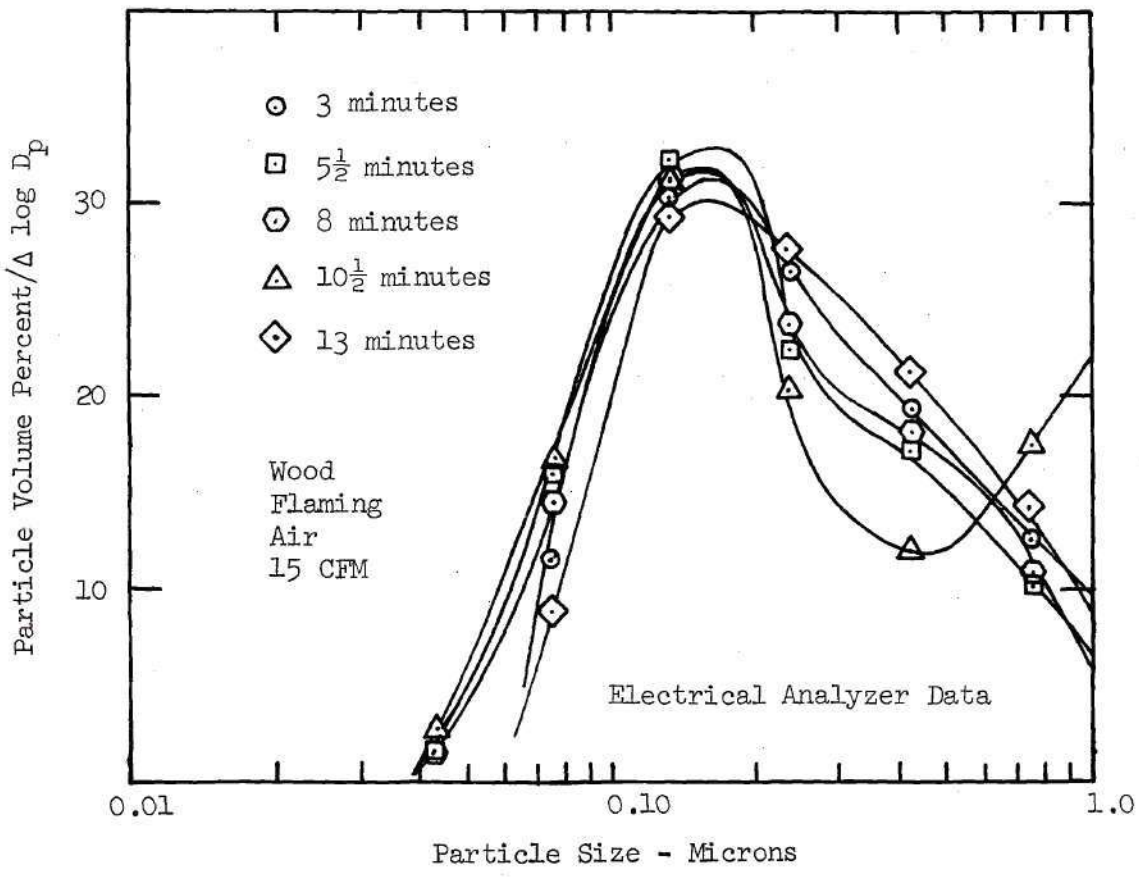

Figure 52. Time Resolved Particle Volume Distribution for Wood Smoke Particles Less Than 1.0 Micron - Flaming in Air

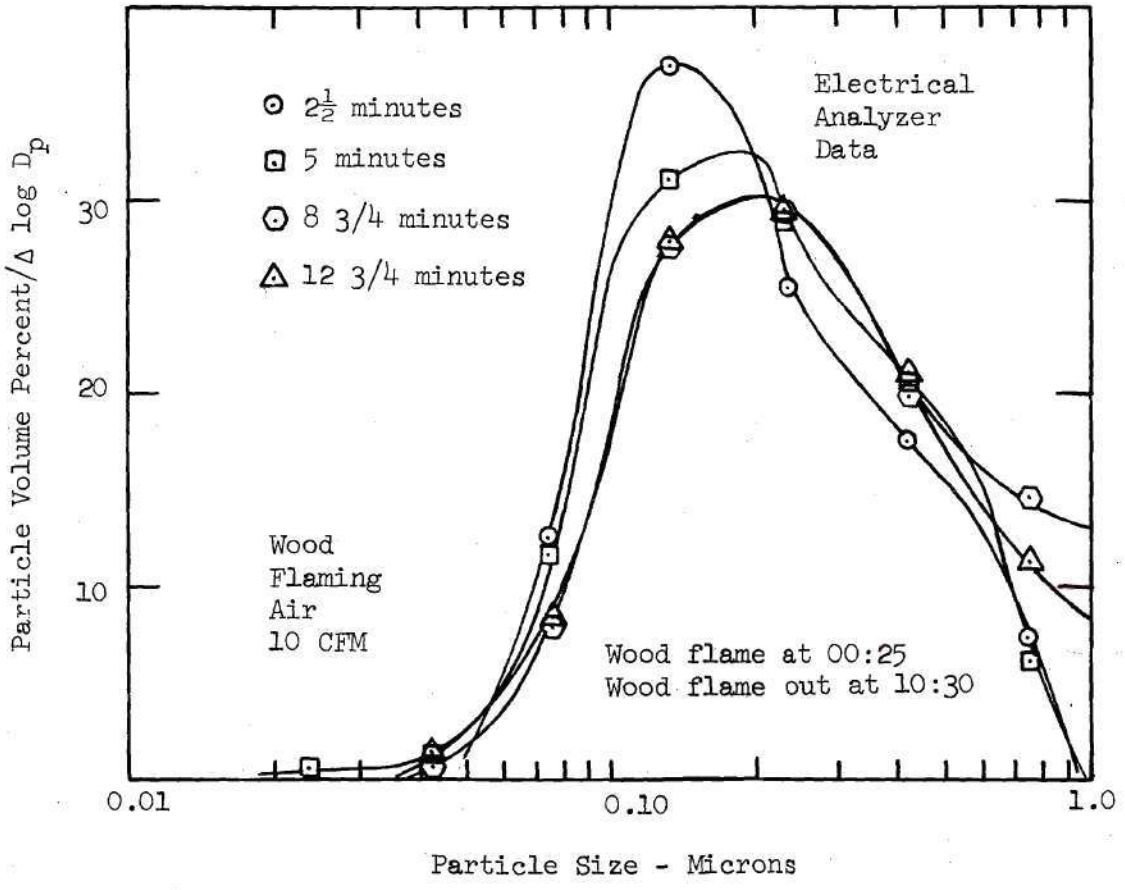

Figure 53. Time Resolved Particle Volume Distribution for Wood Smoke Particles When CPTC Vent Rate is Decreased - Flaming in Air

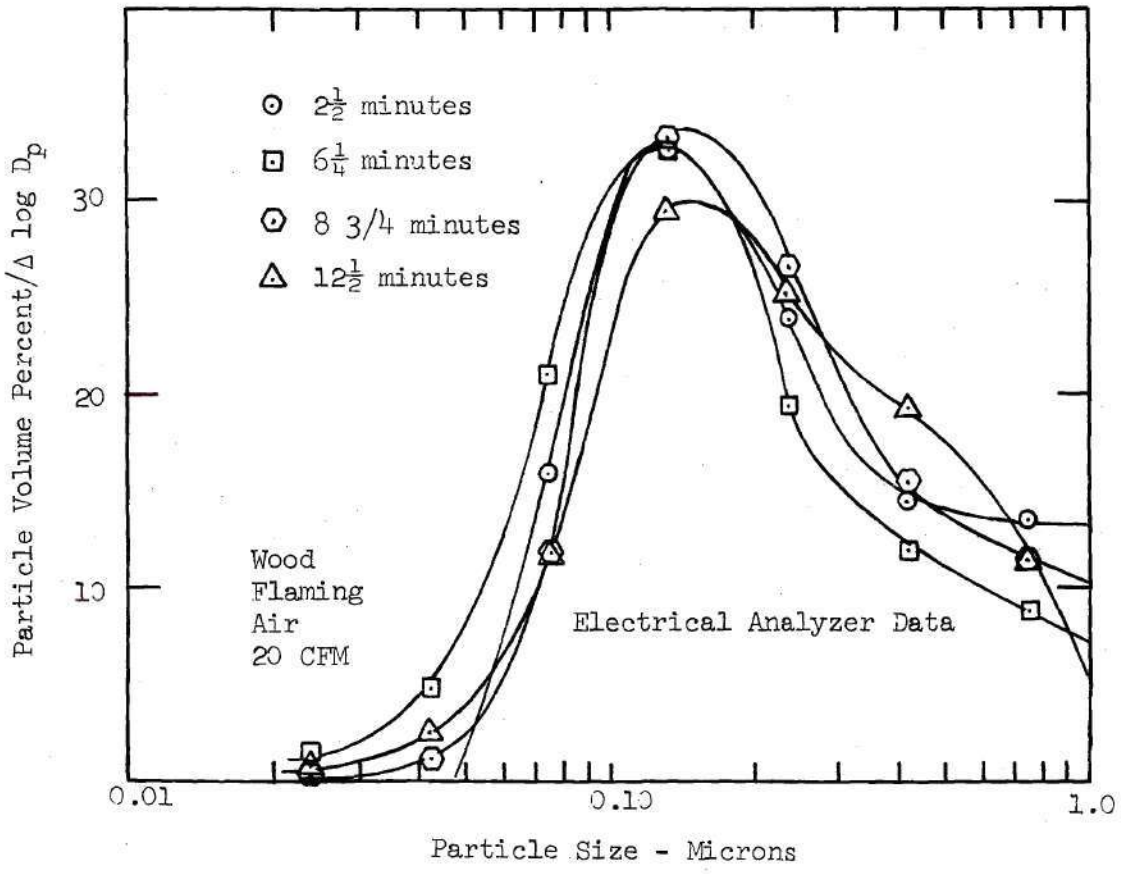

Figure 54. Time Resolved Particle Volume Distribution for Wood Smoke Particles When CPTC Vent Rate is Increased - Flaming in Air

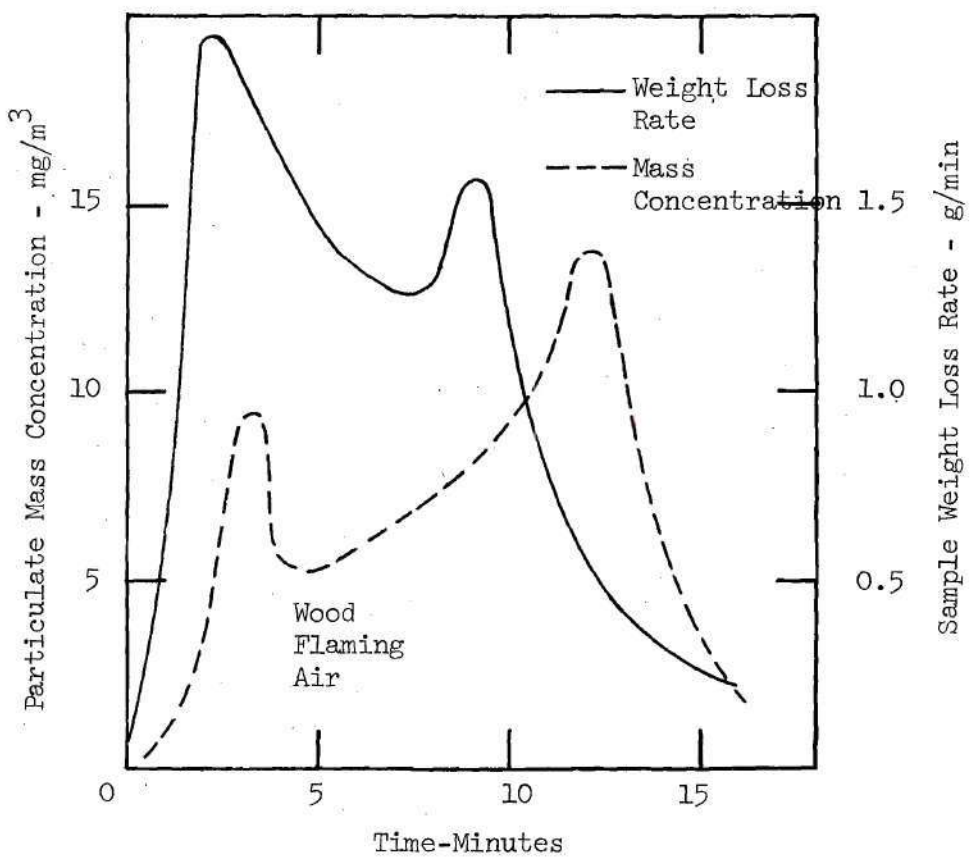

Figure 55. Comparison of Sample Weight Loss Rate With Particulate Concentration for Wood - Flaming in Air

definite peaks during the test. However, it is interesting to note that after the initial peak, sample weight loss rate generally decreases, while particulate mass concentration generally increases. The maximum particulate mass concentration for these conditions is somewhat greater than maximum concentrations measured at 3.2 W/cm^2 under non-flaming conditions, and considerably less than maximum concentrations measured at 6.2 W/cm^2 under non-flaming conditions.

Tests of wood in atmospheres with depleted oxygen concentrations, and using the propane pilot burner, were unsuccessful in regard to sustained flaming of the wood sample. In all tests where oxygen concentrations were below 20 percent, the pilot burner could not maintain flaming conditons at the sample surface. Consequently, smoke produced during these tests was due entirely to pyrolysis of the sample, heated by the propane burner and the radiant heat source at 2.5 W/cm^2. Typical particulate size and concentration data for such a test are given in Figures 56 and 57, for an atmospheric composition of 80 percent N_2, 5 percent O_2, 10 percent CO_2, 5 percent CO. Here, particle sizes are approximately equal to particle sizes measured at the lowest heating rate, i.e., 3.2 W/cm^2, for wood tested under non-flaming conditions. Measured particulate mass concentrations are somewhat higher than those measured at 3.2 W/cm^2 under non-flaming conditions; although they are lower than concentrations measured at 6.2 W/cm^2 under non-flaming conditions.

Discussion of Douglas Fir Results

The flaming combustion of wood or any other polymeric-type

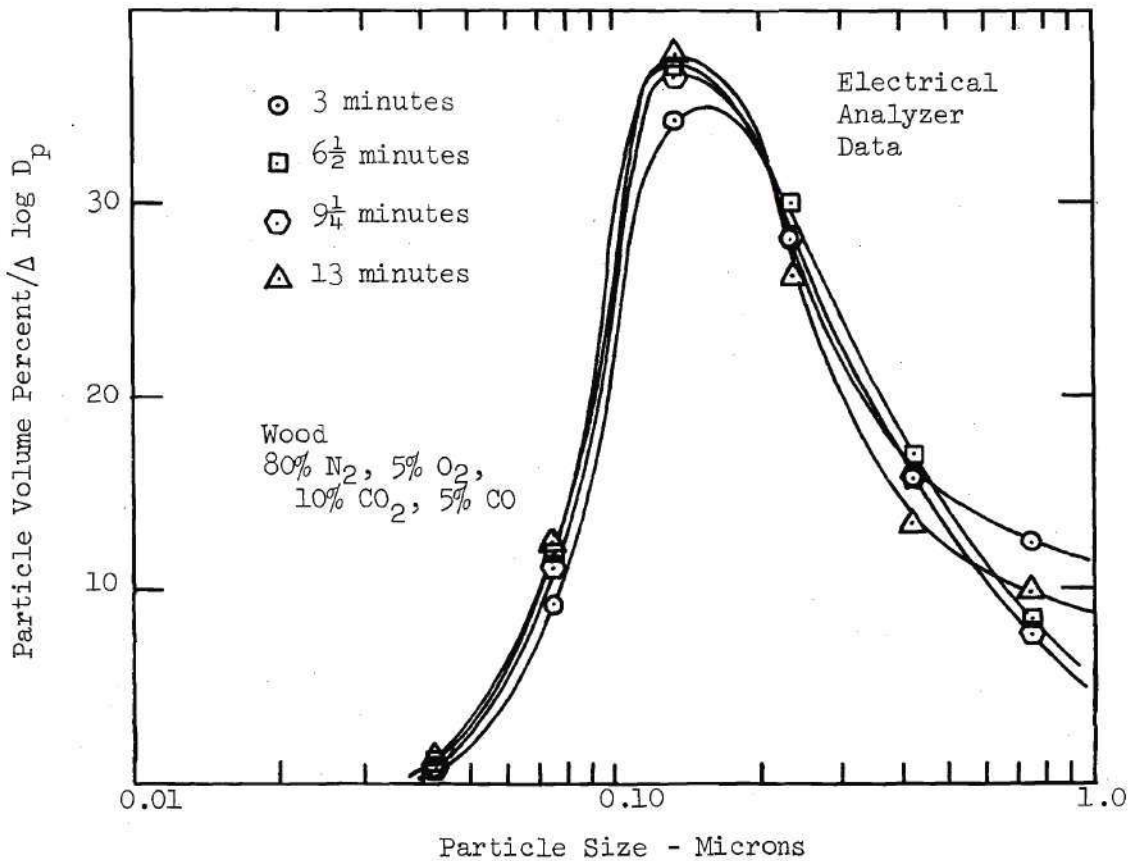

Figure 56. Time Resolved Particle Volume Distribution for Smoke Produced From Smoldering Wood Heated by Propane Flame and 2.5 W/cm^2 Radiant Flux

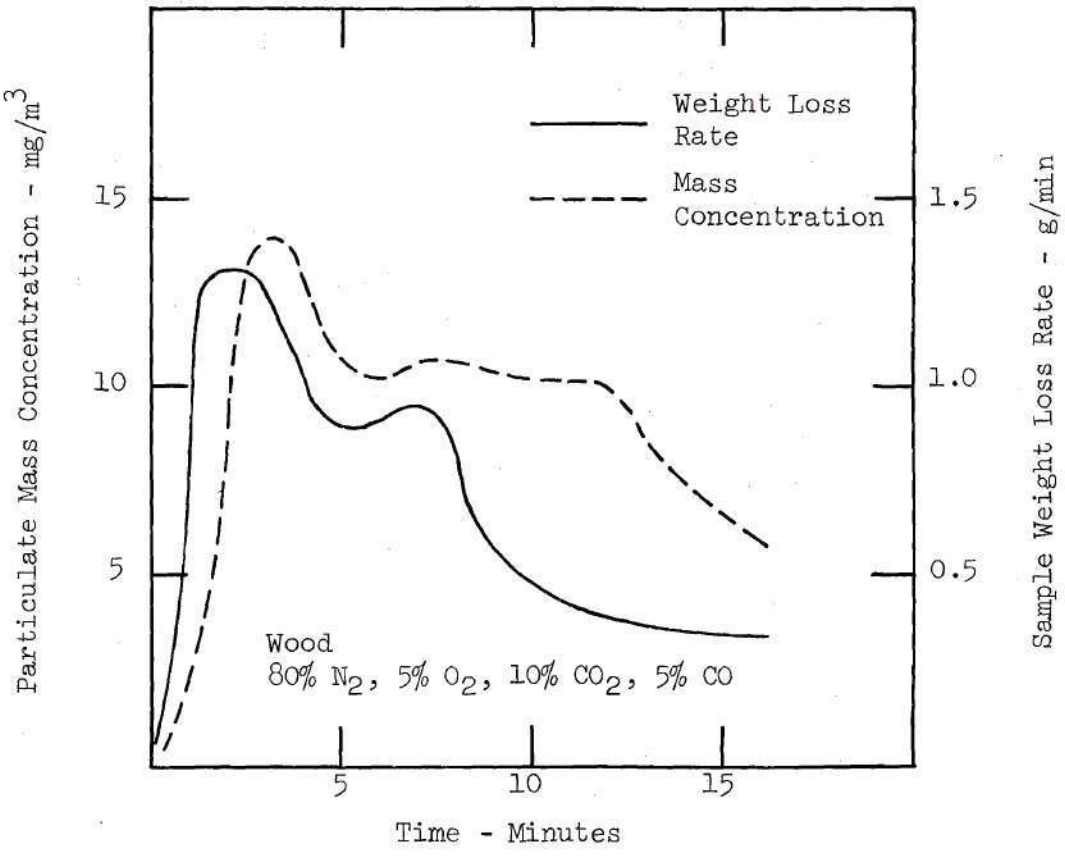

Figure 57. Comparison of Sample Weight Loss Rate with Particulate Concentration for Wood Heated by Propane Flame and 2.5 W/cm^2 Radiant Flux - In 80% N_2, 5% O_2, 10% CO_2, 5% CO

material has been the subject of extensive experimental and theoretical studies, especially in regard to ignition, flame propagation and flame suppression. Polymer and wood flames have generally been characterized as diffusion flames. Heat from the reaction zone is conducted back to the material surface where depolymerization and volatilization of the material provides the fuel that sustains the flaming reaction.[61] Although other researchers have recently argued that some polymer flames may be more "pre-mixed" in nature due to diffusion of unreacted oxygen,[62] the fact remains that fuel is generated by a series of thermal and/or oxidative degradation reactions; and is subsequently reacted exothermically in a flame.

The particulate products then generated under flaming conditions can be from two sources. First, those condensable products which are generated by the degradation of the polymer may escape reaction in the flame, and thus produce particulates of the same nature as generated under strictly non-flaming conditions. However, the dominant portion of solid products from flaming conditions is found to be a black, sooty deposit, and so the following discussion will deal with the generation of soot. The characteristics of unreacted (in a flame) condensable solids and liquids have been reviewed in the discussion of the non-flaming results.

The formation of carbon in flames has been studied extensively, although generally for simplified and well-controlled experimental conditions using simple gaseous or liquid fuels. A good review of carbon formation in gases is given by Palmer and Cullis.[63] An

important aspect of such work to date is the fact that the properties of carbon formed in flames have been found to be relatively independent of the type of flame, the nature of the fuel, and other conditions such as pressure and atmospheric composition.[63] On the other hand, the tendency to form soot has been found to be quite dependent on those conditions.[63] The soot produced in flames most often consists of several spherical particles strung together in necklace-like fashion,[63,64,66] where the small spheres are most frequently between 100 and 500 Å. The appearance of these chain-like particles, as viewed by electron microscope, has been confirmed by in situ optical techniques.[65]

There are several hypotheses concerning the formation of soot particles in flames.[63] However, it is likely that at least two processes are dominant in the formation of the final soot particles.[64] First, the nucleation and growth of the smaller spherical particles must be accounted for; and then the formation of the chain-like particles must be described. The mechanism of nucleation and growth of the smallest particles alone is widely debated although one theory [63] is frequently mentioned. This theory argues that polyunsaturated species in the combustion gases are responsible for nucleation and subsequent growth of the spherical particles. The growth process proceeds by an over-all heterogeneous reaction and/or decomposition of these species to elemental carbon on the hot particle surface, in addition to some coagulation.[63,64,66] The former may also account for the appearance of heavier hydrocarbons usually found

mixed in with combustion generated soot.[63,66] However, experimental difficulties in closing an information gap between nucleation and rapid initial growth of the smaller spheres have prevented complete verification of this, or any other such theory.[66,67] Finally, the formation of the chain-like clusters takes place at an increasing rate as surface growth slows. Random collisions influenced by more pronounced electrostatic interactions have been cited as significant in the appearance of the chain-like particles.

The above-mentioned experimental findings and theories have been established for conditions which are, in many respects, quite different from the conditions studied in this program; i.e., burning polymeric materials. However, some of this information should be applicable to the results reported here for the physical properties of smoke generated during flaming combustion. The characteristic particle sizes measured seem to indicate that long chain agglomerates are formed in flaming wood tests. Size distribution peaks are normally between 1000 and 2000 Å (0.1-0.2 micron). According to the literature, this is indicative of long chain carbonaceous formations. Another possible explanation for such particle sizes, though, is that smaller soot particles could act as nuclei for condensation of unreacted tarry products. Evidence of such a process is indicated in electron microscope photographs of flaming wood smoke particles shown in Reference 29, where particles are apparently spherical in shape.

Although the resultant particle size characteristics were relatively unaffected by CPTC ventilation rates, it was found that

maintenance of stable flaming conditions at the sample surface was very sensitive to vent rate. The fact that particle sizes remained the same over several vent rates is not surprising based on previously reviewed data which indicate that the physical properties of soot formed in flames are relatively independent of atmospheric variables. The sensitivity of flame stability to vent rate is certainly due to local oxygen concentrations, since similar results were observed in atmospheres with depleted oxygen concentrations; i.e., flaming could not be maintained in low oxygen concentrations.

Particulate mass concentration behavior during flaming tests has several interesting aspects. The mass concentration duplicates the major peaks in weight loss at 2-3 minutes and 10-12 minutes; however the trends of the two curves between the peaks are in opposite directions. The relative direction of trends indicates that greater portions of pyrolysis products are escaping without reacting in the flame as the test proceeds. Such a conclusion is based on the fact that for the same sample weight loss rate, particulate mass concentrations are an order of magnitude higher for non-flaming conditions as compared to flaming conditions. This is clearly evident in Figure 14, where the mass concentration drops dramatically when ignition occurs in that "non-flaming" test. During flaming, much of the tarry liquid fraction is converted to gaseous products.

The importance of these results in terms of actual fire hazards is generally the same as previously discussed for the non-flaming results. Since much of the particulate generated during flaming

combustion is simply carbonaceous in nature, it is quite possible that the toxicity factor is not as critical as for non-flaming conditions. On the other hand, the ability of soot to transport toxic gases has been established,[28] and so this factor must remain a concern in terms of toxic effects. Again, the particle sizes measured here can be used in theories predicting the relative ability of a burning material to obscure visibility in actual fire situations. It should also be emphasized that particle sizes measured here are substantially smaller than the one micron average diameter which has been previously assumed in the application of light obscuration theory.[22]

Urethane

Urethane Results

Results of urethane smoke tests conducted under flaming conditions are presented in Figures 58 through 65. However, due to the flame retardant nature of this foam its flaming behavior should first be described. As outlined in Appendix B, a flaming test begins when the propane pilot burner is remotely ignited after a warm-up period required for the radiant heat source. When the burner ignites in urethane tests, a flame covering the entire face of the sample appears almost instantaneously. This flame then quickly rises above the sample and is subsequently extinguished. Normally, this flame front travels no more than 2 or 3 inches above the sample holder before the CPTC ventilation gases dilute and thus quench the flame. The actual "flaming" during these urethane tests occurs, then, for a

period of 30 seconds or less. Sample weight loss data will later show that much of the sample mass loss takes place during this period; where the sample weight was typically reduced after one minute by one-third of the total weight lost for the test. Particulates collected during these tests were, for the most part, "sooty" in nature.

Figures 58 through 62 give particle size data for flaming urethane tests run in five different atmospheric compositions. As in data taken during flaming wood tests, the particle size distributions generally fall within the range of the Electrical Aerosol Analyzer; i.e., less than one micron. Also, since flaming is confined to the first minute of urethane tests, only the first size distribution measured at the beginning of the test is indicative of particle sizes generated during flaming combustion. Later measurements are of particulates generated by the pyrolysis of that foam material remaining after the initial decomposition period; i.e., after the first minute. Notably, there are only slight differences evident between the initial measured size distribution and later size distributions for all atmospheric compositions considered. Where differences are apparent, particle sizes tend to be slightly larger during the period when actual flaming occurs. Those particle size characteristics indicated during the flaming period of urethane tests are quite similar to those measured during flaming wood tests. Particle size distribution peaks are well below 0.5 micron in both cases. Finally, it is clear that changes in atmospheric compositions have little effect on the smoke particle sizes generated during flaming urethane tests.

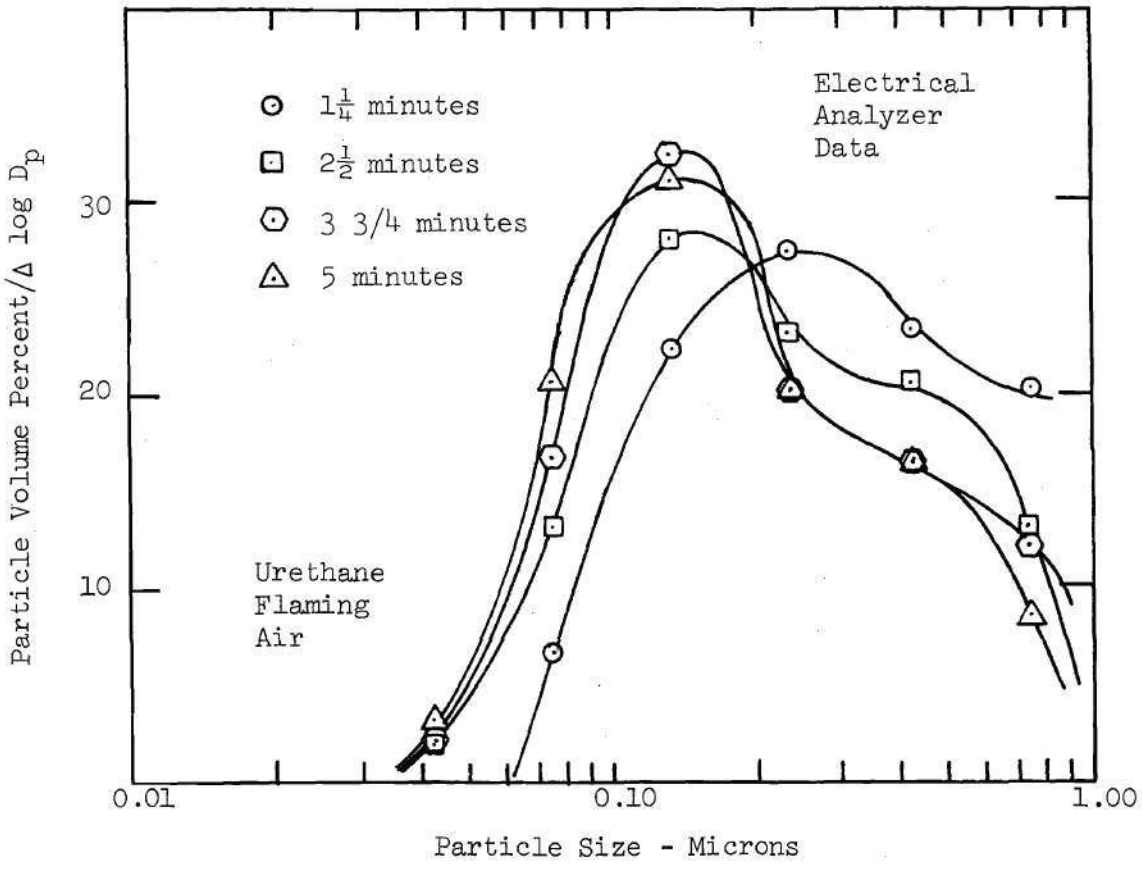

Figure 58. Time Resolved Particle Volume Distribution for Urethane Smoke Particles Less than 1.0 Micron - Flaming in Air

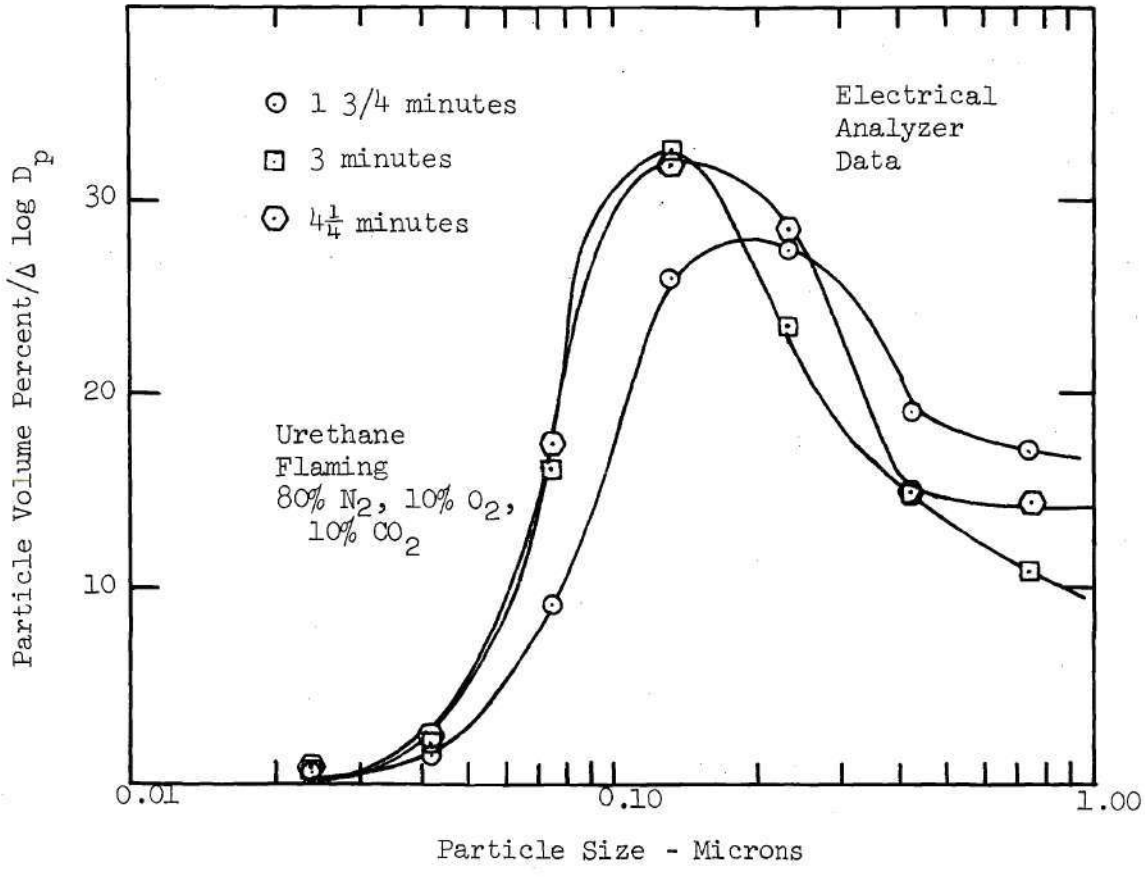

Figure 59. Time Resolved Particle Volume Distribution for Urethane Smoke Particles Less than 1.0 Micron - Flaming in 80% N_2, 10% O_2, 10% CO_2

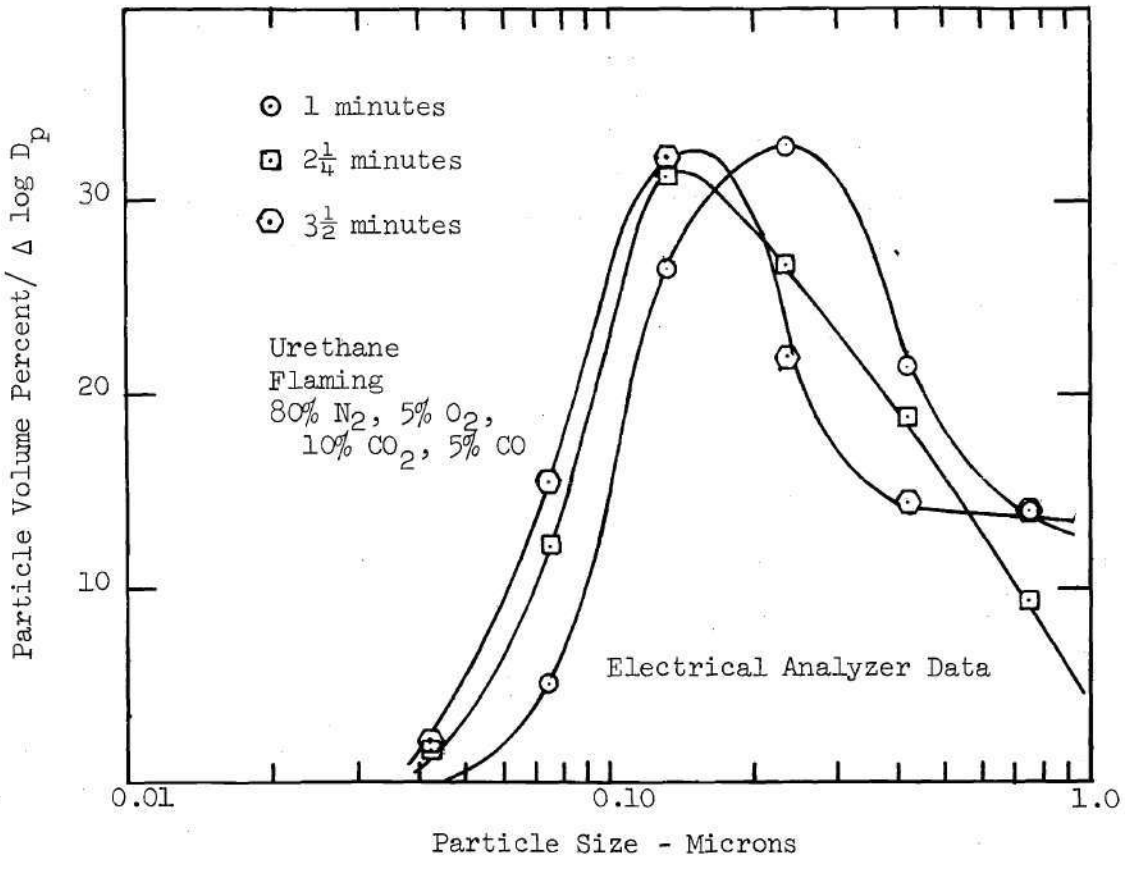

Figure 60. Time Resolved Particle Volume Distribution for Urethane Smoke Particles Less than 1.0 Micron - Flaming in 80% N_2, 5% O_2, 10% CO_2, 5% CO

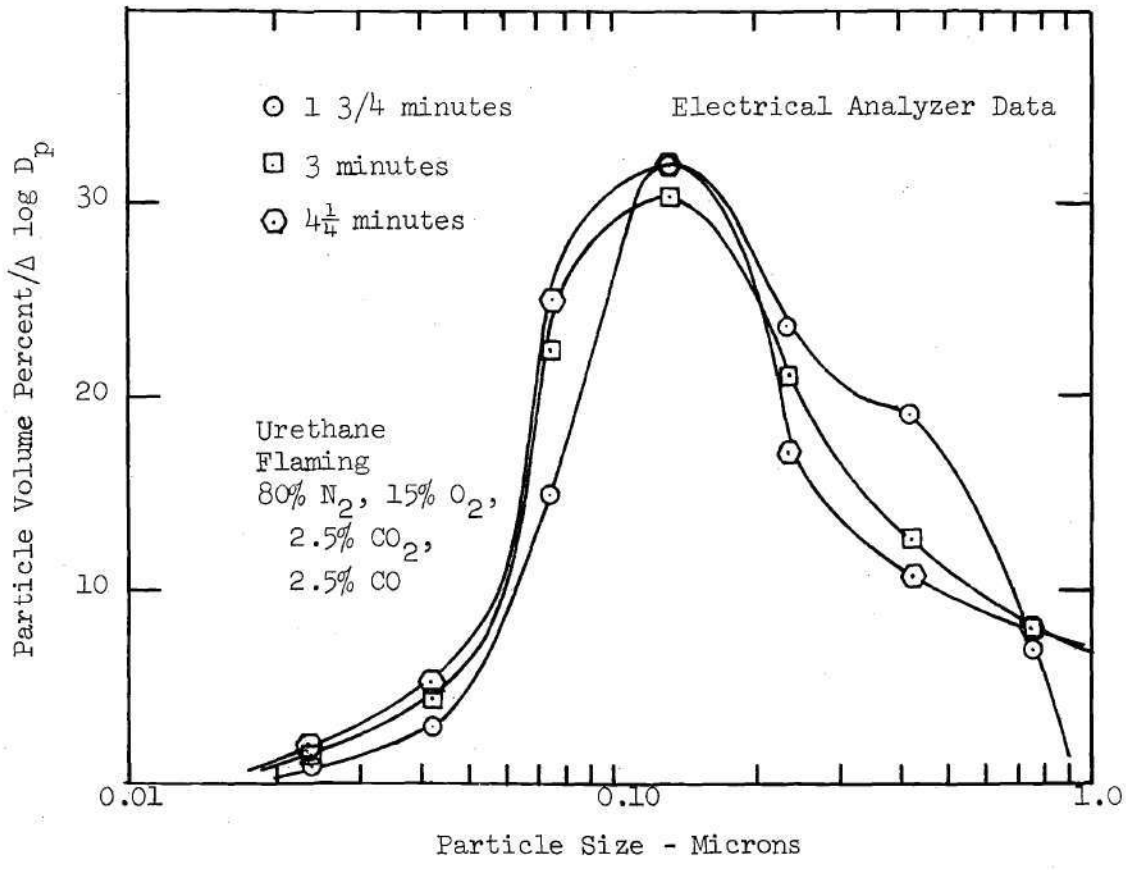

Figure 61. Time Resolved Particle Volume Distribution for Urethane Smoke Particles Less than 1.0 Micron - Flaming in 80% N_2,15% O_2, 2.5% CO_2, 2.5% CO

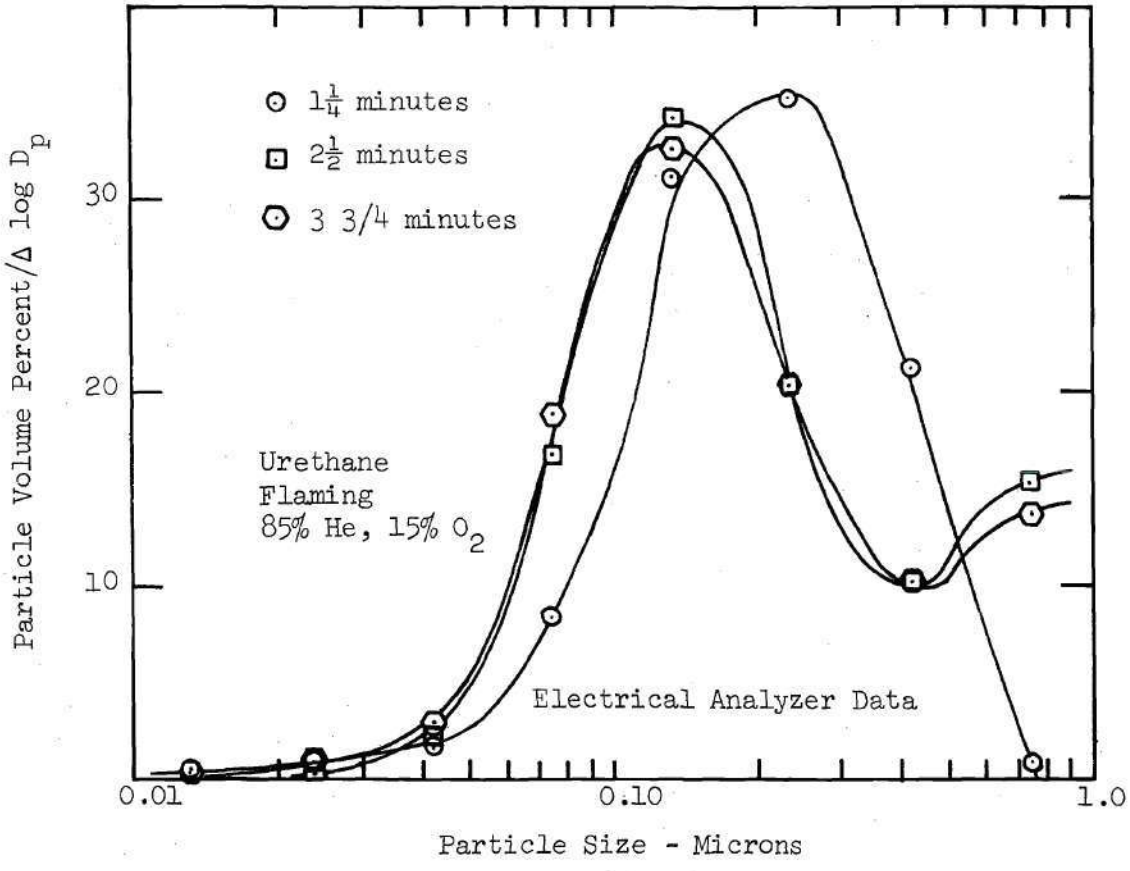

Figure 62. Time Resolved Particle Volume Distribution for Urethane Smoke Particles Less than 1.0 Micron - Flaming in 85% He, 15% O_2

The comparison shown in Figure 63 of particulate mass concentrations measured during tests of the urethane foam under flaming conditions, show qualitatively similar behavior for tests run in several atmospheres. The maximum particulate mass concentrations seem to fluctuate over a range of values, although all are of the same order of magnitude. Figures 64 and 65 give typical weight loss rate data for the flaming urethane foam. Comparisons with the corresponding particulate mass concentrations are also shown in Figures 64 and 65. Maximum particulate mass concentrations are somewhat greater than maximum concentrations measured at 6.2 W/cm^2 in non-flaming tests, and less than maximum concentrations measured at 9.2 W/cm^2 in non-flaming tests.

Discussion of Urethane Results

The type of flame observed for the flame retarded urethane foam probably cannot be classified as the diffusion flame described in the discussion of the flaming wood results. Apparently, more volatile, flammable pyrolysis products build up near the surface of the sample during heater warm-up, and then are quickly ignited when the pilot burner is ignited. Then almost as quickly, the flame retardant additive becomes involved in the reaction kinetics (possibly as some type of intermediary) and subsequently the reaction is interrupted. The combined effects of flame retardant, insulating char layer and depletion of virgin material prevent further adequate production and subsequent ignition of flammable pyrolysis products.

Since previously reviewed information[63] has indicated that

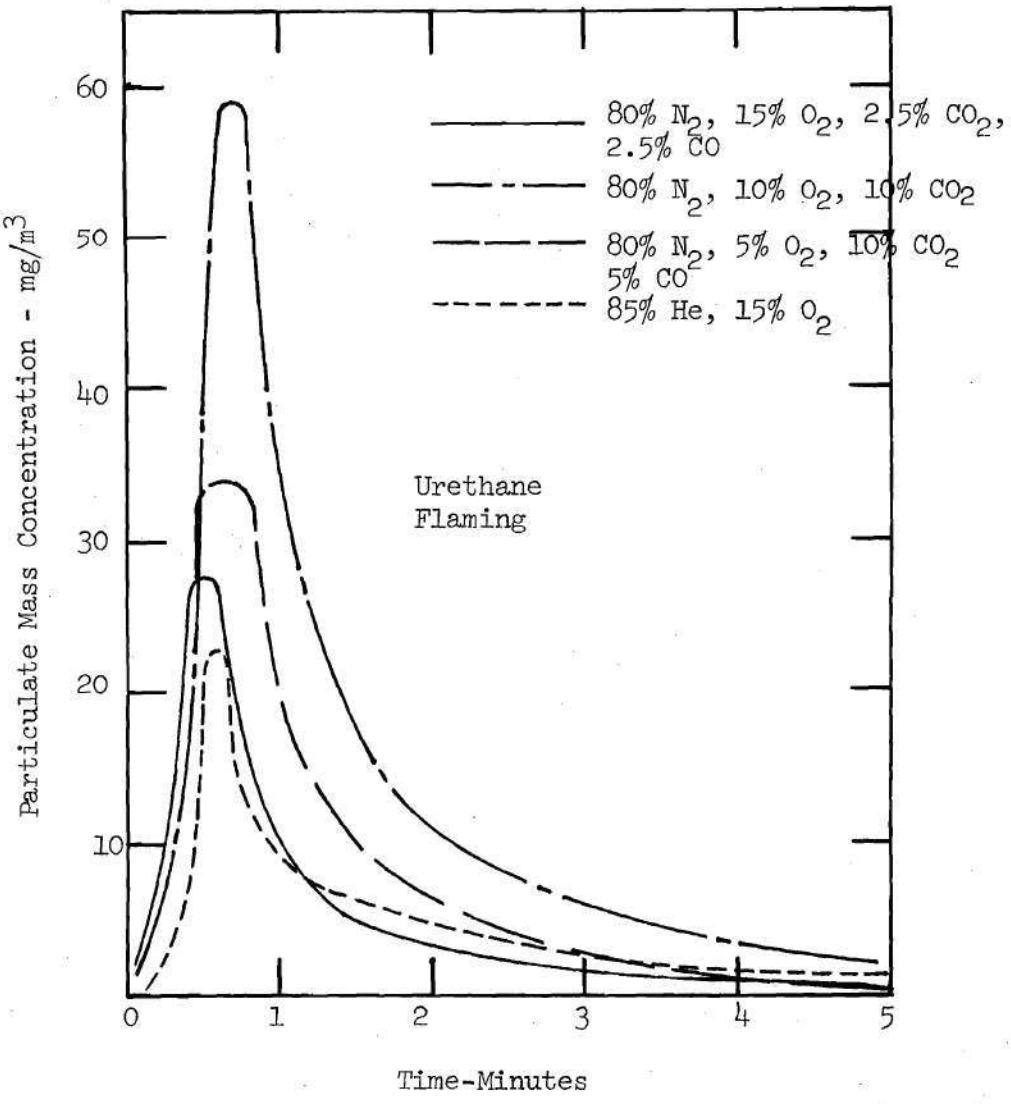

Figure 63. Typical Particulate Mass Concentrations Measured for Urethane Smoke Particles Under Flaming Conditions

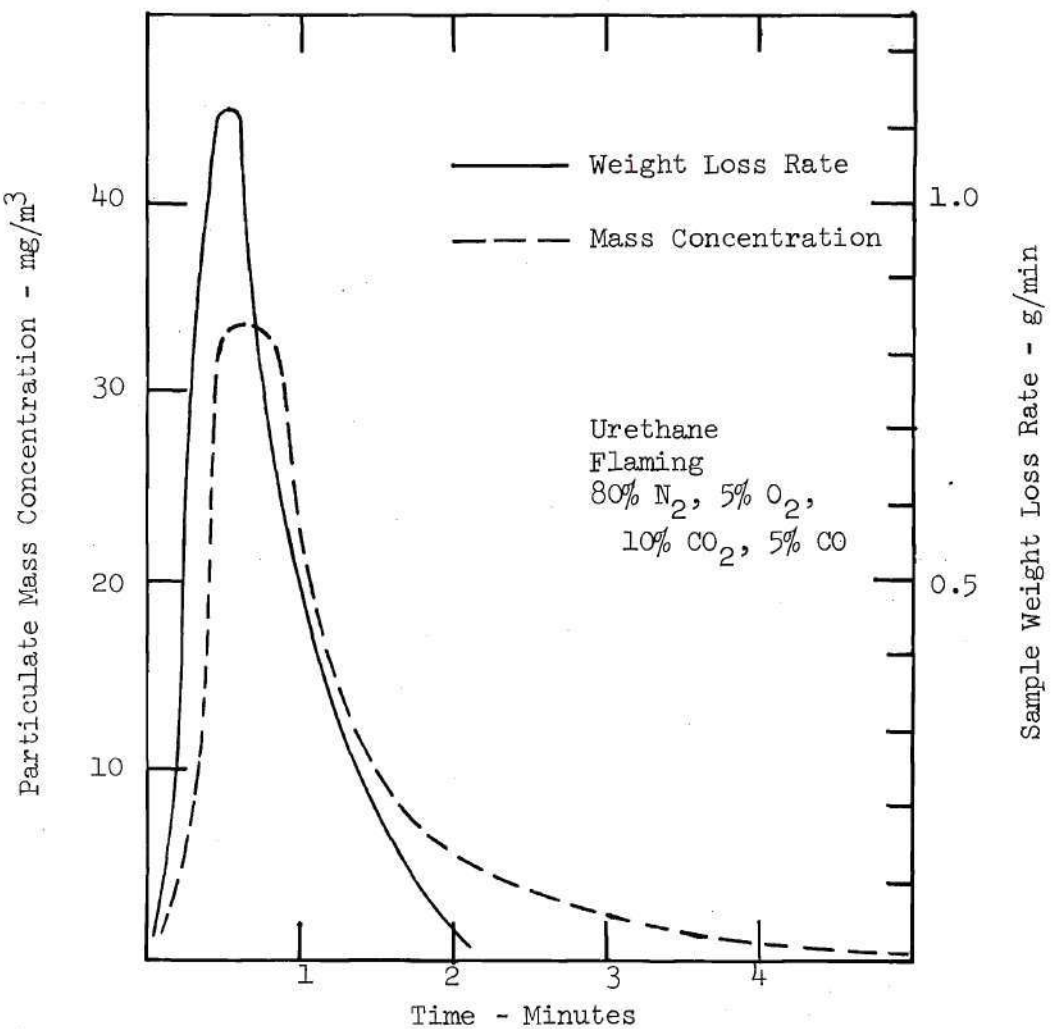

Figure 64. Comparison of Sample Weight Loss Rate With Particulate Concentration for Urethane - Flaming in 80% N_2, 5% O_2, 10% CO_2, 5% CO

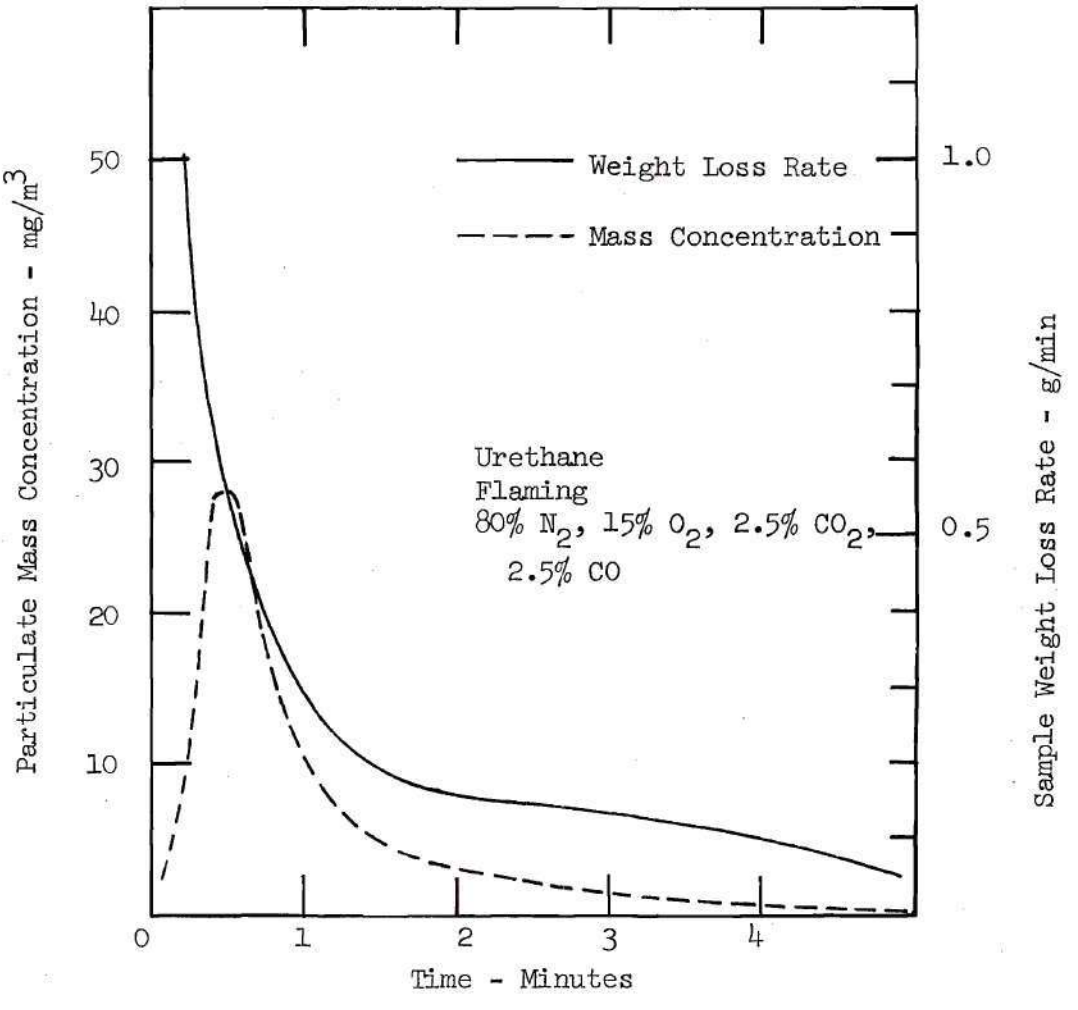

Figure 65. Comparison of Sample Weight Loss Rate With Particulate Concentration for Urethane - Flaming in 80% N_2, 15% O_2, 2.5 % CO_2, 2.5% CO

the physical characteristics of smoke produced in flames is relatively independent of the type of flame (and the type of fuel), the general background provided in the discussion of soot formation from flaming wood should apply equally well here. In fact, the results for flaming urethane seem to confirm this fact, because the size characteristics measured for flaming urethane smoke seem to be very nearly the same as those for wood. Size distribution peaks are near 2000 Å (0.2 micron) with the greatest volume fraction of particles measured well below 0.5 micron. Thus, these particles may be composed of long chain-like formations of smaller spherical soot particles or it may be possible that smaller soot particles act as nuclei for condensible vapors that escape unreacted in the flame. Variations in atmospheric composition had little effect on flame behavior and smoke particle size characteristics for flaming urethane tests. This provides further evidence that soot particles formed under a variety of conditions exhibit the same or similar particle size characteristics.

Measured particulate mass concentrations correlate closely with the weight loss rate behavior of burning urethane samples, thus following trends established under non-flaming conditions. Maximum sample weight loss rates were comparable to maximum weight loss rates measured at a 9.2 W/cm^2 heating rate in non-flaming tests, while maximum mass concentrations in most cases were near maximum mass concentration values measured at a heating rate of 6.2 W/cm^2 in non-flaming tests. Thus, for the same sample weight loss rate, particulate mass concentrations are higher for non-flaming conditions as compared

to flaming conditions. As pointed out in the discussion of flaming wood results, this is due to the reaction of condensable pyrolysis products in the flame, which otherwise contributes to the smoke particulate fraction under non-flaming conditions. The fact that this observed tendency (of flaming samples to generate less particulate mass than non-flaming samples at the same weight loss rate) is less prominent for urethane than it is for wood samples may be due to the fact that particulate products of urethane pyrolysis are less flammable (reactive) than the particulate products from the thermal degradation of wood. Comparison of particulate mass concentration data from several atmospheres shows the behavior to be virtually the same for all atmospheres. Maximum concentrations do vary, although there seems to be no clear correlation with changes in atmospheric composition. Observed variations in maximum particulate mass concentrations might then be due to sample non-uniformities or ambiguities from measurement techniques as discussed in Appendix C. The results are thus presented to show only the typical qualitative mass concentration behavior in the four atmospheres.

Comments relevant to the actual fire hazards created by smoke generated during flaming combustion have been previously presented in the discussion of results from flaming wood tests. Therefore, since particle characteristics for flaming urethane smoke are similar to the characteristics for wood smoke under the same conditions, the discussion regarding the effects of such particulates for wood smoke is also applicable to rigid urethane foam. The reader

is referred to that section for comments on the possible toxic hazards of the particulates observed in flaming combustion, and the potential theoretical applications of these measurements in the area of light obscuration.

Polyvinyl Chloride

PVC Results

Results obtained for tests of polyvinyl chloride plastic under flaming conditions are presented in Figures 66 through 71. Particle size characteristics are shown for all atmospheric compositions tested and representative particulate mass concentrations are presented for two of those vent gas compositions. Andersen Sampler data has again been omitted due to uncertainties caused by small particle sizes and low mass concentrations. The behavior of the PVC sample during a test was similar in some respects to the behavior of samples during non-flaming tests. Specifically, as the temperature of the sample increased, the face of the sample tended to bulge out as described previously in the discussion of non-flaming results. Flaming was generally erratic over the face of the sample, especially after the "bulge" had appeared. Furthermore, flame behavior was extremely erratic in two of the atmospheric compositions; i.e., 80 percent N_2, 5 percent O_2, 10 percent CO_2, 5 percent CO and 85 percent He, 15 percent O_2. This can be attributed to the effects of low oxygen concentrations and interference with the propane pilot flame by the expanded sample face. The sample bulge affected the operation of the pilot flame in most circumstances; however the flaming of the

sample itself was severely affected only in the two atmospheres mentioned above.

The particle size characteristics shown in Figures 66 through 70 are typical of results previously obtained for smoke produced under flaming conditions by other materials. Slight variation in particle sizes is evident during some tests, however this appears to be insignificant. Most of the volume fraction of particles is well below 0.5 micron in diameter, although it seems that these sizes are slightly larger than those measured for wood and urethane under flaming conditions. Variations in atmospheric compositions had no visible effect on particle sizes, in spite of the fact that flaming conditions were adversely affected in two atmospheres. In the atmosphere of 80 percent N_2, 5 percent O_2, 10 percent CO_2, 5 percent CO, the PVC sample burned only for the first two minutes of the test. During the test in helium, the sample flickered infrequently over a two minute period before the test was terminated.

Typical particulate mass concentration data are shown in Figure 71 for two of the atmospheric compositions. Here, the overall order of magnitudes are comparable, although the curves do show different behavior. This is probably due to nonuniform development of the char structure for these flaming PVC tests. As pointed out earlier, the formation of the char adversely affected flaming conditions, which would then cause irregular particulate mass concentration behavior.

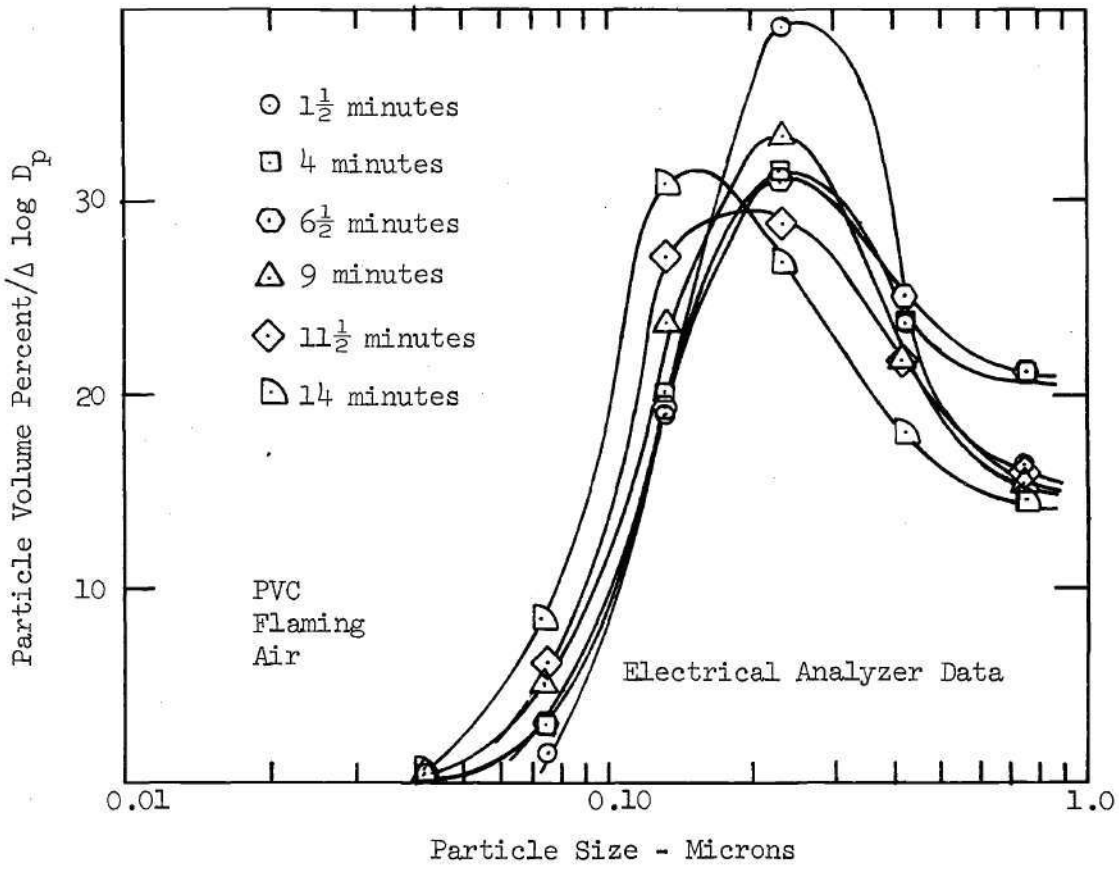

Figure 66. Time Resolved Particle Volume Distribution for PVC Smoke Particles Less than 1.0 Micron - Flaming in Air

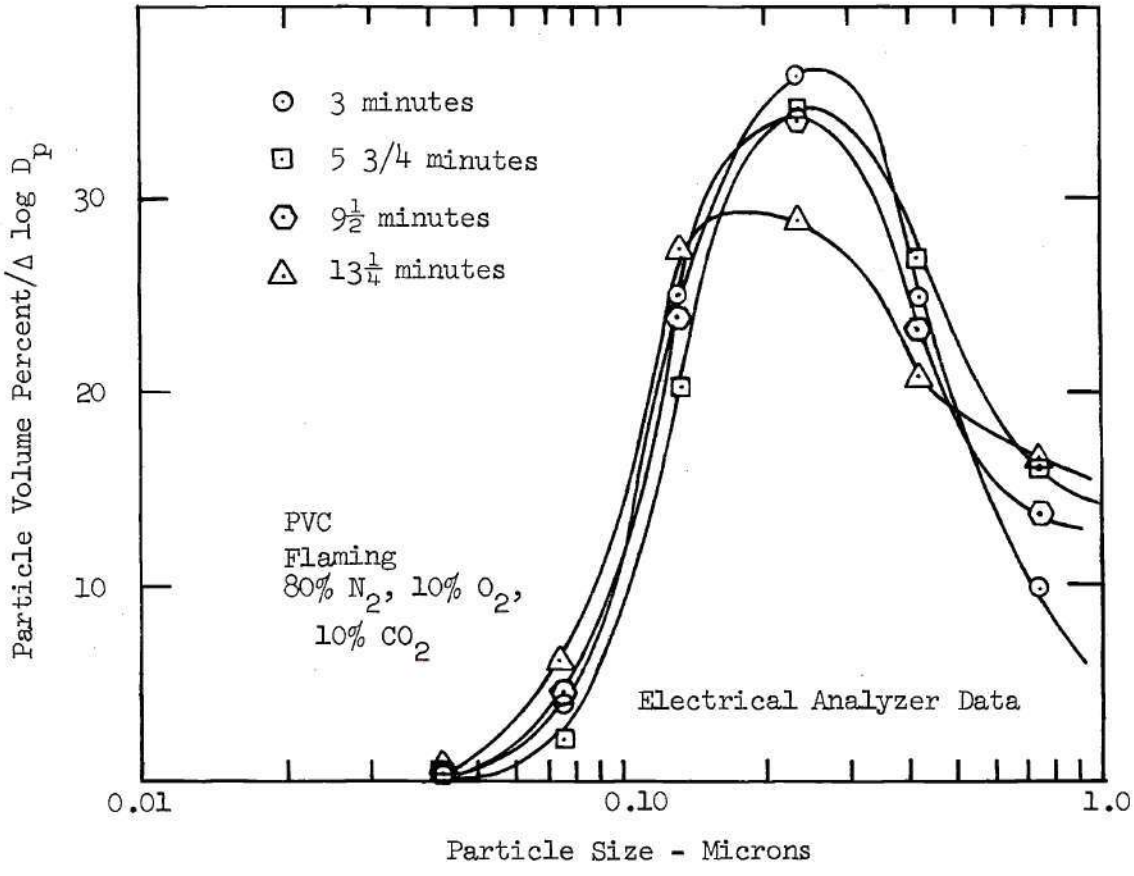

Figure 67. Time Resolved Particle Volume Distribution for PVC Smoke Particles Less than 1.0 Micron - Flaming in 80% N_2, 10% O_2, 10% CO_2

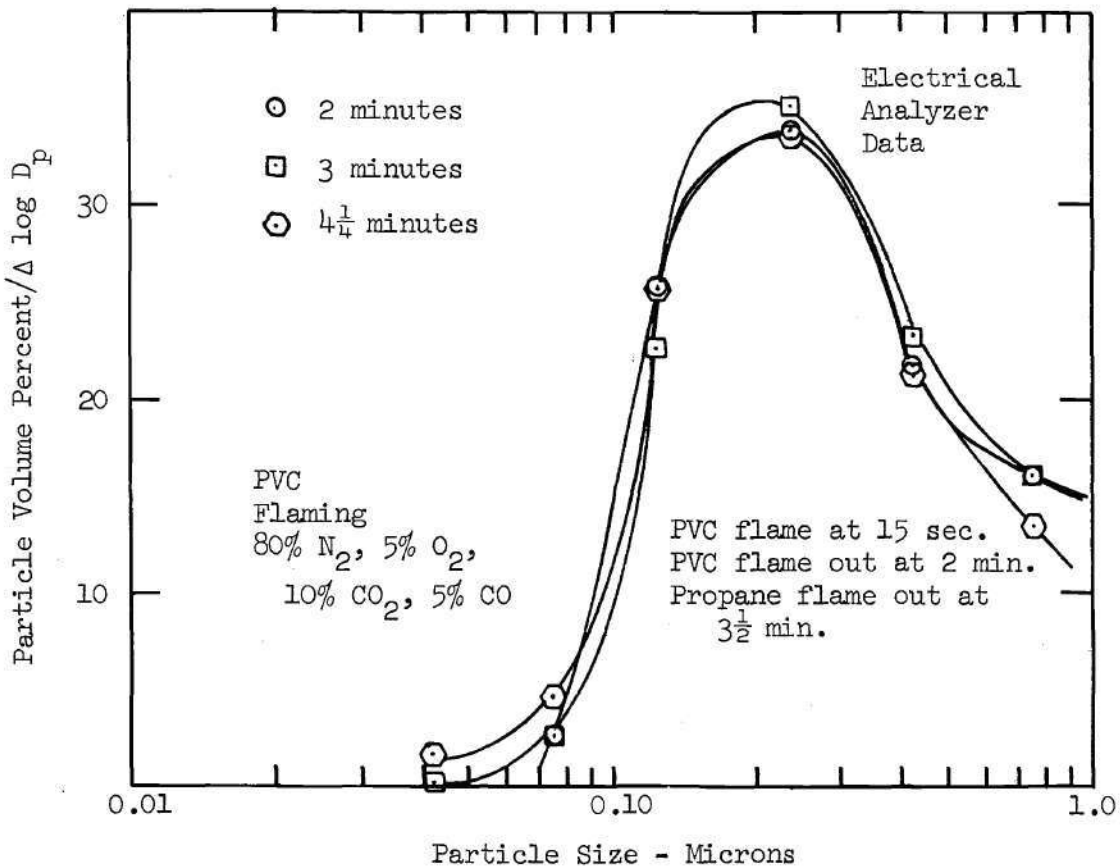

Figure 68. Time Resolved Particle Volume Distribution for PVC Smoke Particles Less than 1.0 Micron - Flaming in 80% N_2, 5% O_2, 10% CO_2, 5% CO

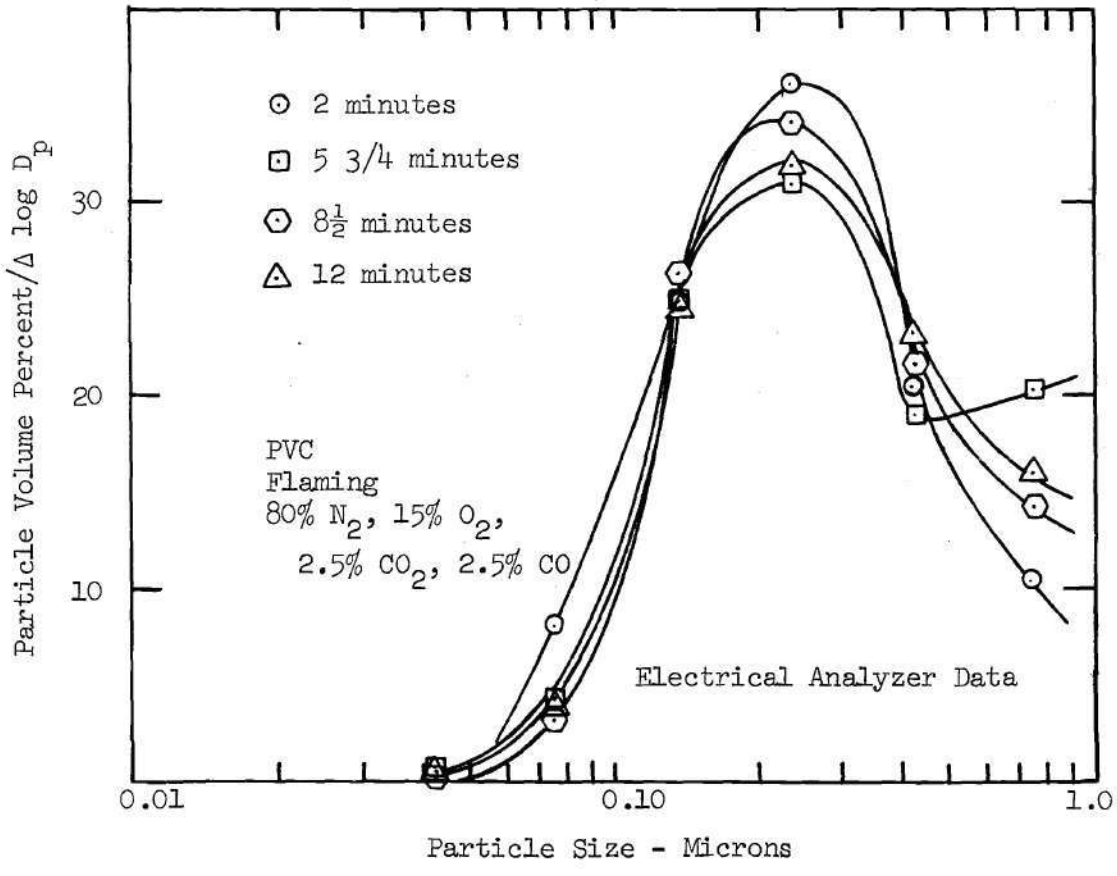

Figure 69. Time Resolved Particle Volume Distribution for PVC Smoke Particles Less than 1.0 Micron - Flaming in 80% N_2, 15% O_2, 2.5% CO_2, 2.5% CO

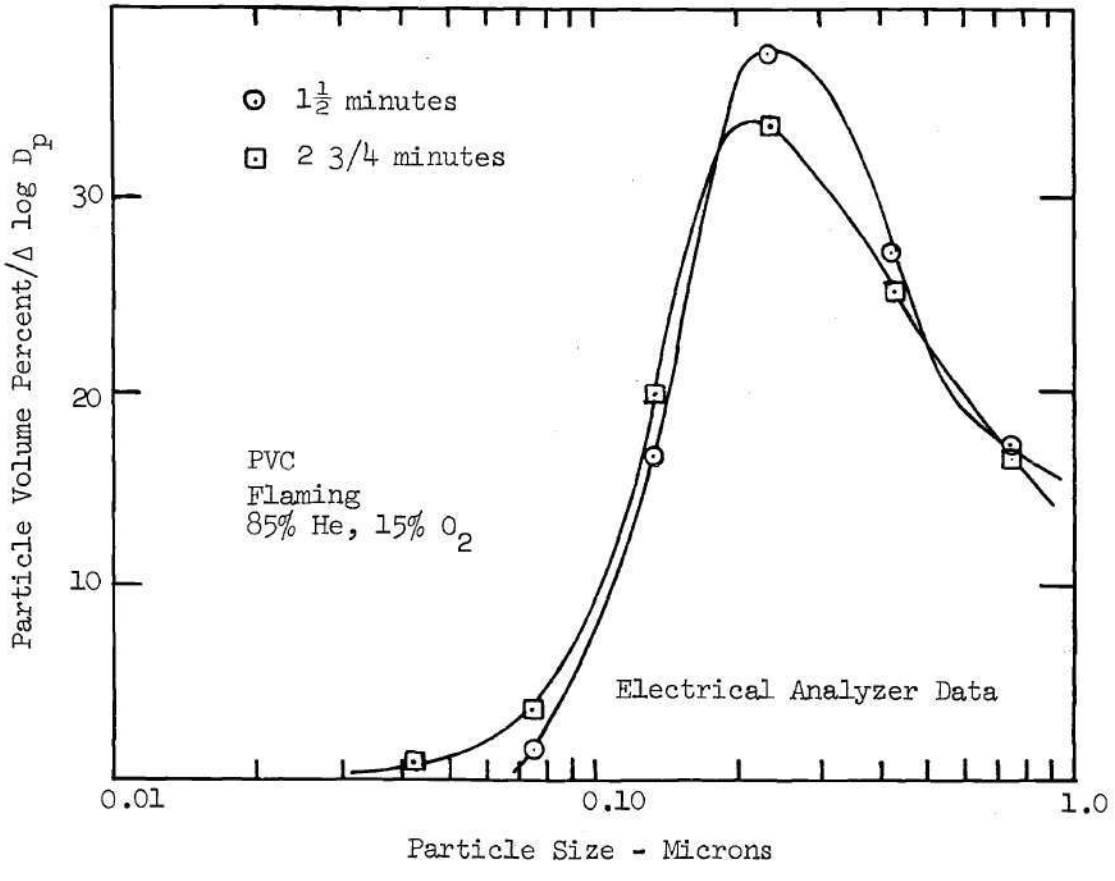

Figure 70. Time Resolved Particle Volume Distribution for PVC Smoke Particles Less than 1.0 Micron - Flaming in 85% He, 15% O_2

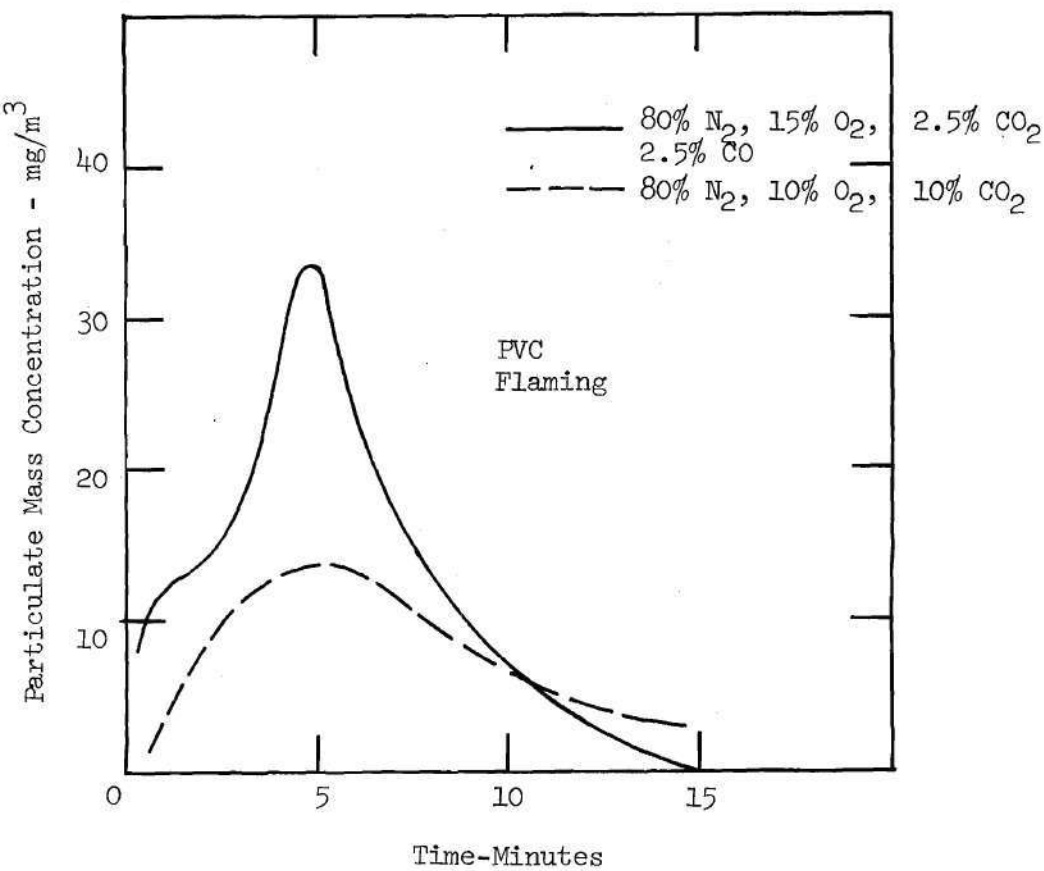

Figure 71. Typical Particulate Mass Concentrations Measured for PVC Smoke Particles Under Flaming Conditions

Discussion of PVC Results

The flaming conditions observed during the tests of PVC using the pilot igniter are typical of the polymer flame characteristics reviewed earlier for wood. However, the greater degree of char formation observed for PVC appears to have adversely affected flame stability. That is, as the char layer forms, heating of interior regions of the sample is inhibited; and the flow of flammable degradation products is slowed. Fuel to the diffusion-type flame is thus restricted and unstable burning conditions are the end result.

Nevertheless, it has become clear from previous discussions of wood and urethane results that the physical properties of smoke particles generated during flaming tests are relatively insensitive to the type of flaming conditions observed during tests. Measurements of flaming PVC smoke are consistent with this conclusion, although particle sizes are slightly larger than for flaming wood and urethane. This may be due in part to the fact that the thermal degradation of PVC generates a number of aromatic hydrocarbons which are particularly noted for soot production.[63] This could then lead to more extensive agglomeration of soot particles resulting in somewhat larger measured particle sizes for flaming PVC smoke. Otherwise, the atmospheric composition and observed flame behavior have little affect on particle sizes. Therefore, consideration of known information relating to smoke formation in flames leads to the same type of mechanisms previously discussed for flaming wood and urethane. Specifically, surface growth of smaller soot particles is probably followed by

agglomeration to large chain-like particles of 3000 Å diameter or greater. In addition, the smaller particles can act as nuclei for the condensation of unreacted condensable degradation products to produce particles greater than 1000 Å (0.1 micron) in diameter.

Particulate mass concentration data for flaming PVC tests in two atmospheres show differences in mass concentration behavior between the two atmospheres. However, this is probably due more to the peculiar behavior of the developing char structure, than to actual effects of atmospheric compositions. Differences in maximum particulate concentrations are not significant in view of the uncertainties of Mass Monitor measurements discussed in Appendix C.

Measurements of the physical properties of smoke produced from burning PVC under flaming conditions have shown the same trends and nearly the same numerical magnitudes as those measurements for flaming wood and urethane. Thus, discussions relevant to toxicity and light obscuration previously given will not be repeated here. The reader is referred to the discussion of flaming wood results in particular. However, it should be emphasized that the results obtained by Stone[28] were specifically obtained for PVC. There he found that soot produced from flaming PVC can transport HCl on the surface of the particles. Therefore, this is definitely a concern from a toxicological point of view in flaming PVC tests, since it has been shown that HCl can be transported deeper into the respiratory system via particles than via a gas phase mechanism.[28]

CHAPTER V

REVIEW AND CONCLUSIONS

In the preceding pages, a systematic investigation into the physical characteristics of smoke particulates generated by burning polymers has been described. Recently developed test methods provide important new information with both practical and theoretical applications. In summary, the following results and conclusions from this research are emphasized.

1. Small-scale test methods have been successfully developed and utilized in a new Combustion Products Test Chamber (CPTC) for the determination of the physical characteristics of smoke particulates. Tests of materials have been carried out under different environmental conditions, especially selected for their relevance to actual fire situations in buildings. Thus, information on the smoking properties of materials may be obtained for conditions not previously considered in other such test programs. The flow-through characteristics of the CPTC allow for accurate control of atmospheric composition and provide uniform conditions for sample combustion. Also, the dilution of smoke by vent gases tends to preserve the characteristics of the aerosol once the smoke has left the immediate vicinity of the sample. Finally, the Aerosol Sampling System developed in conjunction with these test methods has proven to be a reliable means for making particle size and concentration measurements for smoke generated by

materials under flaming and non-flaming conditions. Uncertainties due to the 1/4 inch sampling probe dilution requirements, however, reduce the quantitative value of the particulate mass concentration data.

2. Important new information on the particle size characteristics of smoke particulates generated by burning three commonly used building materials has been provided. Such information has been shown to be important in the analysis of smoke hazards, especially in the areas of toxicology and loss of visibility. Thus, the dangers from the inhalation of smoke particulates and the relative ability of smokes to obscure visibility might then be more adequately determined given the new results provided here.

3. The effects of changes in atmospheric composition on the smoke particulate characteristics measured during the burning of wood, rigid urethane and PVC have been found to be relatively minor. No trends in particle size behavior are evident with variations in oxygen concentration for tests of all three materials under flaming conditions. Measured particle sizes from non-flaming tests of wood samples also showed definite insensitivity to changes in atmospheric composition. Non-flaming tests of urethane and PVC exhibited some changes in particle size characteristics for different ventilation gas mixtures; however these variations are not large and they cannot be definitely correlated with atmospheric composition at this time. Particulate mass concentrations also gave no clear evidence of dependence on ventilation gas compositions within the accuracy of these measurements.

Thus, these results indicate that particulate generation from smoldering materials is quite probably thermal in nature, with no significant secondary chemical reactions (with atmospheric constituents) influencing measured mass concentrations and particle sizes. The fact that the physical characteristics of particulates formed during flaming combustion are relatively independent of atmospheric composition is consistent with previous studies of soot formation in flames.

4. Qualitative and quantitative differences in smoke particulate characteristics have been observed between non-flaming and flaming combustion of all three materials studied. At comparable sample weight loss rates, smoke particles tend to be smaller and particulate mass concentrations lower during flaming combustion. Furthermore, the physical appearance of particulates generated under flaming and non-flaming conditions are considerably different. Observation of particles collected on impaction plates shows a complex mixture of liquid and/or solid organic materials from non-flaming combustion, and a sooty carbonaceous deposit mixed with other liquids and/or solids from flaming combustion. Differences in particulate mass concentrations are due to the reaction of otherwise condensable solids and liquids in the flame, where non-condensable (at room temperature) gases and soot are dominant products. For the same sample weight loss, the concentration of condensable species is thus reduced considerably by the flame and lower mass concentrations are the result when compared to non-flaming conditions. Also, soot generation in flaming combustion clearly does not compensate for the

decrease in particulate mass concentrations due to the reduction in condensable pyrolysis products. Finally, particle sizes observed during flaming combustion indicate the presence of large chain-like sooty agglomerates, whereas particles formed during non-flaming combustion are either liquid droplets or fragments of polymeric materials.

5. In the case of smoldering or non-flaming combustion both particle sizes and particulate mass concentrations were found to depend on the radiant heat flux received at the face of the sample. This was generally the case for all three materials and all atmospheric compositions. Increases in particle sizes and maximum particulate mass concentration levels were most pronounced when radiant heating increased from 3.2 W/cm^2 to 6.2 W/cm^2. For these conditions particle volume distribution peaks increased from below 0.5 micron to near one micron for all three materials. At 9.2 W/cm^2 radiant flux particle sizes were not significantly different from those measured at 6.2 W/cm^2. Upon increase in radiant flux from 3.2 W/cm^2 to 6.2 W/cm^2, maximum particulate mass concentrations increased by an order of magnitude for the three materials tested. However, no definite trends were established for particulate mass concentration levels when the heating rate was further increased to 9.2 W/cm^2. Time-resolved particle volume distribution data show that particle sizes vary with particulate mass concentration levels; e.g., particles are largest when mass concentrations are greatest. Furthermore, particulate mass concentrations are closely related to the rate at which the sample loses mass during the test. These results are found to be especially

significant in view of standard materials smoke test methods which utilize relatively low radiant heating rates. In order to obtain meaningful results in the determination of relative smoke hazards, materials should be tested under conditions more closely related to actual fire situations.

6. Comparison of particle size results from each of the three materials shows that not only do the same trends hold for Douglas fir, urethane and PVC, but also measured quantitative values compare favorably for the same test conditions. Smoke particle sizes measured for each of the three materials under non-flaming conditions at 6.2 W/cm^2 are presented in Figure 72. There are clearly some differences in the results; e.g., urethane particles generated at 6.2 W/cm^2 in non-flaming tests are somewhat larger than those produced in the same manner by wood and PVC. Also, the characteristic size distribution curves are not necessarily similar in shape for the three materials. However, the relative agreement of quantitative values among materials is an interesting aspect of these results.

7. The measurements of particulate characteristics made in this program do not provide the information necessary for a detailed analysis of the fundamental mechanisms involved in particulate generation by burning materials. However, these data do provide information from which some conclusions may be drawn. For example, in the case of non-flaming combustion, it is not clear whether the chemical formation of condensible liquids and/or solids takes place in the solid phase (of the pyrolysis zone) or in the gas phase as the

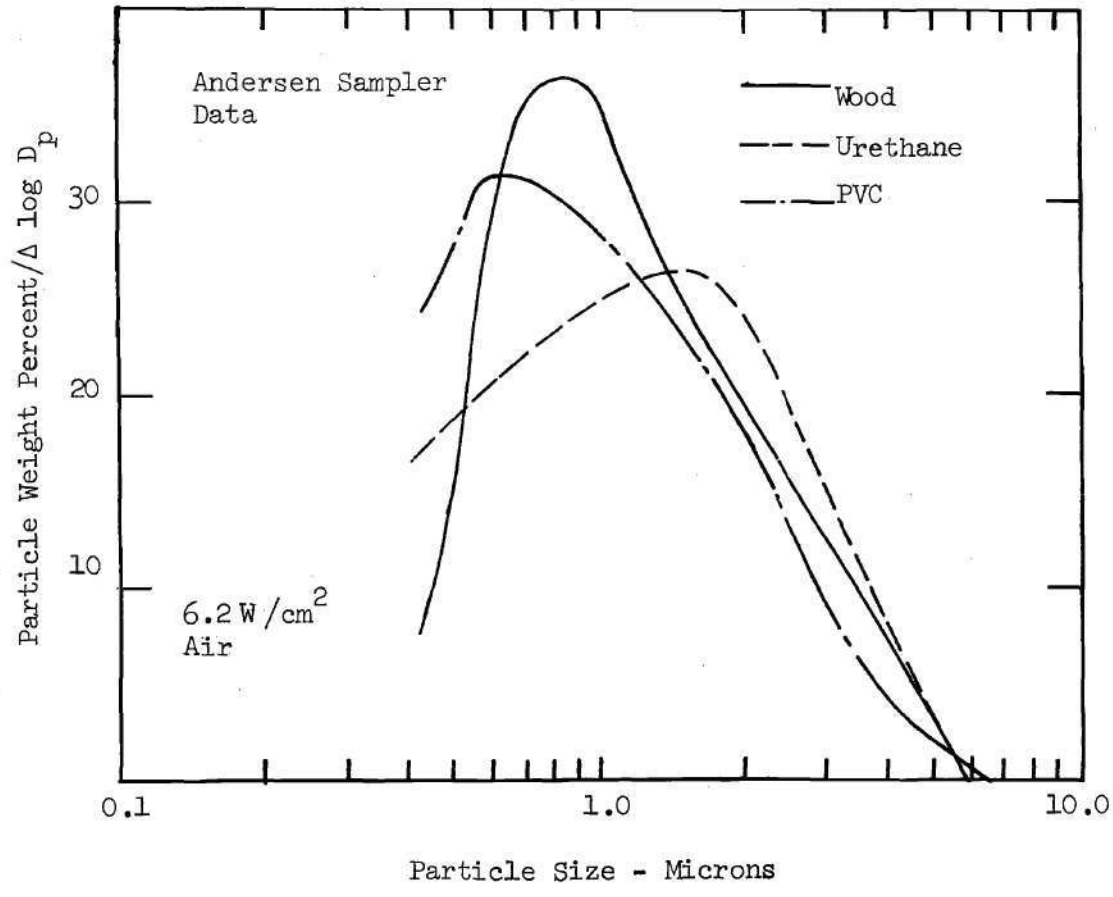

Figure 72. Comparison of Particle Weight Distributions for Wood, Urethane and PVC Non-Flaming

products leave the pyrolysis zone. Yet, it is likely that once the chemical composition of the products is established, the major portion of particulate coagulation and/or condensation takes place in the near vicinity of the pyrolysis zone as discussed earlier (non-flaming results). Particle formation and growth would then be enhanced by increased concentrations of condensable species in a small region near the pyrolysis zone. This accounts for the fact that larger particle sizes are observed when sample mass loss rates and particulate mass concentrations are highest.

Measurements of particle sizes also provide some information on the formation of soot particles generated during flaming combustion. That is, a substantial volume fraction of particles greater than 0.1 micron in diameter indicates the existence of large, chain-like sooty agglomerates, since previous studies have found particles of this size to be composed of a collection of smaller, spherical soot particles to form such larger agglomerates. This conclusion has been confirmed by subsequently taken scanning electron microscope photographs.

As previously mentioned, only a limited number of theories have been developed for modelling the generation of smoke from burning materials. The one developed by Seader and Chien[17] for predicting the optical density of smokes generated in the NBS test chamber indicates a need for the measurements made in this program. However, in order to model smoke production on a more fundamental level, additional information beyond that presented here will be required. Specifically, further efforts in the analysis of smoke particulates

should be directed toward detailed measurements in the near vicinity of a burning sample, and if possible, measurements should be made within a burning sample. Such information might then be effectively used in analyzing the dominant mechanisms in the smoke formation process.

APPENDIX A

EXPERIMENTAL PROCEDURES

This appendix covers the operational aspects of several components of the Combustion Products Test Chamber and the Aerosol Sampling System. This includes calibration and operation of the radiant heat source, implementation of aerosol sampling procedures, and determination of CPTC gas ventilation rates.

Heater Calibration and Operation

In order to provide the required radiative heating levels, the heat source shown in Figure 3 was calibrated for variations in distance from the face of the heater, and voltage input across the four quartz lamps. Measurements of radiant heating levels were taken with a 5/8 inch diameter, water-cooled radiometer (Hy-Cal # R-2059-AX-15-072), where the energy emitted by the lamps is controlled by the a.c. voltage supplied to the lamps. The voltage level is then controlled by a variable transformer.

For calibration, the face of the heater was divided into 20 one inch squares, making a 5 inch by 4 inch imaginary grid. The radiant energy flux was then measured for each grid section at several voltages between zero and 100 volts and at distances (perpendicular from the face) from 1/2 inch to 2 1/2 inches. The average heat flux was then calculated over a 3 inch by 3 inch square in the center of the

heater, corresponding to the area exposed to test samples. Figures 73 and 74 show typical calibration curves for the average energy flux received at the sample face versus distance and voltage, as determined by radiometer measurements. Variations in heat flux from the average over the sample face were found to be less than ten percent.

In actual tests, the incident radiant flux at the face of each sample was adjusted by varying the distance between sample and heater, and also varying the voltage input according to the calibration curves. For example, in tests run at 6.2 W/cm^2 radiant flux, the heater was positioned 1 1/2 inches from the sample and the voltage level set at 84 volts. Finally, it was found that at least one minute of operation was required for the heater to reach steady-state operation. Consequently, for all non-flaming tests (where higher heating rates were used), a cover was positioned over the sample to allow for heater warm-up prior to the actual start of each test. The cover could then be removed once the heater reached steady-state operation and the necessary radiant flux.

Aerosol Sampling Methods

The primary concern in the development of aerosol sampling methods is the preservation of particle size distribution and particulate concentration as the aerosol is withdrawn for analysis (see Figure 5). Variables which affect the results of sampling include isokineticity, gas temperature and sampling system geometry.(68) Therefore, in order to maintain confidence in the measurements made through the aerosol sampling system described in Chapter II, the

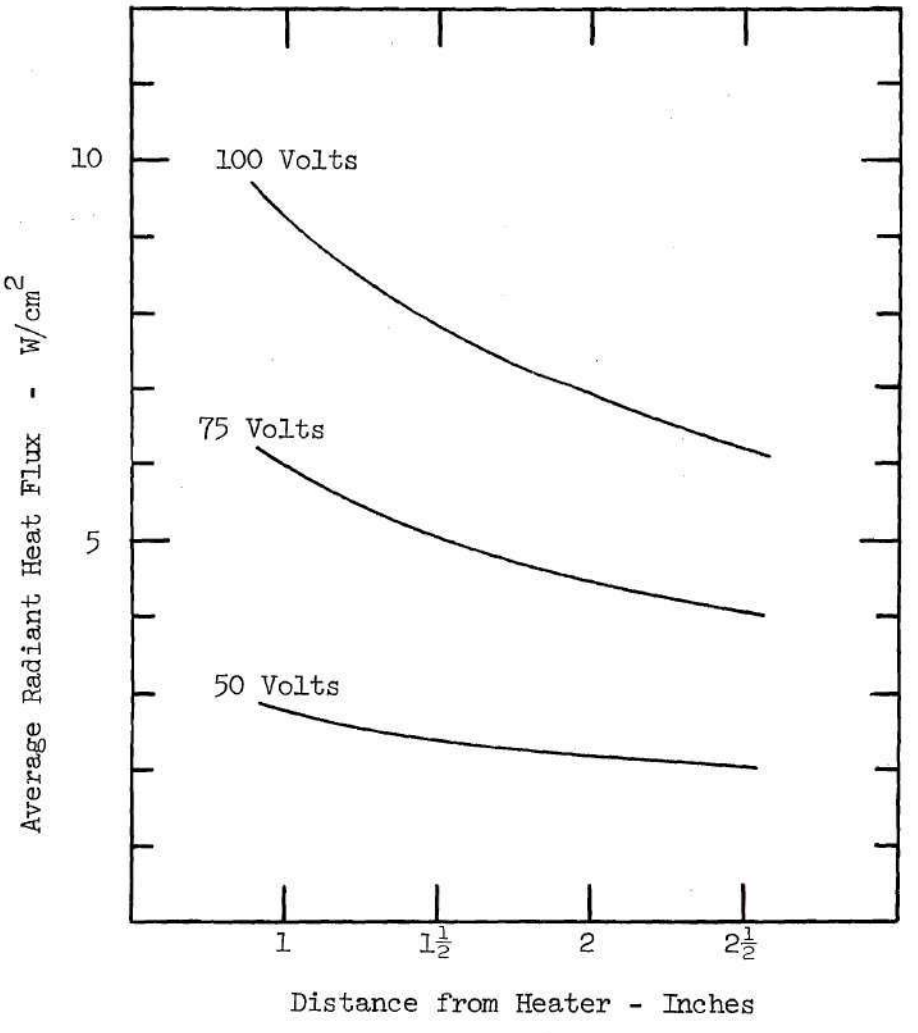

Figure 73. Heater Calibration - Distance

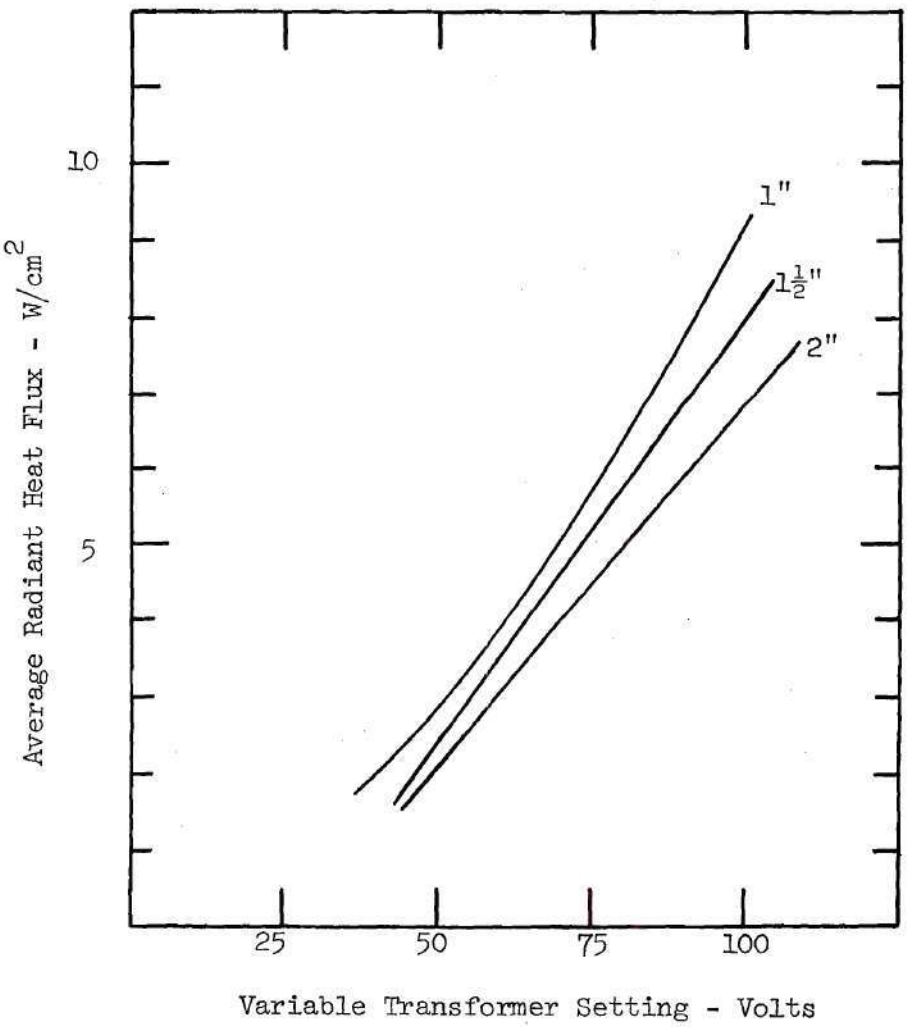

Figure 74. Heater Calibration - Voltage

above-mentioned parameters should be considered in relation to the operational characteristics of that system.

A description of important parameters for both sampling probes is given in Table 3. In the case of the 1/2 inch probe, the aerosol passes through two 90° bends and one 120° bend before reaching the Andersen Sampler. For the 1/4 inch probe, the aerosol passes through four 90° bends prior to being split and directed to the Electrical Analyzer and Mass Monitor inlets. Dilution of the 1/4 inch probe takes place at the second 90° bend as diagrammed in Figure 75. Also shown in Figure 75 is a diagram of the flow splitter used for directing the separate flows to the Electrical Analyzer and Mass Monitor. The 1/8 inch sampling tube supplying the Mass Monitor operates at near isokinetic conditions relative to flow in the 1/4 inch primary supply tube. Finally, all tubing utilized in the Aerosol Sampling System is stainless-steel and is maintained at room temperature.

Subject to the above-mentioned sampling methods developed during the initial stages of the test program, the following comments relevant to factors affecting sampling data accuracy are now in order:

1. Isokineticity - In general, deviations from isokinetic sampling may be expected to give measured differences in particle concentrations from the actual concentrations existing in the suspension.[69] This is primarily due to the inability of particles to follow streamlines in the vicinity of the sampling probe because of particle inertia effects. Isokinetic sampling conditions are met when the sampling orifice velocity equals the flow or wind velocity.

Table 3. Aerosol Sampling System Characteristics

	1/4 Inch Probe	1/2 Inch Probe
Total Length	64 Inches	40 Inches
Total Flow Rate	5 LPM	28.3 LPM
Dilution Ratio	Approx. 6/1	None
Approximate Flow Velocity	370 cm/sec (1)	530 cm/sec
Anisokineticity v/v_o (2)	0.64	6.1
$\left[\frac{\rho v}{18\nu D_c}\right]^{\frac{1}{2}} d$ (3)	Approx. 0.05 (1)	Approx. 0.04

(1) After introduction of 1/4" probe dilution gas.

(2) V_o = Stack velocity based on CPTC ventilation rate of 15 CFM.

(3) Non-dimensional particle size parameter.

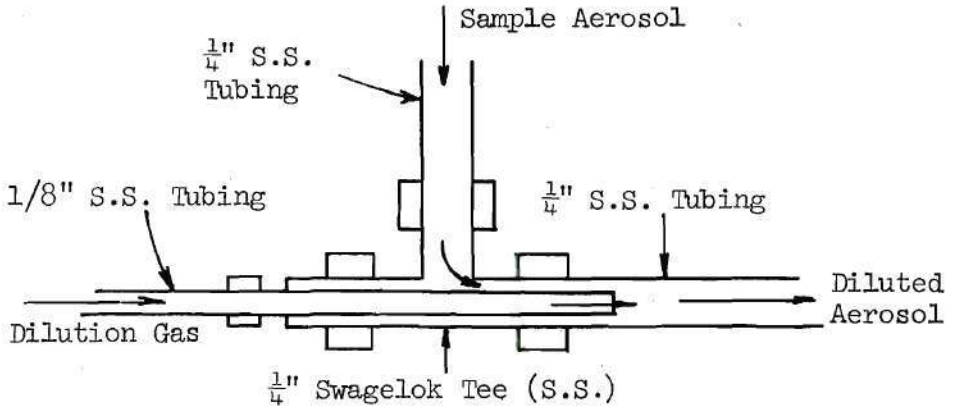

Aerosol Dilution

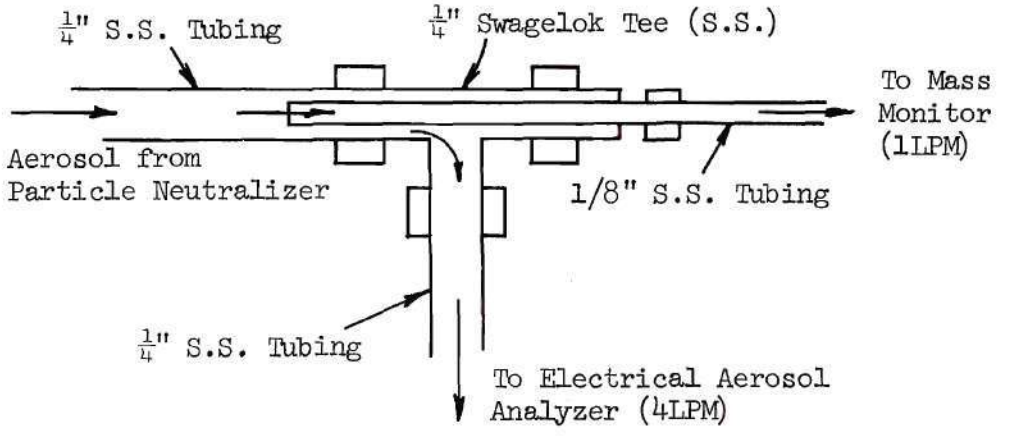

Flow Splitter

Figure 75. 1/4 Inch Sampling Probe Dilution Tee and Flow Splitter Tee

Notably, however, there is evidence to indicate that the sampling of particles below a certain size range is not prejudiced by inertial effects.[69] For particles below 10 microns in size, Sehmel[70] found that the particulate concentrations measured were virtually the same as the actual concentrations, under sampling conditions similar to those of the 1/4 inch probe used here. Also, the application of a semi-empirical equation[71] for the ratio of concentration measured to actual concentration, yields a value of approximately unity; where the formula is valid for sampling conditions characteristic of the 1/2 inch probe. In the latter case, this result is also good for particles less than 10 microns in diameter. Finally, it was determined in the initial stages of this program that measured particle sizes were to be generally near one micron in diameter, and that virtually no particles were greater than 10 microns. Therefore, upon consideration of the above-mentioned data it was concluded that isokinetic sampling is not necessary for the measurements of interest in this study.

2. Gas Temperature - Discussion of the effects of gas temperature on aerosol sampling results, here alludes to the possibility of condensation in the sampling lines prior to particle measurements. The large quantity of products produced during combustion, with their varying volatilities, presents a problem with respect to condensation if they are allowed to cool when sampled from the main flow. Obviously, this would cause measured particle concentrations to be higher than those concentrations which actually exist in the smoke.

However, due to the relatively high chamber ventilation rates used during tests, the temperature of the smoke at the level of the sampling section is generally near or slightly above room temperature. Therefore, since smoke is sampled from the exhaust stack essentially at room temperature, condensation should be negligible in the aerosol sampling lines which are maintained at room temperature.

3. Sampling System Geometry - A number of sharp bends of 90° or greater are found in each of the sampling probe lines. Such bends can be the cause of sampling errors due to particle impaction, under certain circumstances. In recognition of this problem, analytical solutions have been developed for particle impaction on the outside walls of sweeping bends and on body collectors.(69) Nevertheless, for the non-dimensional particle size parameters given in Table 3, the curves in Reference (69) show that the losses due to impaction are negligible for the sampling conditions used in these tests.

Associated with the sampling system design is the necessity for dilution of the aerosol in the smaller 1/4 inch sampling line. The high sensitivity of both the Electrical Aerosol Analyzer and the Mass Monitor require dilution ratios as high as 6/1 for maintaining particle concentrations within the operational limits of the instruments. Generally, the specific dilution rate utilized for each test is dependent on CPTC ventilation rate, material tested, and burning conditions. However, most tests required dilution rates near 6/1, with lower dilution rates (no less than 3.5/1) being used in a few cases. The dilution tee shown in Figure 75 is designed to introduce

the dilution gas as smoothly as possible, in order to prevent coagulation due to excessive turbulent mixing. In all cases, room temperature air is used for sampling line dilution. The larger 1/2 inch sampling line requires no dilution. An indication of typical dilution ratios for the 1/4 inch sampling line is presented in Table 4.

CPTC Ventilation Rates

Ventilation gas flow rates through the Combustion Products Test Chamber were established according to several criteria. First, minimum flow rates were required for each test condition in order to prevent the "build-up" of smoke within the inner shell. Such conditions would then provide for a uniform atmosphere throughout the test and also lessen the probability of particulate deposition on the chamber walls. On the other hand, the rate at which smoke is diluted by the ventilation gases must be limited so that the smoke samples collected on the stages of the Andersen Sampler are large enough to be accurately weighed. Examples of typical CPTC ventilation rates are given in Table 4, for several test conditions. In general, 15 CFM is the flow rate that is most frequently used, particularly in tests where smoke is produced in the greatest quantities. Assuming a flow rate of 15 CFM, the estimated time for smoke to reach the Sampling Section is approximately 20 seconds.

Table 4. Typical CPTC Ventilation Rates and 1/4 Inch Sampling Probe Dilution Ratios

Test Conditions	CPTC Vent Rate	1/4 Inch Probe Dilution
Wood, FL	15 CFM	6/1
Wood, NF, 3.2 W/cm^2	5 CFM	3.5/1
Wood, NF, 6.2 W/cm^2	15 CFM	6/1
Wood, NF, 9.2 W/cm^2	20 CFM	6/1
Urethane, FL	10 CFM	6/1
Urethane, NF, 3.2 W/cm^2	5 CFM	3.5/1
Urethane, NF, 6.2 W/cm^2	5 CFM	5/1
Urethane, NF, 9.2 W/cm^2	10 CFM	5/1
PVC, FL	15 CFM	6/1
PVC, NF, 3.2 W/cm^2	5 CFM	5/1
PVC, NF, 6.2 W/cm^2	15 CFM	6/1
PVC, NF, 9.2 W/cm^2	15 CFM	6/1

FL - Flaming test

NF - Non-flaming test

APPENDIX B

TEST PROCEDURES

This appendix includes the detailed test procedures used in conducting both non-flaming and flaming tests in the Combustion Products Test Chamber.

Test Procedure - Non-Flaming

Step	Comments
1. Sample Preparation	Sample material is normally conditioned at 80°F and 75 percent RH. Samples are then cut to desired shape and thickness.
2. Mount Sample	Sample is placed in holder and mounted on a quartz rod supported by a force transducer, in the center of the inner shell. The distance between sample and heater is adjusted at this time. Also, the force transducer sensitivity is set and checked.
3. Cover Sample	The sample cover is positioned over the sample.

Step	Comments
4. Close Chamber	The perforated plexiglas window to the Inner Shell is fastened in place and the door to the Outer Shell is shut.
5. Set CPTC Flow Rate(s)	Selected flow rates of the ventilation gases are controlled by external needle valves and monitored by float-type flow meters.
6. Start Electrical Size Analyzer Vacuum Pump	This pump requires a warm-up period of 2-3 minutes.
7. Set Selected 1/4 Inch Probe Dilution Gas Flow Rate	The selected dilution flow rate is controlled via needle valve and monitored by float-type flow meter.
8. Activate Electronics in the Electrical Size Analyzer, Mass Monitor and 4-PEN Strip Chart Recorder	
9. Set Flow Rates in Electrical Size Analyzer	Controls are mounted on the instrument.
10. Set Radiant Heater (Zero minus 2 minutes)	For all tests, the incident flux at the sample face is controlled by the variable transformer.

	Step	Comments
11.	Start Andersen Sampler Pump Start Mass Monitor Pump Start Electrical Size Analyzer Cycle Start 4-Pen Strip Chart Recorder Drive Start Sample Cover Withdrawal (Zero minus 15 seconds)	
12.	Sample Completely Exposed (START TEST)	From this point, data is taken continuously until the test is completed. The length of each test is dependent upon the material and test conditions.
13.	Radiant Heater Off Andersen Sampler Pump Off Mass Monitor Pump Off Strip Chart Recorder Off (STOP TEST)	
14.	Electrical Size Analyzer Pump Off	Electrical Size Analyzer sampling is continued until 1/4 inch sampling line is clear of particulates.

Step	Comments
All Gas Flows Off	
All Electronics Off	

Test Procedure - Flaming

Step	Comments
1. Sample Preparation	Sample material is normally conditioned at 80°F and 75 percent RH. Samples are then cut to desired shape and thickness.
2. Mount Sample	Sample is placed in holder and mounted on a quartz rod supported by a force transducer, in the center of the inner shell. The distance between sample and heater is adjusted at this time. Also, the force transducer sensitivity is set and checked.
3. Close Chamber	The perforated plexiglas window to the Inner Shell is fastened in place and the door to the Outer Shell is shut.

	Step	Comments
4.	Set CPTC Flow Rate(s)	Selected flow rates of the ventilation gases are controlled by external needle valves and monitored by float-type flow meters.
5.	Start Electrical Size Analyzer Vacuum Pump	This pump requires a warm-up period of 2-3 minutes.
6.	Set Selected 1/4 Inch Probe Dilution Gas Flow Rate	The selected dilution flow rate is controlled via needle valve and monitored by a float-type flow meter.
7.	Activate Electronics in the Electrical Size Analyzer, Mass Monitor and 4-Pen Strip Chart Recorder.	
8.	Set Flow Rates in Electrical Size Analyzer	Controls are mounted on the instrument.
9.	Set O_2-Air Supply Flow Rate to Propane Burner	The selected flows are controlled via needle valves and monitored by float-type flow meters.
10.	Set Radiant Heater (Zero minus 2 minutes)	For flaming tests, the incident flux at the sample face is 2.5 W/cm^2 and is controlled by the variable transformer.

	Step	Comments
11.	Set Propane Flow Rate to Propane Burner (Zero minus 30 seconds)	Propane flow rate is controlled by needle valve and monitored by float-type flow meter.
12.	Start Andersen Sampler Pump Start Mass Monitor Pump Start Electrical Size Analyzer Cycle Start 4-Pen Strip Chart Recorder Drive (Zero minus 15 seconds)	
13.	Ignite Burner (START TEST)	From this point, data is taken continuously until the test is completed. The length of each test is dependent upon the material and test conditions.
14.	(STOP TEST) Propane Burner Extinguished Radiant Heater Off Andersen Sampler Pump Off Mass Monitor Pump Off Strip Chart Recorder Off	
15.	Electrical Size Analyzer Pump Off	Electrical Size Analyzer sampling is continued until 1/4 inch sampling line is clear of particulates.

Step	Comments
All Gas Flows Off	
All Electronics Off	

APPENDIX C

DATA REDUCTION

Data reduction procedures utilized for the Andersen Sampler, Electrical Aerosol Analyzer and particulate Mass Monitor are outlined in this Appendix. Also included are a brief description and the theory of operation for each instrument.

Andersen Sampler

The Andersen Model 21-000 Sampler utilized in this program is an eight stage, multi-jet cascade impactor which collects particles in aerodynamically graded sizes.[32,72] Air is drawn through the Sampler at one CFM, producing jets of air from each of the 400 holes in each stage. The jets are in turn directed toward an impaction plate below. The hole sizes for each stage are constant, however the sizes decrease for each successive stage. Thus, jet velocities increase from one stage to the next. When the velocity of a particle becomes great enough, inertia will overcome the aerodynamic forces and the particle then sticks to the impaction plate below.[32,72] Otherwise, particles will continue to flow over the collection plate, and down to the next stage. Each stage, therefore, collects smaller particles than the preceding one. Figure 76 shows a cross-section of the Model 21-000 Andersen Sampler.

Aerodynamic diameters for an impaction efficiency of 50 percent

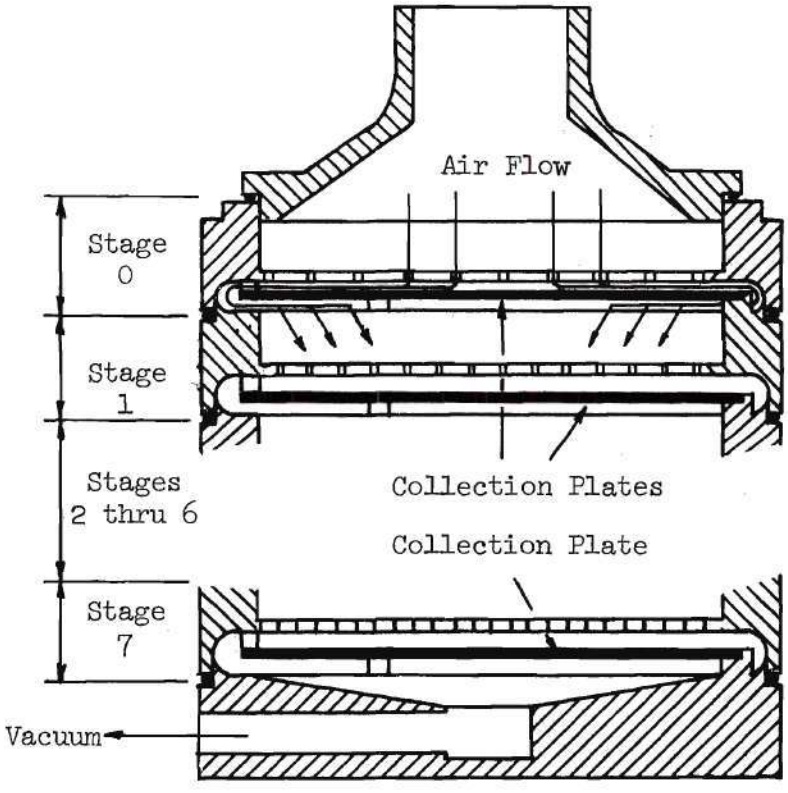

Figure 76. Andersen Sampler - Cross Section (32)

in stages of the Model 21-000 (as determined by the manufacturer) are as follows:

Stage 0	-	11 microns
Stage 1	-	7 microns
Stage 2	-	4.7 microns
Stage 3	-	3.3 microns
Stage 4	-	2.1 microns
Stage 5	-	1.1 microns
Stage 6	-	0.65 microns
Stage 7	-	0.43 microns

The "aerodynamic" diameter is defined as the diameter of an equivalent sphere of unit density having the same terminal settling velocity as the particle in question.[72] The overall collection efficiency of the Model 21-000 is 95 percent or greater for particles larger than 0.43 micron.

In order to trap particles less than the smallest particle size collected within the Andersen Sampler, a Gelman Type A glass fiber filter was mounted behind the Sampler. This back-up filter is 47 mm in diameter and has a collection efficiency of greater than 99.9 percent for particles 0.3 micron in diameter.

The particulates deposited on the collection plates of the Sampler and the glass fiber back-up filter were obtained by the continuous sampling of smoke generated during tests run in the Combustion Products Test Chamber, through the 1/2 inch sampling probe. After

each test, the collection plates and back-up filter are then removed and weighed in order to determine the total mass of particles collected within the calibrated size ranges defined earlier for the Model 21-000. It is assumed that the Sampler has a 95 percent overall collection efficiency. The weight of the particulates collected on the absolute filter is then adjusted in order to account for particles greater than 0.43 micron which may have been deposited on the filter.

Once the particulate weight has been determined for each size range, the data is then converted to particle weight percent and plotted on semi-logarithmic axes. The particle diameter is plotted on the logarithmic scale due to the range and spacing of particle size intervals for the eight stages. Also, prior to calculating particle weight percent for each of the stages, the measured particulate weight values were divided by $\Delta \log D_p$ in order to account for the finite and non-uniform particle size intervals. The corrected particle weight values for each stage were then used to determine particle weight percents for each of the size intervals defined for the Model 21-000 Andersen Sampler. The data is first plotted in bar graph form, and then a curve is manually fitted to the indicated particulate distribution.

Repeatability of particle size distribution data from the Andersen Sampler measurements was well within acceptable limits. An example of data from three different tests of wood under non-flaming conditions is given in Figure 77. This plot is given in bar graph form and shows some variation in particle weight percent for

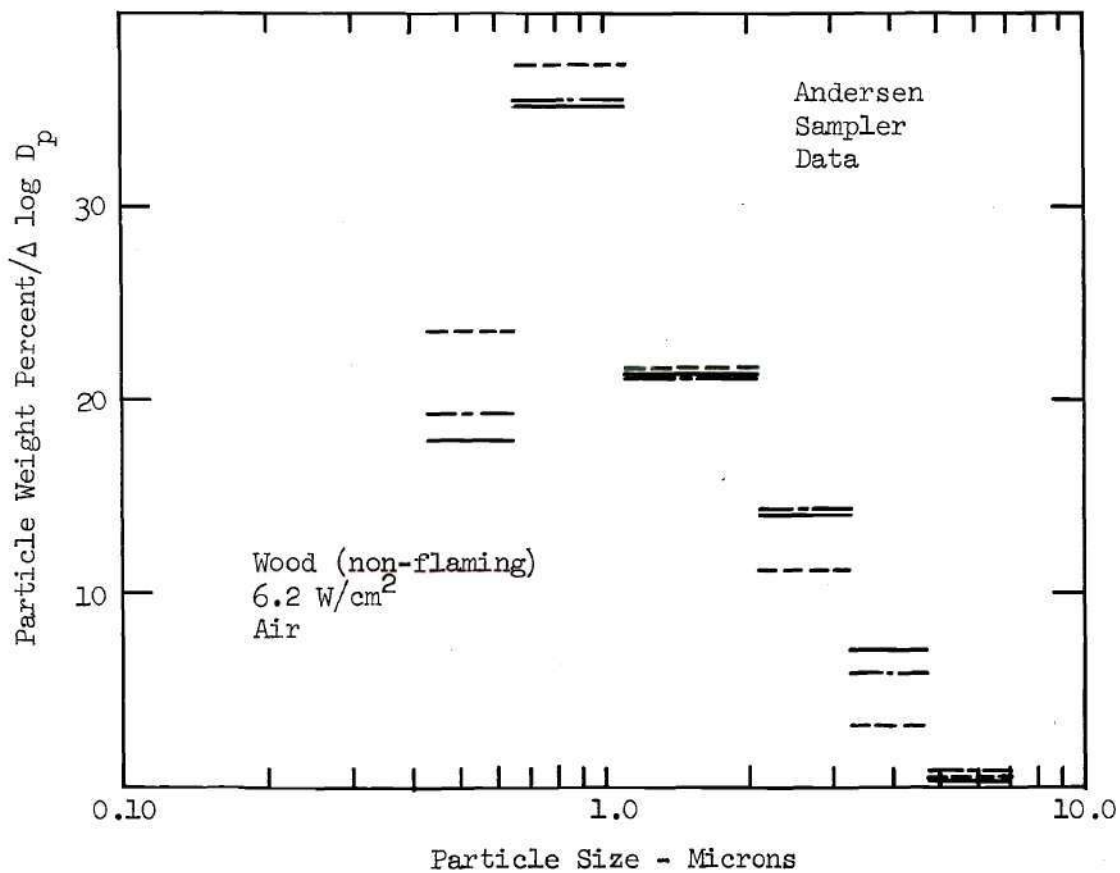

Figure 77. Comparison of Andersen Sampler Data from Three Tests Under the Same Conditions

the same size intervals. However, the general trends indicated for each of the tests is nearly the same and thus the data is essentially repeatable, especially considering the inherent nonuniformity of the wood samples. The repeatable nature of Andersen Sampler data also extends to urethane and PVC samples. However, the tendency of PVC samples to char extensively is the probable cause for somewhat increased scatter in Andersen Sampler data in non-flaming PVC tests. Nevertheless, this scatter did not significantly affect interpretation of the data.

Electrical Aerosol Analyzer

A Model 3030, Electrical Aerosol Analyzer (EAA) manufactured by Thermo-Systems, Inc., has been used to obtain time resolved particle volume distributions for particle sizes less than 1.0 micron.[33,34] The instrument samples smoke aerosol from the 1/4 inch sampling probe line at the rate of 4 liters per minute after the smoke particles have been diluted as described in Chapter II and Appendix A. Particle size measurements are performed by first exposing the aerosol to unipolar gaseous ions in a diffusion charger and then measuring the aerosol electrical mobility with a mobility analyzer. The major components of the instrument also include a current sensor and associated electronic and flow controls.[33,34]

After being electrically charged in the aerosol charger, the size distribution of the aerosol can be calculated from the mobility distribution measured in the mobility analyzer utilizing a monotonic functional relationship between particle size and mobility.[33,34]

The mobility analyzer as shown in Figure 78, consists of a cylindrical condenser with clean air and aerosol flowing down the tube in a laminar stream. For a given voltage on the center rod, particles above a certain critical mobility and less than the corresponding size are deflected to the center rod and collected there. Those particles with a lower mobility and a greater size then pass through the analyzer and are sensed by the electrometer current sensor. Thus, stepwise increases in the voltage on the center rod result in the collection of successively larger particles on the rod and a simultaneous reduction in the current sensed by the electrometer. The change in electrometer current (ΔI) is then converted to particle number density by a simple multiplicative factor for each of the calibrated particle size increments determined by stepwise center rod voltage increases. The particle size range and increments are shown in the data reduction sheet provided in Table 5. The data reduction sheet also gives the applicable multiplying factor necessary to convert changes in electrometer current to number density. All particle size increments are pre-selected by the manufacturer and are programmed automatically. The electrometer current is the final instrument output, and this is recorded on a strip chart recorder.

It should be noted at this point that some early data taken by the Whitby Electrical Aerosol Analyzer was limited in range to a maximum particle size of 0.36 micron. This is evident in results presented for a few cases under non-flaming conditions using 3.2 W/cm^2 radiant flux. This problem arose due to initial incorrect

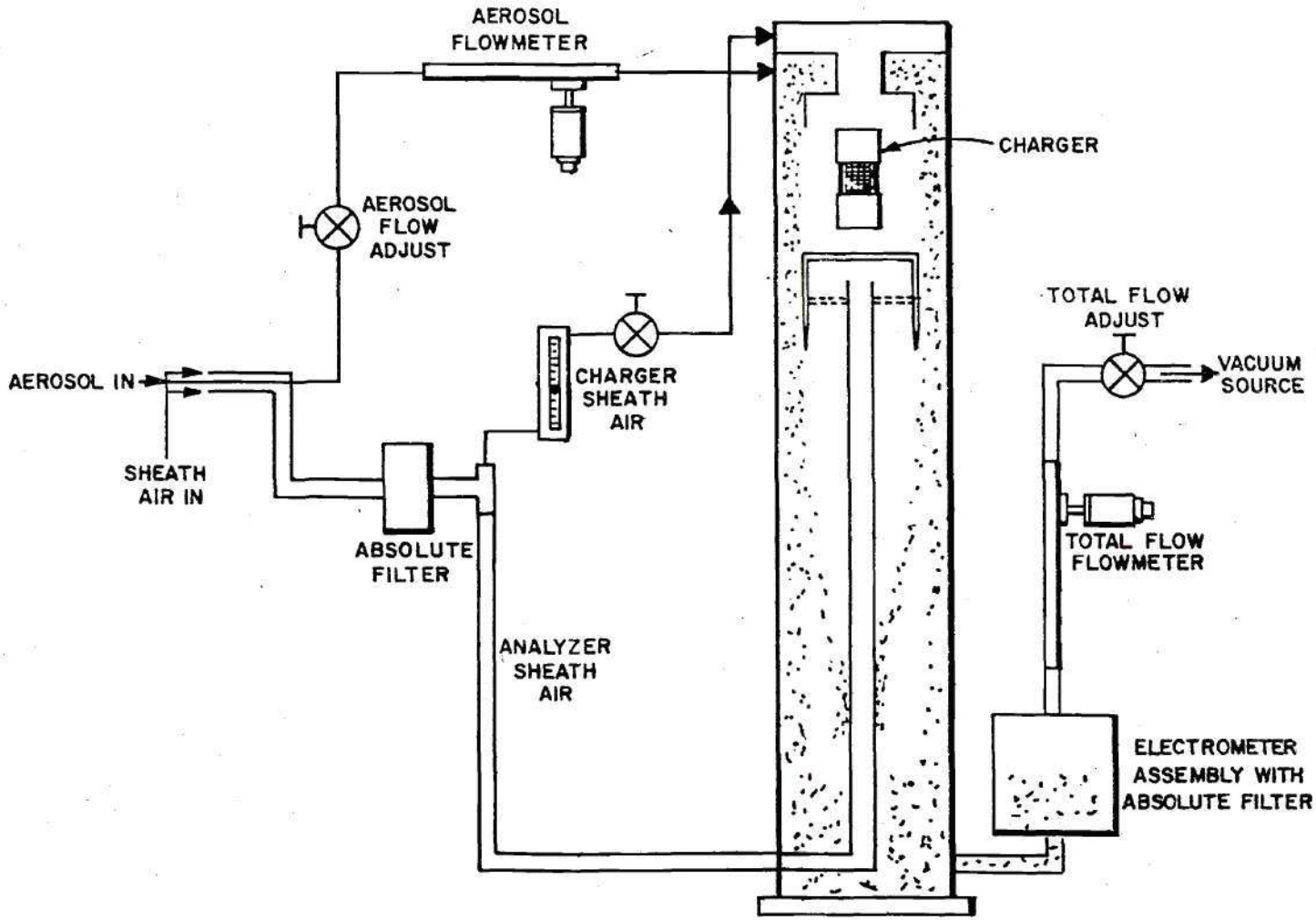

Figure 78. Electrical Aerosol Analyzer - Schematic (34)

Table 5. Data Reduction - Electrical Aerosol Analyzer

D_p, μm	D_{pi}, μm	$\Delta N/\Delta I$	$\Delta \log D_p$	Collector Voltage	I, pA	ΔI, pA	ΔN	$\frac{\Delta N}{\Delta \log D_p \times 4}$	$\frac{\Delta S/\Delta N}{\pi D_{pi}^2}$	$\frac{\Delta S/\Delta \log D_p}{\Delta S \times 4}$	$\frac{\Delta V/\Delta N}{\frac{1}{6}\pi D_{pi}^3}$	$\frac{\Delta V/\Delta \log D_p}{\Delta V \times 4}$
0.0032				19	____							
	0.0042		0.250			____	____	____	5.54(-5)†	____	3.88(-8)	____
0.0056				59	____							
	0.0075	9.52(6)	0.250			____	____	____	1.77(-4)	____	2.21(-7)	____
0.0100				186	____							
	0.0133	4.17(5)	0.250			____	____	____	5.56(-4)	____	1.23(-6)	____
0.0178				588	____							
	0.0237	1.67(5)	0.250			____	____	____	1.76(-3)	____	6.97(-6)	____
0.0316				1870	____							
	0.0422	8.70(4)	0.250			____	____	____	5.59(-3)	____	3.93(-5)	____
0.0562				2600	____							
	0.0750	4.44(4)	0.250			____	____	____	1.77(-2)	____	2.21(-4)	____
0.100				4440	____							
	0.133	2.41(4)	0.250			____	____	____	5.56(-2)	____	1.23(-3)	____
0.178				6600	____							
	0.237	1.23(4)	0.250			____	____	____	1.76(-1)	____	6.97(-3)	____
0.316				8380	____							
	0.422	6.67(3)	0.250			____	____	____	5.59(-1)	____	3.93(-2)	____
0.562				9600	____							
	0.750	3.51(3)	0.250			____	____	____	1.77	____	2.21(-1)	____
1.00				10600	____					÷4		÷4
						ΣN=				ΣS=		ΣV=

† Exponent

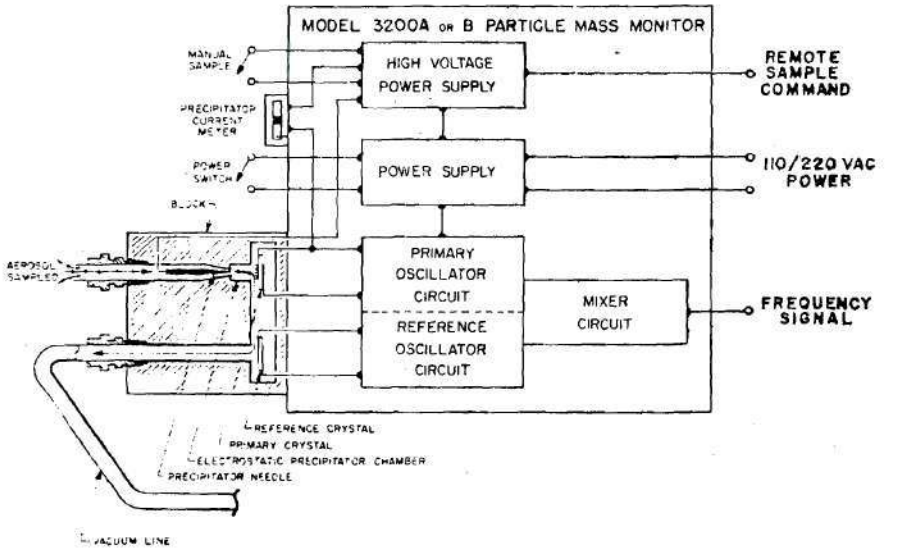

Figure 79. Mass Monitor - Block Diagram [36]

calibration information provided by the manufacturer. Subsequent modifications to the instrument re-established the upper limit of the Electrical Analyzer at 1.0 micron.

Furthermore, the indicated range of particle sizes for which the Electrical Aerosol Analyzer has been calibrated, shows a lower limit of 0.003 micron. However, upon the advice of the manufacturer, the first two size intervals were eliminated from the programmed size increments due to considerable instability at such small particle sizes; especially considering the nature of the smoke aerosol sampled. This also reduced the time required for a complete cycle over the size range of interest from two minutes to approximately 1.5 minutes. Furthermore, it was observed during the test program that most data obtained below 0.01 micron was generally unstable due to the rapid local fluctuations in smoke concentrations and thus all data was effectively limited to the range 0.05-1.0 micron. Since contributions to particle volume fractions from particles less than 0.01 micron are negligible for most conditions, the effective lower size limit did not actually restrict the data presented from the Electrical Analyzer measurements. Also, comparisons of Electrical Analyzer data with in situ light scattering measurements, have shown that the EAA is accurate up to the upper limit of one micron.

In order to compare Electrical Aerosol Analyzer data with Andersen Sampler measurements, particle number concentrations were converted to particle volume concentrations. Particle volume fractions were then calculated in the same manner as previously

computed in the reduction of Andersen Sampler Data. Particle volume distributions for particles less than 1.0 micron were plotted on semi-logarithmic paper. Therefore, volume concentrations for each size increment were divided by $\Delta \log D_p$ before volume fractions were calculated, to account for finite increments. Particle volume distributions calculated for data taken when the upper particle size limit was 0.36 micron, were plotted on linear axes. Thus, volume concentrations for each size increment in this case, were divided by ΔD_p to account for non-uniform and finite intervals. Resultant particle volume fractions for each particle size interval are plotted at the mean particle diameter for that interval, and the distribution curve is fitted through these points. Assuming that particle densities are relatively constant over the size range of interest, Electrical Aerosol Analyzer data can then be readily compared with Andersen Sampler particle weight distribution data. Note also that the normalized particle volume distribution is independent of the dilution ratio utilized for the 1/4 inch sampling probe.

Particulate Mass Monitor

Particulate mass concentration measurements have been made utilizing a Model 3200 B, Particle Mass Monitor manufactured by Thermo-Systems Inc.[36] A schematic of the Mass Monitor is shown in Figure 79. This instrument uses a piezoelectric particle microbalance formed of two identical sensor circuits, each consisting of a quartz crystal and an oscillator. The crystals are mounted in series in an aerosol stream chamber and are vibrated at their resonant mechanical frequency

by their respective oscillators. Just prior to entering the chamber, an electrostatically charged tungsten-tipped needle ionizes all particles in the aerosol stream, causing them to be deposited on the face of the first (primary) crystal's grounded electrode with almost 100 percent collection efficiency.[35,36]

As particles are deposited on the primary crystal its resonant frequency shifts downward, while the resonant frequency of the second (reference) crystal remains constant (with respect to the primary crystal). Instrument electronics continuously monitor the vibration frequencies of the two sensors, compare the frequency outputs, and determine the difference between the two. Thus, as deposition increases on the primary crystal, the difference in frequency (Δf) between the two crystals also increases.[35,36] The difference in frequencies Δf, is then used to calculate particulate mass concentration according to the equation,[36]

$$C = 333 \frac{\Delta f}{\Delta t}$$

where C is mass concentration in $\mu g/m^3$, Δf is frequency shift in Hz, and Δt is the length of sampling period in seconds. The frequency shift output Δf is continuously recorded on a strip chart recorder.

The standard sampling period used in reducing data for most smoke tests run in the CPTC is approximately 30 seconds. This is the sampling time suggested by the manufacturer for mass concentrations encountered in the 1/4 inch sampling probe after dilution. When using a 30 second sampling period, data points were normally taken

every one minute. Thus, for a particular data point, the calculated mass concentration consists of an average over the period beginning 15 seconds before and ending 15 seconds after the indicated time. However, when periods of rapid changes in mass concentration were experienced, the sampling period was reduced to 3 seconds in some cases. When such conditions were encountered, data points were generally taken every 15 seconds to improve resolution. Maximum errors specified by the manufacturer for the Model 3200 B Mass Monitor were $\pm$ 10 percent for the sampling conditions observed in the 1/4 inch sampling probe line.

Since particle concentrations at the Sampling Section of the CPTC were greater than could be directly measured by the Electrical Aerosol Analyzer and the Mass Monitor, sample probe dilution was required in order to maintain concentrations within acceptable levels. The dilution rates used were established by trial and error and are shown in Table 3. Thus, comparisons of particulate mass concentrations required correction of measured mass concentration for the corresponding dilution ratio used in each test. In this manner, measured concentrations were adjusted to show the actual concentration existing in the Sampling Section. Furthermore, all mass concentrations were compared on the basis of the same CPTC flow rate of 15 CFM. That is, if a particular test was run at a flow rate other than 15 CFM, the equivalent mass concentration that would have been measured at 15 CFM was determined in addition to the adjustment for sampling probe dilution.

Finally, it should be noted that the correction of particulate mass concentrations to compensate for sampling probe dilution introduces considerable additional uncertainty into this data. The high dilution ratios required in most tests, in addition to imprecise dilution flow rate control both contribute to this problem. The resolution of the float-type flow meter used to control the flow of sampling probe dilution gas did not provide the accuracy necessary to properly control that flow and this uncertainty is magnified at high dilution ratios. For example, calculations show that for a dilution ratio of 6/1, the additional inaccuracy in particulate mass concentration values is approximately $\pm$ 15 percent. Thus, these results are reliable for comparisons of general trends and order of magnitude differences for various test conditions. However, precise comparisons of data are not possible using the present dilution system.

Force Transducer

Continuous measurements of sample weight loss during tests in the CPTC were made by a Linear Variable Differential Transformer (LVDT) type force transducer manufactured by Schaevitz Engineering (Model FTA-G-100).[73] This force cell contains an elastic mechanical element which, when loaded, is designed to produce a small linear deflection of the core of a linear variable differential transformer resulting in a voltage output linearly proportional to axial load.[73] A constant a.c. voltage source is supplied by a Hewlett-Packard carrier amplifier and the voltage output in millivolts is recorded on a strip-chart recorder. The particular model used here has a 0-100 g. range,

with better than 0.2 percent linearity and 0.1 percent resolution. Signal output was normally calibrated at 3 mV/g for wood and PVC samples and 30 mV/g for urethane samples.

Data taken from the strip-chart recorder was converted to weight loss rate for comparison with particulate mass concentrations. This was done by calculating the weight loss of the sample for the previous minute. Thus, in most cases, the weight loss rate in grams per minute was an "average" over that previous minute. This approach was used in order to eliminate random fluctuations in weight loss so that general trends could be studied. However, in cases where better resolution was required (i.e., when the characteristic weight loss rate is extremely rapid) the time interval selected for weight loss rate determination was reduced to 30 or 15 seconds as required. This was particularly necessary in measuring the weight loss of urethane samples at high heating rates in non-flaming tests and in flaming tests.

BIBLIOGRAPHY

1. Gaskill, J. R., "Smoke Hazards and Their Measurement - A Researcher's Viewpoint," J. Fire and Flammability, 4, 279 (1973).

2. "Operation School Burning," National Fire Protection Association, Boston, Mass. (1959).

3. Fuchs, N. A., The Mechanics of Aerosols, Pergamon Press (1964).

4. Task Group on Lung Dynamics, Health Physics, 12, 173 (1966).

5. Silverman, L., Billings, C. E., and First, M. W., Particle Size Analysis in Industrial Hygiene, Academic Press, New York (1971).

6. Aerosol Measurements, Proceedings of a Seminar on Aerosol Measurements, edited by W. A. Cassat and R. S. Maddock, NBS Special Publication 412, Washington, D. C. (May 1974).

7. "ASTM Standard Method of Test for Surface Burning Characteristics of Building Materials (E 84-68)," Annual Book of ASTM Standards, Part 14 (1968).

8. "ASTM Method of Test for Surface Flammability of Building Materials Using an 8-ft Tunnel Furnace (D 286-65)," Annual Book of ASTM Standards, Part 17 (1965).

9. "ASTM Method of Test for Measuring the Density of Smoke from the Burning or Decomposition of Organic Materials (D 2843-70)," Annual Book of ASTM Standards (1970).

10. Gross, D., Loftus, J. J., and Robertson, A. F., "Method of Measuring Smoke from Burning Materials," Fire Test Methods-Restraint and Smoke-1966, ASTM STP 422, 166 (1967).

11. Lee, T. G., "The Smoke Density Chamber Method for Evaluating the Potential Smoke Generation of Building Materials," NBS Technical Note 757 (January 1973).

12. Christian, W. J., and Waterman, T. E., "Ability of Small Scale Tests to Predict Full-Scale Smoke Production," Fire Technology, 7, 332 (1971).

13. Gaskill, J. R. and Veith, C. R., "Smoke Opacity from Certain Woods and Plastics," Fire Technology, 4, 185 (1968).

14. Gaskill, J. R., "Smoke Development in Polymers During Combustion," J. Fire and Flammability, 1, 183 (1970).

15. Einhorn, I. N., Birky, M. M., Grunnet, M. L., Packham, S. C., Petajan, J. H. and Seader, J. D., "The Physiological and Toxicological Aspects of Smoke Produced During the Combustion of Polymeric Materials," Annual Report NSF-RANN Grant G. I.-33650-FRC/UU-12, UTEC 73-164, The Flammability Research Center, University of Utah, Salt Lake City, Utah (1973).

16. Einhorn, I. N., Birky, M. M., Grunnet, M. L., Packham, S. C., Petajan, J. H. and Seader, J. D., "The Physiological and Toxicological Aspects of Smoke Produced During the Combustion of Polymeric Materials," NSF-RANN GI-33650-FRC/UU-19, UTEC 74-060, The Flammability Research Center, University of Utah, Salt Lake City, Utah (1974).

17. Chien, W. P., Seader, J. D. and Birky, M. M., "Monitoring Weight Loss in an NBS Smoke-Density Chamber," Fire Technology, 9, 289 (1973).

18. Chien, W. P. and Seader, J. D., "Smoke Development at Different Energy-Flux Levels in an NBS Smoke-Density Chamber," Fire Technology, 10, 187 (1974).

19. Mickelson, R. W., and Einhorn, I. N., "The Effects of Additives on the Smoking Tendency of Urethane Foams," Proceedings of the Division of Organic Coatings and Plastics, American Chemical Society, 28, 272 (1968).

20. Hilado, C. J., "Smoke from Cellular Polymers," Fire Technology, 5, 130 (1969).

21. Brenden, J. J., "How Fourteen Coating Systems Affected Smoke Yield From Douglas Fir Plywood," Forest Products Lab, Madison, Wis., Report No. 18, FSRP FPL-214 (1973).

22. Seader, J. D. and Chien, W. P., "Physical Aspects of Smoke Development in an NBS Smoke-Density Chamber," J. Fire and Flammability, 6, 294 (1975).

23. Saito, F., "Smoke Generation from Organic Materials," Japan Building Research Institute, Research Paper No. 33 (1968).

24. Tsuchiya, Y., and Sumi, K., "Smoke Producing Characteristics of Materials," J. Fire and Flammability, 5, 64 (1974).

25. Coleman, W. E., Scheel, L. D., and Gorski, C. H., "The Particles Resulting From Polytetrafluoroethylene (PTFE) Pyrolysis in Air," American Industrial Hygiene Assn. Journal, 29, 54 (1968).

26. Paabo, M., and Comeford, J. J., "A Study of Decomposition Products of Polyurethane Foam Related to Aircraft Cabin Flash Fires," Dept. of Transportation, FAA-RD-73-46, Washington, D. C. (1973).

27. Woolley, W. D., "Nitrogen-Containing Products from the Thermal Decomposition of Flexible Polyurethane Foams," British Polymer Journal, 4, 27 (1972).

28. Stone, J. P., Hazlett, R. N., Johnson, J. E. and Carhart, H. W., "The Transport of Hydrogen Chloride by Soot from Burning Polyvinyl Chloride," J. Fire and Flammability, 4, 42 (1973).

29. King, Thomas Y., "Smoke and Carbon Monoxide Generation from Burning Selected Plastics and Red Oak," Proceedings-Fire Safety Research, NBS Special Publication 411, 165 (1973).

30. "Investigation of the Properties of the Combustion Products Generated by Building Fires," Proposal submitted by Prof. Ben T. Zinn to the National Science Foundation RANN Program, School of Aerospace Engineering, Georgia Institute of Technology, Atlanta, Georgia (1973).

31. "Properties of Combustion Products from Building Fires-Project Summary Report," Proceedings NSF/RANN Conference on Fire Research, Georgia Institute of Technology, Atlanta, Georgia, 167 (May 1974).

32. Andersen, A. A., "A Sampler for Respiratory Health Hazard Assessment," American Industrial Hygiene Assn. Journal, 27, 160 (1966).

33. Liu, B. Y. H., Whitby, K. T., and Pui, Y. H., "A Portable Electrical Aerosol Analyzer for Size Distribution Measurement of Submicron Aerosols," presented at the 66th Annual Meeting of the Air Pollution Control Assn., Chicago, Ill. (1973).

34. Operating and Service Manual, Model 3030 Electrical Aerosol Size Analyzer, Thermo-Systems Inc., Saint Paul, Minn. (1974).

35. Chuen, R. L., "Particulate Mass Measurement by Piezoelectric Crystal," Aerosol Measurements, NBS Special Publication 412, Washington, D. C. (1974).

36. Instruction Manual, Model 3200 Particle Mass Monitor, Thermo-Systems Inc., Saint Paul, Minn. (1974).

37. Roberts, A. F., "A Review of Kinetics Data for the Pyrolysis of Wood and Related Substances," Combustion and Flame, 14, 261 (1970).

38. Tsoumis, G., Wood as a Raw Material, Pergamon Press (1968).

39. Hilado, C. J., Flammability Handbook for Plastics, 2nd ed., Technomic (1974).

40. Backus, J. K., "Flame Resistant Rigid Foams," Advances in Urethane Science and Technology, 1, Technomic (1971).

41. Waterman, T. E., "Room Flashover-Criteria and Synthesis," Fire Technology, 4, 25 (1968).

42. Butler, C. P., "Measurements of the Dynamics of Structural Fires," Stanford Research Institute, Annual Report, Contract DAHC 20-70-C-0219 (1970).

43. Wiersma, S. J. and Martin, S. B., "Measurements of the Dynamics of Structural Fires," Stanford Research Institute, Annual Report, Contract DAHC 20-70-C-0219 (1971).

44. "A Study of Room Fire Development: The Second Full-Scale Bedroom Fire Test of the Home Fire Project," edited by P. A. Croce, Factory Mutual Research, FMRC No. 21011.4 (1975).

45. Courtney, W. G., "Condensation During Heterogeneous Combustion," Eleventh Symposium (International) on Combustion, The Combustion Institute, Pittsburgh, Pa., 237 (1967).

46. Zinn, B. T., Cassanova, R. A., Powell, E. A., Bankston, C. P., and Tsoukalas, S. N., "Experimental Determination of the Physical and Chemical Properties of Smoke," presented at the Polymer Conference Series, Flammability of Materials, University of Utah (July 1975).

47. Browne, F. L., "Theories of the Combustion of Wood and Its Control," U. S. Forest Products Laboratory, Report No. 2136 (1958).

48. Wood Chemistry, 2, edited by Louis E. Wise and Edwin C. Jahn, Reinhold Publishing Corp., New York, N. Y. (1952).

49. Private Communication of Unpublished Data provided by Dr. George Mulholland, National Bureau of Standards (October 1975).

50. Roberts, A. F. and Clough, G., "Thermal Decomposition of Wood in an Inert Atmosphere," Ninth Symposium (International) on Combustion, The Combustion Institute, Pittsburgh, Pa., 158 (1963).

51. Tinney, E. R., "The Combustion of Wooden Dowels in Heated Air," Tenth Symposium (International) on Combustion, The Combustion Institute, Pittsburgh, Pa., 925 (1965).

52. Roberts, A. F., "Problems Associated with the Theoretical Analysis of the Burning of Wood," Thirteenth Symposium (International) on Combustion, The Combustion Institute, Pittsburgh, Pa., 893 (1971).

53. Davies, C. N., Stanford Research Institute Journal, 5, 123 (1961).

54. Geddes, W. C., "Mechanism of PVC Degradation," Rubber Chemistry and Technology, 40, 177 (1967).

55. Woolley, W. D., "Decomposition Products of PVC for Studies of Fires," British Polymer Journal, 3, 186 (1971).

56. Madorsky, S. L., Thermal Degradation of Organic Polymers, Interscience Publishers (1964).

57. Winkler, D. E., "Mechanism of Polyvinyl Chloride Degradation and Stabilization," Journal of Polymer Science, 35, 3 (1959).

58. Stromberg, R. R., Straus, S., and Achhammer, B. G., "Thermal Decomposition of Polyvinyl Chloride," Journal of Polymer Science, 35, 355 (1959).

59. Tsuchiya, Y. and Sumi, K., "Thermal Decomposition Products of Polyvinyl Chloride," Journal of Applied Chemistry, 17, 364 (1967).

60. Talamini, G. and Pezzin, G., "Polyvinyl Chloride Thermal Dehydrochlorination," Makromolekulare Chemie, 39, 26 (1960).

61. Fristrom, R. M., "Topical Report: The Chemistry of Polymer Flames-Propagation and Suppression," Johns Hopkins University, Applied Physics Laboratory, APL/JHU FPP TR4 (1971).

62. Stuetz, D. E., Diedwardo, A. H., Zitomer, F., and Barnes, B. P., Journal of Polymer Science: Polymer Chemistry, 13, 585 (1975).

63. Palmer, H. B. and Cullis, C. F., "The Formation of Carbon from Gases," Chemistry and Physics of Carbon, 1, edited by P. L. Walker, Dekker, New York, N. Y. (1965).

64. Wersborg, B. L., Howard, J. B. and Williams, G. C., "Physical Mechanisms in Carbon Formation in Flames," Fourteenth Symposium (International) on Combustion, The Combustion Institute, Pittsburgh, Pa., 929 (1973).

65. Jones, A. R. and Wong, W., "Direct Optical Evidence for the Presence of Sooty Agglomerates in Flames," Combustion and Flame, 24, 139 (1975).

66. Homann, K. H., "Carbon Formation in Premixed Flames," Combustion and Flame, 11, 265 (1967).

67. Wersborg, B. L., Fox, L. K. and Howard, J. B., "Soot Concentration and Absorption Coefficient in a Low-Pressure Flame," Project Squid, Technical Report MIT-86-PU, Massachusetts Institute of Technology (1974).

68. Smith, F. H., "The Effects of Sampling Probe Design and Sampling Techniques on Aerosol Measurements," Air Force Systems Command, Washington, D. C., Report No. AEDC-TR-74-119 (1975).

69. Cadle, R. D., Particle Size, Reinhold Publishing Corp., New York, Chapter 2 (1965).

70. Sehmel, G. A., "Sub-Isokinetic Sampling of Particles in an Air Stream," Batelle-Northwest, AEC Contract No. AT(45-1)-1830 (1966).

71. Davies, C. N., "The Entry of Aerosols Into Sampling Tubes and Heads," British Journal of Applied Physics, 1, 921 (1968).

72. Air Sampling Instruments, American Conference of Governmental Industrial Hygienists (1972).

73. "Force Transducers - Technical Bulletin 5001," Schaevitz Engineering, Pennsauken, N. J. (1970).

VITA

Clyde Perry Bankston was born in Atlanta, Georgia on May 19, 1949. He attended elementary school in Birmingham, Alabama and junior high school in Jacksonville, Florida. Mr. Bankston graduated from Terry Parker Senior High School, Jacksonville, Florida in June 1967. He entered the Georgia Institute of Technology in September of 1967 and received the degree of Bachelor of Aerospace Engineering with Highest Honor in June of 1971.

From August 1971 to March 1972, Mr. Bankston was on active duty in the U. S. Navy and was stationed at NAS Lakehurst, New Jersey. In March 1972, he returned to the Georgia Institute of Technology as a graduate student in the doctoral program. He received the degree of Master of Science in Aerospace Engineering in August of 1973.

Mr. Bankston is a member of Phi Eta Sigma, Sigma Gamma Tau, Tau Beta Pi, Phi Kappa Phi, American Institute of Aeronautics and Astronautics and the Combustion Institute. He is also a participating member of the U. S. Naval Reserve program.

On June 15, 1974, Mr. Bankston married the former Mary Lynn Gay of Lakeland, Florida.